

# A novel mode of reproduction in *Listeria monocytogenes* L-forms

**Doctoral Thesis****Author(s):**

Staubli, Titu

**Publication date:**

2014

**Permanent link:**

<https://doi.org/10.3929/ethz-a-010273693>

**Rights / license:**

In Copyright - Non-Commercial Use Permitted

Diss. ETH No. 22242

# A novel mode of reproduction in *Listeria monocytogenes* L-forms

A dissertation submitted to attain the degree of  
DOCTOR OF SCIENCES of ETH ZURICH  
(Dr. sc. ETH Zurich)

presented by  
TITU STAUBLI  
MSc ETH Zurich

born on 20.01.1984  
citizen of  
Zurich ZH, Switzerland

accepted on the recommendation of  
Prof. Dr. Martin J. Loessner, examiner  
Dr. Yves Briers, co-examiner  
Dr. Markus Schuppler, co-examiner

2014



# Table of Contents

<b>1</b>	<b>Summary</b>	<b>1</b>
<b>2</b>	<b>Introduction</b>	<b>9</b>
2.1	<i>Listeria monocytogenes</i> . . . . .	9
2.1.1	Taxonomy, morphology and characteristics of <i>Listeria</i> . . . . .	9
2.2	<i>L. monocytogenes</i> infection . . . . .	10
2.3	Bacterial cell cycle . . . . .	10
2.3.1	Bacterial chromosome segregation . . . . .	12
2.4	Bacterial cell wall . . . . .	14
2.5	Bacterial membrane . . . . .	15
2.6	Cell wall-deficient bacteria . . . . .	18
2.6.1	Definition of L-forms . . . . .	18
2.6.2	History . . . . .	19
2.6.3	Bacterial L-form cells . . . . .	20
2.6.4	<i>Listeria monocytogenes</i> L-forms . . . . .	21
2.6.5	<i>Listeria</i> L-forms reproduction . . . . .	22
2.6.6	<i>Bacillus subtilis</i> L-forms . . . . .	24
2.6.7	<i>Escherichia coli</i> L-forms . . . . .	26
2.7	Pathogenicity of <i>Listeria</i> L-forms . . . . .	28
2.8	L-forms may provide insights on the primordial life . . . . .	29
<b>3</b>	<b>Manuscript 1</b>	<b>43</b>



<b>4</b>	<b>Manuscript 2</b>	<b>69</b>
<b>5</b>	<b>Manuscript 3</b>	<b>95</b>
<b>6</b>	<b>Conclusion and Outlook</b>	<b>111</b>
<b>7</b>	<b>Addendum</b>	<b>115</b>
7.1	<i>Listeria</i> L-forms membranes comprise significantly more polar phospholipids . . .	115
7.2	Imaging analysis suggests a generation time of 265 minutes . . . . .	116
7.3	DNA content and surface area correlate linearly over time . . . . .	117
7.4	Three Dimensional Structured Illumination Microscopy of stable L-forms . . . . .	118
7.5	Production of GUV with <i>Listeria</i> lipid extracts . . . . .	119
7.6	<i>Listeria</i> protoplasts escape at the middle of the lateral wall . . . . .	120
<b>8</b>	<b>Material and Methods</b>	<b>125</b>
8.1	Methods . . . . .	125
8.1.1	Lipid composition analysis by mass spectrometry . . . . .	125
8.1.2	Infection of THP1-macrophages with EGDe L-forms . . . . .	125
8.1.3	Imaging analysis . . . . .	126
8.1.4	Time-lapse of protoplast escape from its enveloping wall . . . . .	126
8.1.5	<i>Listeria</i> L-forms lipids were extracted using a two-step protocol . . . . .	126
8.1.6	Generation of GUVs out of <i>Listeria</i> L-forms lipid extracts . . . . .	127
8.2	Culture Media . . . . .	128
8.3	Buffers and Solutions . . . . .	129

# Abbreviations and Designations

ActA	Protein for actin polymerization	lmo	Prefix of <i>Listeria</i> genes
Amp	Ampicillin	kD	1000 Dalton
Amp <sup>R</sup>	Resistance to Ampicillin	LB	Luria-Bertani (media)
ATP	Adenosine triphosphate	LLM	<i>L. monocytogenes</i> L-form medium
BHI	Brain Heart Infusion	MetOH	Methanol
bp	Base-pair	NaOH	Sodium hydroxide
BTME	BODIPY <sup>®</sup> TR methyl ester	NaCl	Sodium chloride
Cm	Chloramphenicol	OD	Optical density
Cm <sup>R</sup>	Resistance to Chloramphenicol	o/n	Overnight
CFP	Cyan Fluorescent Protein	PCR	Polymerase chain reaction
CFU	Colony Forming Units	PFA	Paraformaldehyde
DAPI	4',6-diamidino-2-phenylindole	PG	Peptidoglycan
DNA	Deoxyribonucleic acid	pH	Potential of hydrogen
DMSO	Dimethyl sulfoxide	PLC	Phospholipase C
ds	double-strand	PrfA	Positive Regulatory Factor A
DS	Droplet solution	PS	Phospholipid solution
EDTA	Ethylenediaminetetraacetate	qPCR	quantitative PCR
EP	Eppendorf tube	RBS	Ribosomal binding site
EtOH	Ethanol	rpm	Round per minute
GFP	Green Fluorescent Protein	rRNA	Ribosomal ribonucleic acid
GUVs	Giant Unilamellar Vesicles	RT	Room temperature
HCl	Hydrogen chloride	SAP	Shrimp alkaline phosphatase
LLO	Listeriolysin O	SDS	Sodium dodecyl sulfate
InlA	Internalin A	SOE	Splice overlap extension
InlB	Internalin B	SOC	Super optimal broth media
IPTG	Isopropyl $\beta$ -1-thiogalactopyranoside	w/o	water oil emulsion

**Units**

m	Meter
min	Minutes
g	Gram
<i>g</i>	g-force
s	second
A	Ampere
mol	Mole
rpm	Round per Minute
°C	Degree celcius
l	Liter
V	Volt
F	Farad

# 1 Summary

Bacteria have the ability to adapt in response to a changing environment and have developed strategies to ensure their survival under a range of disadvantageous conditions. Exposure to compounds interfering with cell wall integrity or synthesis (antibiotics and lytic enzymes) may cause the bacterial cell to lose its cell wall. Despite the severe response, they do not die off immediately. Provided that there is the right osmotic environment, bacteria cannot only survive for a long period of time, but are actually capable of switching to a new mode of replication. In the absence of the cell wall, bacteria can not divide by binary fission instead, they employ a range of different compensatory mechanisms. Replicating cell wall-deficient variants are commonly referred to as L-forms. Their emergence has been reported for several Gram-positive and Gram-negative bacterial species. Although several studies exist on L-forms of pathogenic bacteria being associated with chronic diseases, their role has not yet been fully elucidated.

*Listeria monocytogenes* is a Gram-positive, rod-shaped bacterium and opportunistic human pathogen that is ubiquitous in the environment. In the light of *L. monocytogenes* as the causative agent of listeriosis, there is need for a better understanding of survival strategies applied in the presence of cell wall targeting antibiotics. The aim of this study was to investigate a new mode of replication of *L. monocytogenes* L-forms. L-forms were generated by exposing parental *L. monocytogenes* to the cell wall synthesis interfering drug penicillin G, followed by growth in osmotically stabilizing media. Upon transition to the wall-less state, *Listeria* L-form cells display a spherical shape and measure up to 30  $\mu\text{m}$ .

The first part of this thesis includes growth characterization of L-forms derived from the *L. monocytogenes* strain EGDe. Determination of growth kinetics indicated a significant slower

growth rate, reaching stationary phase after 2 days. In order to elucidate the new proliferation mechanism several methods were used. Microscopic analysis revealed that *Listeria* L-forms divide by forming intracellular and extracellular vesiculation. Time-lapse microscopy of extracellular reproduction cycles demonstrated a high degree of membrane dynamics leading to progeny cells produced by budding-like, protrusions and fragmentation processes. In the early growth phase L-form cells tend to be interconnected by thin strands filled with cytoplasm. Fluorescence Loss in Photobleaching (FLIP) experiments confirmed that these structures form a continuum, and there is an actual exchange of cytoplasmic material occurring. Reproduction by internal vesiculation apparently also involves the formation of vesicles within vesicles (VWVs). Fluorescent markers as well as isolation and sub-cultivation of VWVs by micromanipulation unraveled the viability of these internal budding structures.

In the second part I focused on the molecular level to investigate what is driving replication. L-forms feature a distorted structural organization characterized by polyploidy and the dispensability of many cell division proteins. Usually, bacterial cell division is tightly orchestrated by various proteins in order ensure the faithful production of two identical daughter cells. The presence of multiple chromosomes indicates the loss of synchronization of cell division, DNA replication and segregation. Furthermore, it was demonstrated that the cell division key player FtsZ is not required for L-form reproduction. I therefore conclude that proliferation of L-forms likely represents an undirected and random process which may not always give rise to viable progeny cells. Generation of heteroploid L-forms, containing two different types of chromosomes, was employed to monitor faith of DNA distribution. The resulting spontaneous and rapid differentiation of heteroploid to monoploid L-forms supports the hypothesis of the absence of a chromosome segregation machinery. We found that L-forms exhibit an enhanced permeability for extracellular DNA and proteins, most likely to be accounted by an increase in membrane fluidity. Moreover, L-forms were observed to undergo membrane fusion resulting in heteroploids. Both processes could have fueled evolution driven by competition and selection of the best adapted vesicles. Due to the primitive mode of reproduction and the dispensability of sophisticated cell division machinery, L-forms are now considered to represent a prokaryotic

model system to probe primordial cellular reproduction.

Our findings not only highlight the enormous plasticity and adaptability of bacterial survival and multiplication, but also offer a glimpse back into the distant past and the putative origins of self-replication in ancestral cell types.



# Zusammenfassung

Bakterien sind in der Lage Überlebensstrategien zu entwickeln und können sich so verändernden Umweltbedingungen anpassen. Werden sie zum Beispiel einem Zellwandsynthesehemmer ausgesetzt führt dies zum Verlust der Zellwand. Trotz dieser beträchtlichen Veränderung sind die Bakterien dank einem alternativen Replikationsmechanismus weiterhin fähig sich in einem osmotisch günstigen Milieu weiter zu vermehren. Im Gegensatz zu den Prokaryoten, welche von einer Zellwand umgeben sind, teilen sich die zellwandlosen Bakterienformen nicht durch binäre Zellteilung sondern verfügen über eine Reihe an alternativen Vermehrungsweisen. Replikationsfähige zellwandlose Bakterien nennt man L-Formen. Sowohl aus Gram-negativen, als auch Gram-positiven Bakterien können L-Formen entstehen. Obwohl schon mehrere Studien publiziert wurden, die einen Zusammenhang zwischen chronischen Erkrankungen und L-Formen untersuchten, konnte bis heute keine einstimmige Aussage über deren Pathogenität gemacht werden. Die vorliegende Arbeit befasste sich mit der Untersuchung von L-Formen des pathogenen Bakteriums *Listeria monocytogenes*. Es handelt sich um ein Gram-positives, stäbchenförmiges und ubiquitär vorkommendes Bakterium welches als opportunistischer Krankheitserreger gefürchtet wird. Das Ziel dieser Dissertation war, den Replikationsmechanismus von *Listeria monocytogenes* L-Formen zu charakterisieren. Es ist von zentraler Bedeutung, die Vermehrungsstrategien besser zu verstehen, da diese möglicherweise bei der Therapie von Listeriose Patienten eine entscheidende Rolle spielen. Zellwandlose Listerien wurden erzeugt, indem man parentale Listerien dem Antibiotikum Penicillin G aussetzte und anschliessend in einem osmotisch stabilen Medium kultivierte. Ich beobachtete, dass die Zellen nach der Modifikation und dem Ablösen der Zellwand eine runde Form annehmen und einen Durchmesser von bis zu 30  $\mu\text{m}$  aufweisen.



Der erste Teil der Arbeit umfasst die Charakterisierung des Wachstumsverhaltens von L-Formen des Stammes EGDe. Untersuchungen haben gezeigt, dass im Gegensatz zu den parentalen *Listerien*, die L-Formen erst nach 2 Tagen ihre stationäre Phase erreichen. Um den Replikationsmechanismus der zellwandlosen *Listerien* zu studieren, kamen verschiedene Methoden zum Einsatz. Mikroskopische Analysen haben ergeben, dass sich *Listerien* L-Formen sowohl mittels intrazellulären, als auch extrazellulären Vesikeln replizieren. Anhand von Videoaufnahmen über die Zeit der kompletten Replikationszyklen, konnte die enorme Membrandynamik aufgezeigt werden, welche nötig ist um Nachkommenzellen zu generieren. Eine entscheidende Beobachtung war, dass L-Formen in der frühen Wachstumsphase dazu tendieren, sich untereinander zu verbinden. Experimente mit Hilfe der "Fluorescent Loss in Photobleaching (FLIP)" Mikroskopie bestätigten den Austausch von zytoplasmatischem Material zwischen den L-Form Zellen. Die Vermehrungsweise via interner Vesikelbildung geschieht durch die Bildung von so genannten "vesicle within a vesicle (VWV)". Die Lebensfähigkeit der VWVs wurde anhand von fluoreszierenden Farbstoffen sowie Isolierung und Subkultivierung der einzelnen Vesikel demonstriert.

Im zweiten Teil der Arbeit fokussierte ich mich auf die molekularen Mechanismen. Es galt nachzuvollziehen, was die treibende Kraft des alternativ entstandenen Teilungsmechanismus darstellt. Die zellulären Prozesse in L-Formen scheinen weniger genau reguliert zu sein als bei ihren parentalen Verwandten, welche einen äusserst präzisen Zellteilungsvorgang aufweisen. Die Ungenauigkeit ist gekennzeichnet durch die Polyploidie und Entbehrlichkeit vieler Zellteilungsproteine. Das Vorhandensein mehrerer Chromosomen impliziert den Verlust der Synchronisation der Zellteilung, DNA Replikation und Chromosomensegregation. Zudem wird das Zellteilungsschlüsselprotein FtsZ in *Listerien* L-Formen für das Wachstum nicht gebraucht. Aufgrund dieser Indizien schliesse ich, dass die Proliferation der zellwandlosen *Listerien* unstrukturiert, völlig zufällig abläuft und deshalb nicht immer zu lebensfähigen Nachkommen führt.

Aufgrund des primitiven Replikationszyklus und den Verzicht ausgeklügelter Zellteilungsmechanismen, werden die L-Formen auch als Modellsystem herbeigezogen, um die möglichen Eigenschaften der ersten Zellen auf Erden zu studieren. Ein wichtiges Erkenntnis diesbezüglich war,

dass L-Formen eine höhere Membranpermeabilität besitzen und extrazelluläre DNA sowie Proteine aufnehmen können, was höchstwahrscheinlich mit der höheren Membranfluidität einhergeht. Weitere Beobachtungen haben ergeben, dass L-Formen fusionieren und so heteroploide Zellen bilden können. Solche Prozesse hätten die Evolution von Protozellen beschleunigen und favorisieren können. Die hier präsentierten Resultate zeigen nicht nur die enorme Plastizität und Anpassungsfähigkeit von Bakterien auf, sondern ermöglichen uns auch einen interessanten Einblick in die Vergangenheit und Vorfahren von Prokaryoten.



## 2 Introduction

### 2.1 *Listeria monocytogenes*

#### 2.1.1 Taxonomy, morphology and characteristics of *Listeria*

*Listeria* has been first described in 1926 by E.G.D. Murray who isolated *L. monocytogenes* from a infected guniea pigs and rabbits [1]. *Listeria* belongs to the order *Bacillales* and the family *Listeriaceae*. It is a member of the Firmicutes, Gram-positive bacteria featuring low G/C content in their DNA. Close relatives include *Bacillus*, *Clostridium*, *Brochothrix*, *Enterococcus*, *Streptococcus* and *Staphylococcus* [2]. *Listeria* is a rod-shaped, Gram-positive cell with a size of about 0.5-3  $\mu\text{m}$  x 0.5  $\mu\text{m}$ , and can live as a facultatively anaerobic and facultatively intracellular pathogen. It is ubiquitous, well adapted to life in diverse environments ranging from water, various food products, and life in the cytosol of eukaryotic cells [3]. The adaptability is represented by the ability to grow at 1-45°C and to survive in media with high salt concentrations (10% (w/v)) and low pH [4]. The optimum growth temperature of *Listeria* ranges from 30 to 37°C, but growth can be observed from 1 to 45°C [5, 6]. Brain heart infusion (BHI) is the medium *Listeria* grow best in. At temperatures up to 30°C, *Listeria* shows a characteristic tumbling motility governed by the flagella which is produced in a temperature-dependent manner [7, 8]. The expression of the *flaA* gene is repressed at 37°C, resulting in no or weakly motility [7]. To date, there are eight species of the genus *Listeria* known, however, only two are considered to be a pathogenic. *L. monocytogenes* is able to infect human and animals, whereas *L. ivanovii* is an animal pathogen [5, 9, 10]. The rest of the *Listeria* species have been regarded as non-pathogenic [5, 11].

## 2.2 *L. monocytogenes* infection

*L. monocytogenes* infections occur mostly by ingestion of contaminated food. The main source of infection often originates from raw food that was not subjected to pasteurization [12]. In healthy individuals, *L. monocytogenes* infection is often restricted to a gastroenteritis. On the contrary, in immunocompromised, elderly people or pregnant women, *L. monocytogenes* can cause severe infections which manifests as meningitis, meningoencephalitis, or septicemia which can result in a 25-30% death rate [2].

*L. monocytogenes* features different strategies to cope with harsh conditions (low acidity, osmolarity, oxygen tension and bile) found in the gastrointestinal tract. The crucial step in *L. monocytogenes* infection comprises the ability to cross the intestinal barrier [12]. Invasion of host epithelial cells is governed by various surface proteins including InlA and InlB, which bind to receptors on the host cell [3]. InlA binds to the host E-cadherin whereas InlB interacts with the hepatocyte growth factor (HGF) receptor [13]. The attachment to these receptors induces internalisation by the host endocytic machinery. In order to escape from the phagosome, *L. monocytogenes* secretes pore-forming listeriolysin O (LLO), in combination with two phospholipases C (PLC) which support rupture of the vacuole membrane [14, 3]. Once in the cytosol, ActA assembles asymmetrically on the bacterial surface and recruits host cell actin to polymerize into an actin tail. This machinery propels *L. monocytogenes* through the cell and enables spread into adjacent cells [15, 16]. Due to the cell-to-cell spread, *Listeria* ends up enveloped by double membrane vacuole where escape is assisted by phosphatidylcholine-specific Phospholipase C encode by the *plcB* gene [2].

## 2.3 Bacterial cell cycle

Cell division is a tightly regulated process in order to ensure faithful inheritance of genetic material into new daughter cells. The sophisticated eukaryotic cell division system has been elucidated in detail [18, 19]. On the contrary, the explicit mechanisms of bacterial cell division has not been fully resolved yet. For a long time, prokaryotes were considered to be devoid of

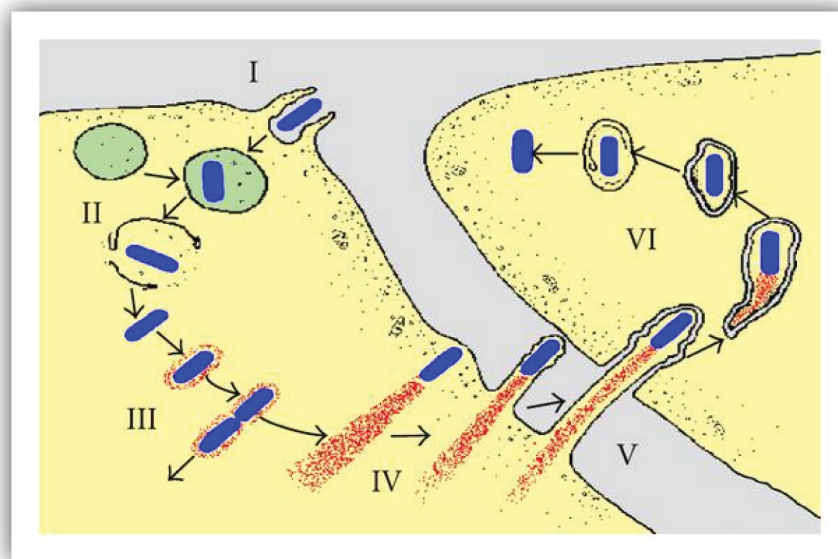


**Figure 1:** *L. monocytogenes* intracellular infection cycle represented in a cartoon. (I) Cell entry mediated by the cell surface proteins InlA or InlB, (II) escape from the phagolysosome induced by the pore-forming virulence factor LLO and PlcA, (III) actin recruitment and replication, (IV) asymmetrical ActA localization followed by actin-polymerization leads to intracellular movement, (V) Formation of listeriapods and subsequent spreading into neighbouring cells, (VI) Lysis of the two-membrane vacuole is mediated by LLO and PlcB. [17]. Adapted from Tilney and Portnoy [15].

cytoskeleton elements. Later it was revealed that similar cytoskeleton elements known from eukaryotic cells are also present in bacteria. The key player in bacterial cell division localizing first to the division site is the conserved tubulin-like protein FtsZ. Polymerization of FtsZ leads to the formation of the so called Z ring which acts as a scaffold by attracting other cell division proteins to the division plane to form the divisome. The Z-ring then executes constriction of the cell envelope and facilitates cytokinesis [20, 21]. The position of the formation of the Z-ring is crucial in generating two daughter cells of equal size. Two regulatory systems (Min and nucleoid occlusion system (NO)) are known to be responsible for proper positioning of the Z-ring [21]. The Min system consists of three components (MinC, MinD and MinE) which inhibits the FtsZ polymerization throughout the cell except for midcell. This is achieved by the establishment of gradient of the negative regulator MinC, exhibiting a minimum concentration at midcell. MinC promotes disassembly of FtsZ, antagonizing cell division on other places else than in the middle of the cell. The gradient of MinC is abolished by MinD and MinE. MinD is an ATPase and binds to the cell membrane in an ATP-dependent manner, and it recruits MinC. MinE displaces MinC and stimulates MinD ATPase, causing the release of the Min proteins from the membrane. Subsequently, MinD undergoes nucleotide exchange to generate MinD-ATP which then binds together with MinC at the other pole [22]. As a result of this periodic migration of the Min system components, the assembly of the Z ring is constrained to the middle of the cell.

### 2.3.1 Bacterial chromosome segregation

The faithful duplication and transmission of genetic information to daughter cells is a fundamental step and must therefore be tightly regulated. Eukaryotes utilize a conserved mitotic apparatus in which various proteins act at the centromeres to direct chromosome segregation [23, 19, 24]. Although bacteria miss the classical eukaryotic mitotic apparatus, chromosome segregation is undeniably an active process, tightly connected to other cellular events such as DNA replication and compaction. In prokaryotes, the mechanism of chromosome partition is less well understood than in eukaryotic cells.

Up to now there are three major models describing the chromosome segregation in bacteria.

By far the most influential hypothesis about bacterial segregation was the *replicon model*, suggesting that the chromosomes are attached to the membrane. Hence, as a results of bacterial growth, the bacterial chromosome segregation could be achieved passively as a by-product of cell elongation. The second model opposes the replicon model and is based on the fact that the speed of movement of the chromosome segregation is too fast to be accounted for cell growth. It rather proposes a *non-dedicated model* where the force produced by the DNA polymerase or RNA polymerase would help to separate the daughter chromosomes [25]. Intriguingly, it was also suggested that DNA segregation may be also a self-organizing process, driven by separation of transertion domains [26].

The most recent model proposes a *mitotic-like apparatus* conducting the chromosome segregation. A DNA partitioning (Par) system related to the one found in plasmids segregates chromosomal origin regions on DNA replication [27]. The system consists of two trans-acting factors (ParA and ParB), and conserved *parS* sites which are located in close proximity to the origin of replication (*ori*). ParA is an ATPase and able to form dynamically unstable actin-like filaments. ParB is a DNA-binding protein that interacts with ParA and binds to *parS* sites. Upon duplication of chromosomes the ParB proteins bind to *parS* sites forming complexes which then act as initiation of ParA filament formation. Continued insertion of ParA-ATP onto the filament ends physically pushes the chromosomes copies apart. Nucleotide hydrolysis within the polymers then leads to destabilization of the filament [28]. It is important to point out bacteria seem to live surprisingly happy in the absence of the ParABS system, implying that there may be other mechanisms at work.

In addition to the par system, several other proteins are known to be involved in active chromosome partitioning. The actin homologues MreB and Mbl (in *B. subtilis*), responsible mainly for cell shape regulation, are also involved in chromosomes segregation, as their depletion leads to a defect in chromosome partitioning [29]. A further important player is the highly conserved "structural maintenance of chromosomes" (SMC) condensation complex which has been shown to be recruited to the *oriC* by parB [30]. Lack of the SMC complex results in a more severe chromosome segregation defect than a parB or parA null mutant. In *B. subtilis*, the



SMC complex is required for chromosome compaction and faithful DNA copy segregation. The exact mechanism still remains elusive, but it has been suggested that the SMC present at the origin would act as "organization center" interacting with multiple regions of the chromosomes that are hundreds of kilobases away [30].

## 2.4 Bacterial cell wall

Bacteria are not only surrounded by a lipid membrane but are also enveloped by a cell wall that confers stability, rigidity and defines cell shape. The integrity plays a critical role for cell viability. The cell wall is a complex and multilayered structure, which falls into one of two major groups: Gram-negative bacteria contain a thin peptidoglycan layer located between the inner and outer membrane decorated with lipopolysaccharide. In contrast, Gram-positive bacteria are surrounded only by one lipid membrane, but feature a thick cell wall ranging from 15 to 80 nm [31, 32]. The peptidoglycan layer consist of alternating of  $\beta$ -1,4-linked *N*-acetylglucosamine (GlcNAc) and *N*-acetylmuramic acid (MurNAc) strands, which are cross-linked by peptide side chains [31]. In *Listeria* a 5-residue stem peptide is attached to MurNAc residue consisting of "L-Ala- $\gamma$ -D-glutamic acid-*meso*-A<sub>2</sub>pm-D-Ala" [33]. The cross-linking occurs via the  $\omega$ -amino group of the *meso*-diaminopimelic acid (*m*-DAP) at position 3 and a carboxyl group of the D-Ala at position 4 of a neighbouring stem peptide [34].

The murein is also decorated by many proteins which are anchored to the peptidoglycan. LPXTG constitutes the biggest family and represents surface proteins that are covalently attached to the peptidoglycan [35].

The peptidoglycan biosynthesis occurs in two different compartments. The first step proceeds within the bacterial cytoplasm and includes the assembly of the disaccharide-peptide monomer. It requires six reactions mediated by MurA to MurF which then leads to the formation of the UDP-MurNAc-pentapeptide precursor from UDP-GlcNAc. In order to facilitate the transport of the hydrophilic precursors, the integral membrane protein MraY facilitates transfer of the MurNAc-pentapeptide to the undecaprenyl phosphate carrier (C55-P), located on the cytoplasmic side of the membrane, leading to generation of the so-called lipid I. The final step before translocation

across the membrane involves addition of GlcNAc to lipid I, executed by the transferase MurG, resulting in lipid II. The complete disaccharide penta peptide unit is then transferred through the membrane by a not fully elucidated mechanism. The second part of the peptidoglycan pathway includes the polymerization of the units into nascent strands and attaching them to existing cell wall structure. A glycosyltransferase catalyses the formation of the glycan chains, whereas a transpeptidase is responsible for cross-linking of the peptide cross-bridges.  $\beta$ -lactam antibiotics (such as penicillins and cephalosporins) target the transpeptidases and inhibit the cross-linking, causing bacterial cell lysis [36, 37, 31].

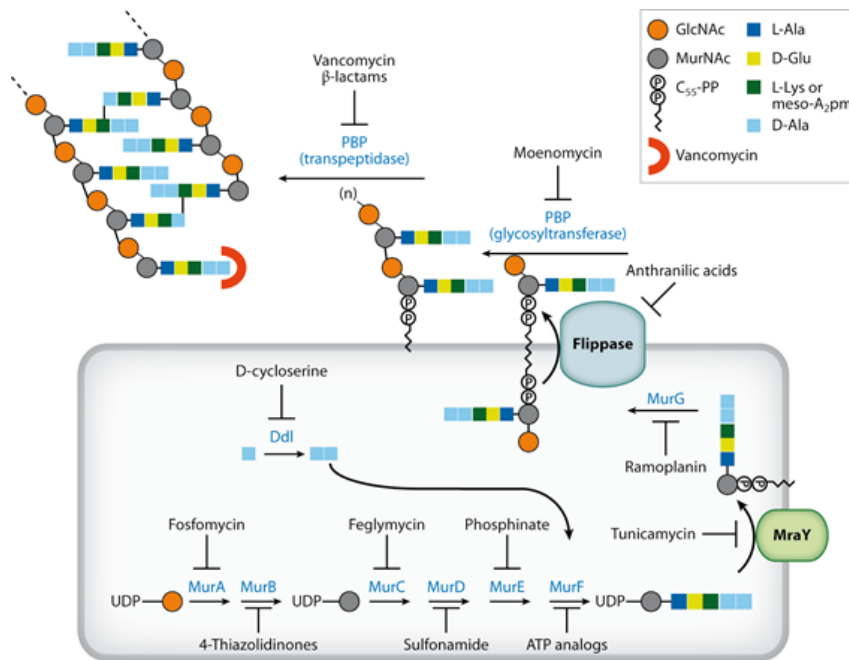


**Figure 2:** Overview of the peptidoglycan-biosynthesis pathway. The assembly of the peptidoglycan is a complex process involving approx. 20 enzymes. The biosynthesis occurs both in the cytoplasm as well as at the inner and outer side of the membrane [36].

## 2.5 Bacterial membrane

The cellular membrane constitutes a crucial structure for the existence of life by separating the cytoplasm from the outside. It enables a selective permeability for the import and export of aqueous-soluble compounds. The cellular membrane mainly consists of lipids intersected by

proteins. Bacterial membranes are composed of three principle phospholipids such as the zwitterionic phosphatidylethanolamine (PE), the anionic phosphatidylglycerol (PG), and cardiolipin (CL). The composition of the membrane of Gram-negative and Gram-positive bacteria varies significantly in the ratio of these components. Furthermore, the lipid constitution highly depends on the growth phase. Cardiolipin constitutes almost 50% of the cellular membrane of *L. monocytogenes*, followed by PG with about 20%, and phosphoamino-lipids (20%). The rest of the bilayer is composed of different other pospholipids [38].

The phospholipid production is preceded by the type II fatty acid synthesis (FAS II) which consists of the following reactions. The first steps include the conversion of acetyl-CoA to malonyl-CoA by acetyl-CoA carboxylase (ACC). This intermediate serves as signalling molecule by regulating FapR activity, therewith also controlling the entire FAS II cyle [39]. Subsequently, the malonyl transacylase FabD transfers the malonyl group to ACP forming malonyl-ACP, the decisive factor for the initiation and elongation cycle. The following reactions include the enzymes FabF/G/Z and FabI, finally resulting in the production of acyl-ACP. Each consecutive cycle produces addition of two methylene groups. The first step in the phospholipid synthesis is initiated by the peripheral membrane proteins PlsX which transfers the acyl group from the long chain-acyl-ACP to the inorganic phosphate ( $\text{PO}_4$ ). Next, the integral plasma-membrane protein PlsY acylates the 1-position of glycerol-3-P producing lysophosphatidic acid (LPA), followed by acylation of 2-position of LPA catalyzed PlsC. The resulting component posphatidic acid (PA) represents the key precursor in the formation of membrane phospholipids. A wide range of polar head groups can now be attached to the basic PA core structure giving rise to PE, PG or CL. [40]. The synthases PssA, PgsA and ClsA, catalyzing the committed step in PE, PG and CL synthesis, predominantly localize to the septal membranes [41]. It is assumed that the synthases are recruited and guided by the divisome in order to synthesize phospholipid membranes in concert with the peptidoglycan synthesis [42].

In the last decade, it has become apparent that lipids are not homogeneously distributed within the plasma membrane, but show lateral inhomogeneities in composition [43]. These inhomogeneities are called membrane microdomains or lipid rafts, which are characterized by

a more ordered and tightly packed structure than the surrounding bilayer [43]. These domains play an important role in signal transduction and establishment of distinct protein localisation patterns within the cell. For instance, cellular asymmetry is governed by microdomains which is crucial in many cellular processes of various organisms [44].

For a long time it has been surmised that lipid rafts only exist in eukaryotic cells. However, over the last years, microdomains have also been observed in bacterial membranes, attributing an essential function in recruiting specifically cell division proteins within the bacterial cell [44]. For instance, cardiolipin domains form at the cell poles and division sites, thereby selectively recruiting DnaA (initiation of DNA replication at *oriC*) and MinD [45]. Hence, membrane composition constitutes an essential part of the tightly regulated cell division mechanism.

In order to exert all functions, the cytoplasmic membrane needs to be maintained at the optimal membrane state which is mainly defined by the fluidity of the membrane [46]. The fluidity provides information on the viscosity and is regulated by the confirmation of the lipid bilayer. In bacteria, two different conformations are possible. A rigid "gel-phase" (ordered phase) and more "liquid-crystalline phase" (disordered phase) which are determined by the fatty acids moiety of the phospholipids. Unsaturated, branched and short acyl chains enlarge the space between the lipids and therefore increase their fluidity, whereas long and saturated fatty acids lead to a more compact membrane structure [47]. The length of the fatty acids chains is also decisive. Bacteria contain fatty acids ranging from C<sub>12</sub> to C<sub>24</sub>, mostly 14 and 20 carbons [48, 49]. Longer chains are able to penetrate deeper into the bilayer thereby increasing the interactions between the hydrophobic chains which results in a more rigid structure [50, 51]. On the contrary, shorter fatty acids moieties intersect to a lesser extent, leading to less restricted inter-chain forces. As a consequence, phospholipids comprised of shorter acyl chains contribute to membrane disruption and a more "fluid" character of these barrier structures.

Usually, an intact bacterial membrane requires a largely fluid bilayer [52]. Given these physical properties, it becomes obvious that bacterial membrane fluidity is dependent on environmental factors (i.e. temperature, pH, nutrients and chemicals). Shifting organisms from high to low temperatures leads to the incorporation of unsaturated fatty acids as they exhibit a much lower

transition temperature in comparison to saturated ones. As a result, bacteria are able to regulate its membrane fluidity, to ensure cell viability [53].

As elucidated above, microdomains play an important role in various cellular functions. Hence, there has been much interest in the detection of these rafts in membranes. Microdomains are characterized by a high degree of liquid ordered phase whereas the surrounding membranes exhibit a liquid disordered phase [54]. Detection occurs by taking advantage of these physical differences. Specific solvent-polarity dependent dyes such as Laurdan can be excited to increase its dipole moment, thereby causing a reorientation of the surrounding water molecule dipoles. This induced reorientation of the proximate molecules requires energy resulting in a red shift of the Laurdan emission spectrum. In more loosely packed membranes (disordered phase), water molecules are able to penetrate deeper and produce a larger dipole moment. This results in a red shift in emission, which can be detected spectroscopically or microscopically [55]. The degree of microdomains, and thereby membrane fluidity, is represented by the generalised polarization GP (value) which is defined by the ratio of the following emission intensities:

$$\frac{I_{435}-I_{495}}{I_{435}+I_{495}} = GP$$

The GP value ranges from -1 to +1, where a higher value indicates a more rigid, and a lower value a more fluid membrane structure [56]

## 2.6 Cell wall-deficient bacteria

### 2.6.1 Definition of L-forms

L-forms are cell wall-deficient variants of bacteria which are able to grow and divide as spheroplasts or protoplasts. They can be differentiated by the degree of absence of cell wall, as well as their ability to revert to the parental form [57]. Spheroplasts-type L-forms still exhibit remnants of the cell wall whereas protoplast-type L-forms are completely devoid of any cell wall components. Both types can exist in a stable and an unstable form. Unstable L-forms are able to revert to normal walled parental bacteria, whereas stable spheroplasts and protoplasts-type L-forms are unable to re-acquire a cell wall. It is important to point out that some parasitic

species of bacteria such as mycoplasma also lack cell wall but are not considered as L-forms, as they are not derived from bacterial cells normally surrounded by a peptidoglycan layer. Most likely, they have lost the cell wall retrospectively as a consequence of host cell adaptation.

### 2.6.2 History

The term L-forms was introduced in 1935 by Emmy Klienerberger, when she first observed cell-wall deficient bacteria in cultures of *Streptobacillus moniliformis*. Klienerberger described them as spherical, osmosensitive cells growing on plates of hypertonic complex medium containing serum [58] and named them L-forms in honor of the Lister institute in London where she was employed. Originally, she proposed L-forms as morphological variants of *S. moniliformis*; however, at that time morphology was considered invariable and Klienerberger finally discarded her idea. A few years later in 1939, Harvard Medical School researcher Louis Dienes observed that L-forms could adapt a state again which is indistinguishable from parental *S. moniliformis*. Hence, he suggested that L-forms are derived from normal bacterial cells, however, may keep the ability to revert to the parental state [59]. In the following years, L-forms were isolated from other bacteria species but in contrast to the work of Dienes, these L-forms were found to be stable and thus unable to return to their original morphology [60]. The hypothesis of L-forms not being surrounded by a structured peptidoglycan layer has been supported by electron microscopy as well as by chemical analysis [60]. In 1942, L-forms were shown to be insensitive to penicillin which provided a simple tool for isolating cell wall-deficient bacteria [61]. Later on, it turned out that treatment with penicillin does not primarily select L-forms but rather induces L-form transition and growth [62, 63]. During the following decades (1950-1980), most research on L-forms focused on the potential role in human infections. Several studies disclosed the persistence of L-forms in human cells [64, 65, 66], leading to the hypothesis that unstable L-forms of certain bacterial pathogens are able to survive in human tissues and at some point may revert to their parental form causing infections of the host. Many results of studies about L-forms could not be confirmed by experimental approaches [57]. Currently, we are experiencing a revival of research on L-forms. Over the past five years several papers on L-forms have been published [57, 67, 68, 69, 70, 39, 71, 72,

73] also investigating molecular aspects of L-form proliferation using modern tools. Besides a better understanding of L-forms, the study of cell-wall deficient cells also provides an improved understanding of bacterial cell division and maintenance.

### 2.6.3 Bacterial L-form cells

The peptidoglycan (PG) is a rigid network that defines the structure of most bacterial lineages. It consists of chains of two alternating sugars (N-acetylglucosamine and N-acetylmuramic acid) which are cross-linked by peptides. The cell wall network confers stability as well as rigidity and defines the bacterial cell shape. Its integrity is therefore of great importance. In consideration of the crucial role of the peptidoglycan layer, it is intriguing that some bacteria are capable of switching to a wall-deficient L-form state [57]. More surprisingly, bacteria lacking a cell wall are not only able to survive but are capable of reproduction and multiplication. In some bacteria the loss of cell wall leads to acquirement of a complete new mode of replication (see 2.6.5, 2.6.6, 2.6.7, Manuscript 1 and 2).

Initially, L-forms had been described as antibiotic-resistant or persistent bacteria associated with various infectious diseases [74]. However, their role as causative agents remained unclear (see 2.7). L-forms can be derived from various bacteria, including Gram-positive and Gram-negatives. In the laboratory, induction of stable L-forms is usually performed by selective cultivation in an osmoprotective medium. The first step includes growth of parental cells in media supplemented with inhibiting concentrations of cell wall synthesis interfering substances such as penicillin. Single colonies are then transferred on to fresh medium still containing cell wall inhibitors. Subsequently, stabilization occurs by gradually reducing the concentration or completely omitting the inhibitors in the media. Although the generation of L-forms seems straightforward, the entire procedure is time consuming and not very well controllable. In order to improve and increase the success rate, detailed knowledge on the molecular level of this process is required. During the last few years, L-form research has been mainly focusing on the bacteria *L. monocytogenes*, *B. subtilis* and *E. coli*. Despite the fact that L-forms derived from these bacteria exhibit several similarities, they also demonstrate the many differences regarding modes of replication. The

three types of L-forms will be reviewed in the following sections.

#### 2.6.4 *Listeria monocytogenes* L-forms

Between 1950 and 1980, significant research was conducted focusing on the potential role of L-forms in human cells [64, 65, 66]. It was during that time when *L. monocytogenes* L-forms were first observed. Various descriptions of their morphology and induction protocols were reported [75, 76, 77, 78]. However, the techniques available back then did not allow in-dept knowledge on the division mechanism and the molecular cell biology of cell wall-deficient *L. monocytogenes*. In 2009, Dell'Era *et al.* (2009) presented insights on the cell biology and the new mode of reproduction of *L. monocytogenes* L-forms ScottA [67]. They described an induction method by growing *Listeria* L-forms cells on "*Listeria* L-form agar medium" (LLM) containing penicillin G at 32°C. After two to eight weeks, characteristic "fried-egg" like appearance of transient L-forms become visible. Stable L-forms are then obtained by repeated passages in LLM soft-agar, followed by step-wise decrease and final removal of penicillin G. Due to the lack of the rigid peptidoglycan layer, L-forms distinguish extremely from their parental form (Figure 3). Growth kinetics experiments showed that *L. monocytogenes* L-forms feature a much slower growth rate compared to parental *Listeria* cells. Whereas the latter reach late log phase/early stationary phase after 16-20 h of incubation under standard culture conditions, *L. monocytogenes* ScottA L-forms need 6-8 days after passage from inoculation into fresh LLM soft-agar until this growth phase.

Stable *L. monocytogenes* derived L-forms are non-motile and devoid of the rigid peptidoglycan cell wall. This is in line with the finding that Internalin A is absent from the L-form surface, whereas Internalin B is present [67]. The absence of Internalin A is due to the lack of peptidoglycan to which the protein is attached to via SrtA [35]. Internalin B is indirectly associated with the cytoplasmic membrane, and still present on the L-form surface. Although L-forms do not possess a murein sacculus they still produce peptidoglycan precursors. The lipid II molecules has been found on the surface in a homogeneous pattern. Whether a production of peptidoglycan precursors is a prerequisite for *L. monocytogenes* L-form growth and division remains currently



unknown.

L-forms can grow in the presence of cell wall-active drugs. It is therefore not surprising that *L. monocytogenes* L-forms exhibit a different transcription profile compared to the parental form. The majorities of genes affected are involved in metabolism and stress response. Several cell shaping and cell wall synthesis genes are down-regulated, whereas most up-regulated genes are involved in stress responses or fulfill regulatory functions. The largest group of up-regulated genes constitutes genes of unknown function though [67].

### 2.6.5 *Listeria* L-forms reproduction

*L. monocytogenes* L-forms do not divide by simple binary fission but use an alternative mode of reproduction. The detailed mechanism of multiplication of *Listeria* L-forms had not been elucidated yet. *L. monocytogenes* L-forms derived from strain ScottA form characteristic internal vesicles which are considered as reproduction units [67, 73]. The vesicles seem to originate from lipid accumulations residing at the inner side of the mother cell membrane. It is possible that overproduction of lipids drives the membrane to fold inwards and to pinch off, giving rise to the intracellular vesicles. It may be that at the time of the creation, vesicles incorporate a small amount of cytoplasmic material containing all the essential biomolecules to continue cellular processes. At some point, the mother cell collapses and releases the internal vesicles into the extracellular space, which may then start their own life (Figure 4). Microscopic analysis disclosed that only a small fraction of the vesicles become metabolically active. The viability of intracellular progeny was monitored by *L. monocytogenes* L-forms expressing constitutively GFP. Most of the internal vesicles are devoid of fluorescent protein, and only a small minority contain a GFP signal. Additional viability staining using a colourless tetrazolium dye confirmed this result. This dye is reduced to red a formazan compound in compartments where free electrons are present, indicating respiratory activity and an oxidative metabolism. Whereas the vast majority of internal vesicles did not become fluorescent, some showed clear signs of metabolic activities. The results are in agreement with the hypothesis of internal vesicles becoming only active upon release from the mother cell. As long as the mother cell retains its membrane potential, there is no possibility

for the progeny to establish their own. The hypothesis was supported by time-lapse microscopy where freshly released cells, devoid of a GFP become fluorescent within 2 min of the burst of the mother cell [73]. As the maturation of GFP requires longer than just a few minutes, it is assumed that pre-synthesised molecules are already present in the vesicles. The release most likely involves a change in the environment, allowing the GFP molecule to become fluorescent. As the last step during GFP maturation requires oxygen, deprivation of oxygen within the vesicles would deliver a reasonable explanation. Another possibility might be a lower pH that within the vesicles, preventing the GFP molecules from proper folding.

Unlike parental cells where cell division is tightly orchestrated by several proteins, L-forms appear to be rather disorganized. The presence of polyploidy in L-forms reflects their disorder. The average number of chromosomes per cell was determined for *L. monocytogenes* Scott A L-forms which contain in average about 18 chromosomes [73]. Due to the loss of synchronization of cell division, DNA replication and segregation, *L. monocytogenes* L-forms likely distribute their genetic material in a passive manner. Multi-nucleation might account for the absence of a tightly regulated system and enable faithful inheritance of a complete chromosome.

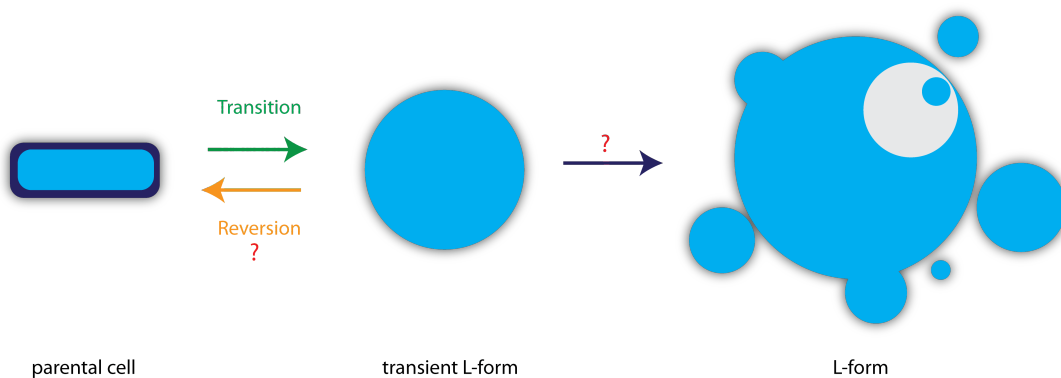


**Figure 3:** Generation of *Listeria* L-forms occurs by exposure to antibiotics targeting the cell wall synthesis. This leads to an escape out of the peptidoglycan layer and conversion into a transient L-forms. Some of them may then acquire the capabilities to turn into replicating and stable L-forms (adapted from [67, 73])

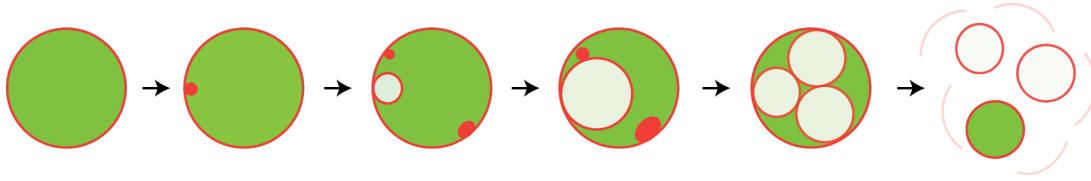


**Figure 4:** Hypothetical creation of internal vesicles in *Listeria* L-forms. Lipid accumulations of different sizes (red dots) residing at the periphery of the mother cell originate from an overproduction of lipids. It is assumed that they represent the phospholipid pool and nucleation site for the generation of new vesicles (adapted from [73])

### 2.6.6 *Bacillus subtilis* L-forms

L-forms derived from *B. subtilis* can be generated by the two step method described by Leaver *et al.* [69] and Mercier *et al.* [39]. They reported the apparent requirement of two genetic changes for successful *B. subtilis* L-form reproduction. The first genetic change was introduced into the *ispA* gene encoding a polyisoprenoid synthase [69] that catalyzes the formation of essential lipids involved in peptidoglycan and teichoic acid synthesis and assembly. Genome sequence comparison of freshly derived L-forms with the genome of its parental cells revealed a single amino acid substitution in the *ispA* gene. The modification predisposes *B. subtilis* to grow and multiply without a wall with about a 1000-fold increase in the frequency of L-form formation compared to the wildtype [69]. The second and more significant mutation induces an increase in membrane production. Simple excess of membrane synthesis seems to be sufficient to drive the new mode of cell division. L-forms can acquire an over-synthesis of membrane fatty acids by two mutations. The first one directly leads to an up regulation of the FAS II system via *AccDA* overproduction. *AccDA* encodes the catalytic subunit of acetyl-coenzyme A-carboxylase. A single point mutation in the upstream sequence of *accD* is sufficient to induce a massive amount of fatty acid [39]. Overproduction of lipids can also be achieved by indirect inhibition of the peptidoglycan precursor pathway by inhibiting for instance the *murE* operon. The exact mechanism why disruption of the peptidoglycan synthesis results in a overproduction of fatty acids in *B. subtilis* is still elusive.

Long-term time-lapse imaging revealed a novel propagation mechanism used by *B. subtilis* L-forms (Figure 5). Initially, the L-form requires a specific escape step to bulge out of the

rod-shaped cell wall sacculus, which includes the formation of a breach at the middle of the lateral side of the normally intact cell wall. Exposure to antibiotics targeting the cell wall or lytic enzymes enables such an escape as the cell wall integrity is reduced at the position where the peptidoglycan synthesis takes place. Once the protoplasts have successfully slipped out of the cell wall, the cells increase in size followed by a period when a series of shape perturbations occur, which is characterized by the formation of transient blunt protrusions. These show a dynamic behavior appearing and retracting, finally re-emerging at different points on the cell surface. In the end, the cells form a pseudopodium-like protrusion which elongates for a period of about 70 min and then resolves into five more-or-less round bodies. These particles represent viable progeny which are metabolically active and able to undertake further reproduction [69, 71] (Figure 5).

Recently, further analysis has been published providing insights on the molecular mechanisms of *B. subtilis* L-form cell division [39]. Genes usually involved in bacterial cell division were assessed for their necessity in *B. subtilis* L-forms. The results revealed no evidence for involvement of cytoskeleton proteins in *B. subtilis* L-form reproduction. Most prominently, the cell division key player FtsZ, responsible for recruiting other important proteins and generating a constriction force, seems not required for proliferation. Instead, successful reproduction depends on the precise biophysical properties of the cellular membrane. [69, 39]. Membrane fluidity seems to be a decisive factor which has to be maintained in order to ensure faithful proliferation in *B. subtilis* L-forms. This is in accordance with the finding that mutants deficient in the synthetic pathway for branched-fatty acids (BFACs) are not able to undergo scission and separation of progeny cells [72].

The intriguing question as to whether L-forms are able to revert to its parental form had been unanswered for a long time. Very recently though, Kawai *et al.* have addressed this question. They demonstrated that *B. subtilis* L-forms are indeed able to re-acquire a cell wall. *B. subtilis* L-forms were generated as described above and then transformed with a set of genes responsible for a successful PG synthesis. Parental *B. subtilis* cells appeared on plates without penicillin G, confirming the capability of reversion. Interestingly, *B. subtilis* L-forms do not require an existing

cell wall template to regenerate its peptidoglycan layer and restore a rod-shape morphology.

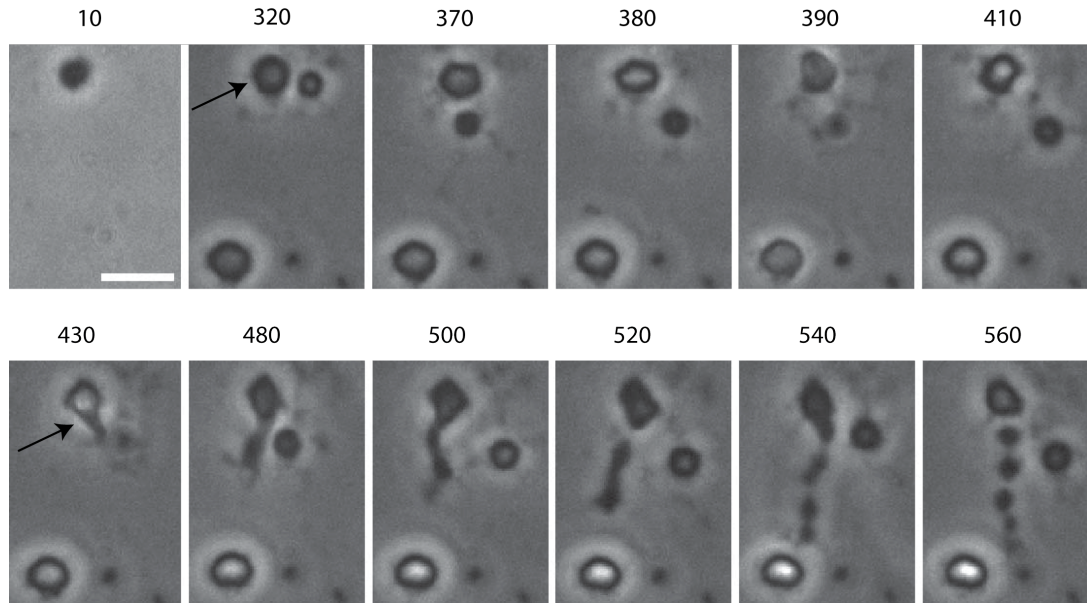


**Figure 5:** Novel mechanism of proliferation of *B. subtilis* derived L-forms. At 430 min the marked cell begins to form a protrusion which elongates for a period of time. In the end, the protrusion resolves giving rise to five round progeny cells which are able to undertake further reproductions [69].

### 2.6.7 *Escherichia coli* L-forms

*E. coli* is a Gram-negative bacterium surrounded by two lipid membranes, separated by thin layer of peptidoglycan. Due to the inner and outer membrane, *E. coli* L-forms show a different behaviour as observed for Gram-positive L-forms. The most prominent difference is the involvement of FtsZ in *E. coli* L-form division, which ranges from binary fission-like division, asymmetrical fission to the formation of small buds [79]. It has been suggested that unstable L-forms of *E. coli* retain low amounts of cell wall material [80]. In fact, unstable L-forms depend on the cell wall precursor D-glutamate and diaminopimelic acid (2<sup>nd</sup> and 3<sup>rd</sup> amino acid of the peptide stem) as well as activity of MurA, the enzyme that catalyzes the first reaction in the synthesis of the muramic acid side chain. Lack of any of these cell wall specific components prevents L-form propagation. Furthermore, direct measurement revealed that these cell wall-deficient cells still contain about 7% peptidoglycan of the amount in parental *E. coli* cells. This

amount of peptidoglycan is by far insufficient to form a complete cell wall. Thus, unstable *E. coli* L-forms require the ability to synthesize small amounts of peptidoglycan and this residual synthesis is essential for their propagation [80].

Recent findings shed new insights into the molecular mechanisms underlying unstable *E. coli* L-form formation and survival [68]. Microarray analysis revealed significant changes in the transcription profile of *E. coli* parental cells and L-forms which included the overexpression of many genes involved in stress responses and of unknown function. Furthermore, screening of *E. coli* deletion mutant library for mutants defective in forming L-forms identified various genes involved in cell envelope stress, DNA repair, iron homeostasis pathway, outer membrane biogenesis, and drug efflux /ABC transporters. Complementation of the identified mutations confirmed their role in L-form formation.

A more detailed analysis on the genetic level of an *E. coli* mutant, having lost the ability to form a cell wall, disclosed two mutations in the *dcw* region [79]. This region harbors essential genes for cell division and murein synthesis which are conserved among many eubacteria [81, 82]. One mutation affects the *ftsQ* gene, leading to a truncated protein. FtsQ is a membrane protein and localizes at the Z-ring where it recruits other proteins for division. The protein domain responsible for this recruitment is missing in this truncated FtsQ protein. In contrast to *E. coli* L-forms, this mutation is lethal in parental *E. coli*, most likely because of the impaired localization of divisome proteins. Analysis of the primary sequence of other *fts* genes such as *ftsZ*, the main component of the Z ring, in the L-form genome revealed no alterations though. Another mutation causes a frame shift resulting in a premature stop in the gene *mraY*. It encodes for an integral membrane enzyme which catalyzes the binding of building blocks for cell wall synthesis. If this process cannot occur, the synthesis of the murein sacculus and other extracellular polysaccharides (LPS) can also not take place, leading to an inhibition of cell wall synthesis. These results show that *E. coli* L-forms do not require the function of FtsQ and MraY which are required for all bacteria containing murein-based cell walls [79]. However, it is not clear whether these mutations are responsible for L-form transition or may have arose during propagation over years under laboratory conditions.

Very recently, a new study has been published providing further details on the molecular mechanism of *E. coli* L-form reproduction. Billings *et al.* [83] have been able to monitor the conversion to L-form and the reversion to parental cell by time-lapse microscopy. The entire process was conducted in a micro-fluid system which allowed to remove the inducing agent cefsulodin while recording the entire process. Exposure to the antibiotic induced the formation of bleb-like bulges due to defects in the peptidoglycan layer. The newly formed cells would then grow and eventually detach from the rest of the cell. Within about an hour after removal of cefsulodin, the spherical L-forms started to re-acquire rod-shaped morphologies. Cylindrical protrusions in combination with cytokinesis finally resulted in parental cells within a few generations [83]. Experiments using the MreB inhibitor A22 revealed the necessity of functional MreB filaments to regenerate the cell wall. Application of quantitative imaging analysis demonstrated a co-localization of MreB and insertion of new peptidoglycan material which occurs preferentially at negatively curved region of the cell. The authors ascribe MreB a decisive role in directing the establishment of a new cell wall by being able to sense the membrane curvature [83].

## 2.7 Pathogenicity of *Listeria* L-forms

The question of whether cell wall-deficient bacteria (L-forms) may still be pathogenic has been under debate for a long time. There are several publications describing a possible role of L-forms in various diseases [84, 85, 86]. Due to the absence of the cell wall, L-forms have been thought to be able to evade the immune system and end up as persisters, possibly responsible for chronic diseases [74, 87]. L-forms have been assumed to play a role in Crohn's disease, endocarditis, rheumatic fever, meningitis, urinary tract infectious and several other diseases [88, 89, 85, 90]. However, studies which would provide detailed information on the role of pathogenicity of L-forms are lacking. Re-isolation of L-forms out of tissues presented a severe problem. Moreover, the detection method to identify cell wall-deficient bacteria leave little to be desired. Due to these reasons, bacterial L-forms have not been regarded as clinically significant by the majority of researchers.

In a very recent publication by Schnell *et al.* [91], pathogenicity of stable *L. monocytogenes* L-

forms was investigated. The expression of virulence genes required for the intracellular life cycle of *L. monocytogenes*, were found to be significantly down-regulated. These findings indicate that *L. monocytogenes* L-forms are unable to escape into the cytosol and to spread into neighboring cells. The intriguing question whether *L. monocytogenes* L-forms could possibly evade the immune system was addressed by measuring pro-inflammatory cytokines. The analysis revealed that cell-wall deficient *Listeria* could be still recognized by activated macrophages, and the lack of peptidoglycan does not lead to permanent attenuated recognition by the innate immune system. Interferon- $\beta$  is exclusively induced upon cytosolic entry of pathogenic *L. monocytogenes* [92, 93] and was therefore evaluated upon infection of macrophages with L-forms. Results indicated that *L. monocytogenes* L-form are being entrapped in the phagosome due to the absence of IFN- $\beta$  response in comparison to parental *L. monocytogenes*. In conclusion, stable *L. monocytogenes* L-forms can be regarded as non-pathogenic variants of their walled counterparts.

Future research should address the pathogenicity of transient L-forms, which retain the ability to revert to its parental form. Transient L-forms possibly occur in natural environments and under conditions where beta-lactam antibiotics are present. Yet, such experiments will require development of a reliable *in vivo* detection and differentiation method for transient L-forms.

## 2.8 L-forms may provide insights on the primordial life

It is surmised that the first hypothetical pre-structure of the first cell (protocell) may have formed about 4 billions years ago [94, 95, 96, 97, 98, 99, 100]. The structures hypothetically enabled spatial compartmentalization of chemicals, thereby allowing simple biochemical processes to occur. The first protocells did not feature all the properties to form viable entities and to undergo self-maintenance as well as self-reproduction but rather represented a temporary structure between a non-living matter and life. How the transition from a hypothetical pre-structure to the first living matter, and the subsequent evolution to sophisticated cells occurred remains elusive. In order to investigate possible prebiotic life, most approaches have used lipid vesicles as a model system [101, 102, 96, 98]. Vesicles composed of defined lipids enabled to specifically investigate properties under conditions that may have existed on early earth. The



high degree of vesicle dynamics depending on the lipid composition and chemical environment has provided interesting discoveries. Production of intra- and extra-vesicles, formation of protrusions or fission-like processes are interesting features observed in artificial vesicles. It is assumed that these dynamical shape variations, driven only by physiochemical forces, may represent a putative early mode of cellular development [98, 103, 104].

Bacterial L-forms have gained of increasing interest as they divide by a simple mechanism that involves shape perturbations, resembling the behaviour of artificial vesicles. Due to the morphological similarities of giant lipid vesicles and cell wall-deficient bacteria, L-forms have been regarded to possibly mimic behaviour of early form of life [70, 105] (see Figure 6). Over the past billions of years, contemporary cells have evolved sophisticated attributes. Acquisition of incremental complexity have lead to tightly regulated proliferation mechanisms. The fact that L-forms seem to reproduce by an unorganized and less coordinated mechanism supports the hypothesis that they may represent ancestral characteristics.

The reason why bacteria are still able to revert to such a primitive division mode may be ascribed to the evolution of the cell wall. Genes responsible for the synthesis of peptidoglycan are present throughout the bacterial kingdom. It is envisaged that the "last universal common ancestor" (LUCA) already possessed some kind of a cell wall [106]. On the contrary, the progenitor of this common ancestor may have been wall-less, and used an extrusion-resolution mode of proliferation as described in bacterial L-forms. Later on in evolution, bacteria acquired cell walls and developed a new highly organized mechanism to drive cell division. However, bacteria may have retained the old proliferation system for "emergency" use, in case of cell wall damage which can occur when cells are exposed to antibiotics or other cell-wall interferences.

Laboratory-derived lipid vesicles can be applied to pursue a bottom-up approach, and to probe the first living entity. Primitive, as well as more sophisticated cellular functions, can be assessed under very defined conditions. However, they are still abiotic and limited to a certain degree of complexity. Bacterial L-forms represent a living but simple system and therefore may provide valuable information on the evolution of early cells.

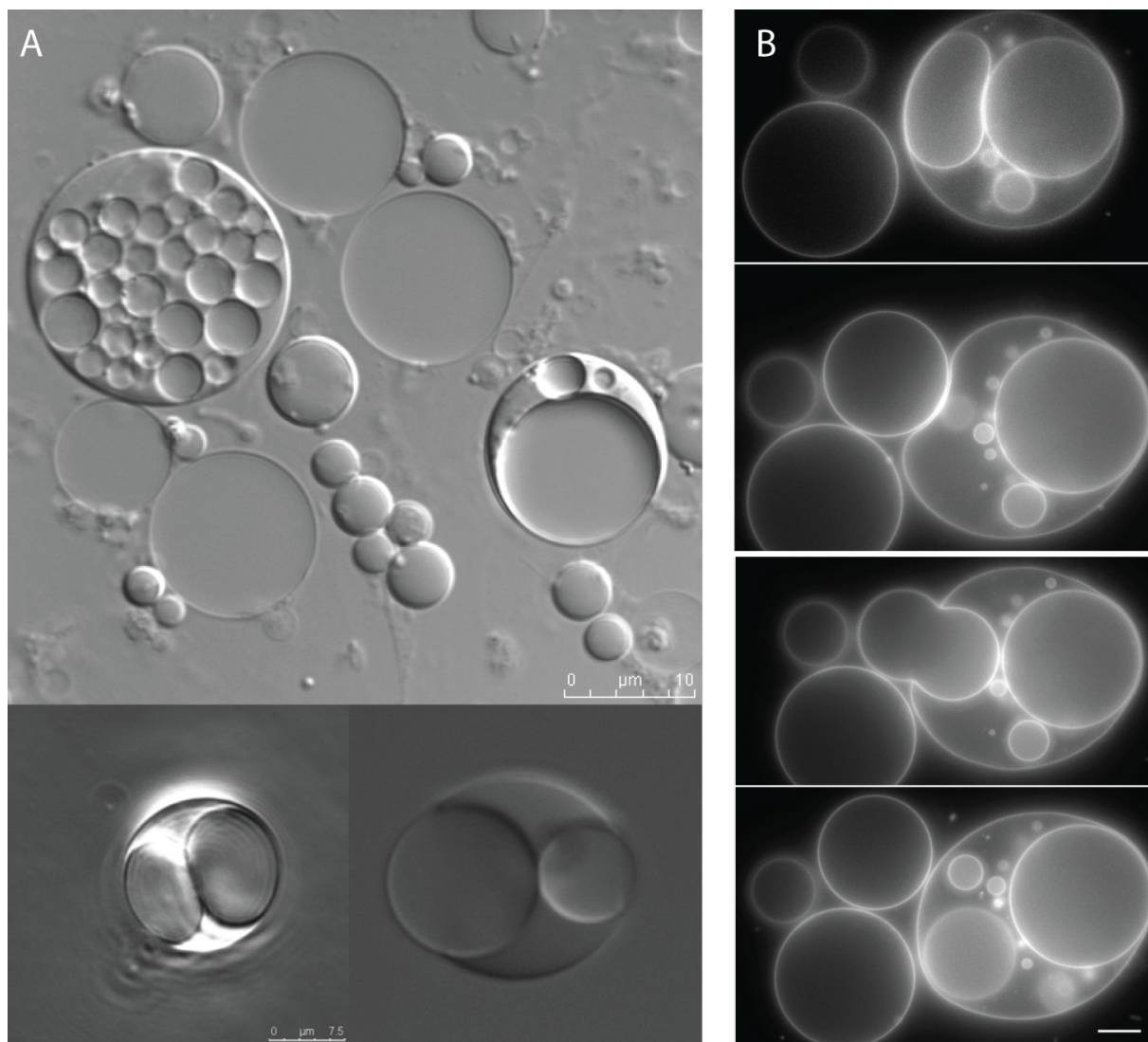


**Figure 6:** *Listeria* L-forms and GUVs share morphological similarities. They are both surrounded only by a lipid bilayer, and are able to form internal as well as external lipid vesicles. A: *L. monocytogenes* L-forms grown in LLM-soft-agar and imaged with DIC. B: GUV produced with the following lipids and ratio: POPC:SM:Ch:GM1 (45:30:25:8). The GUV were then loaded with a saturated galactose solution and then diluted with MilliQ water to establish an osmotic gradient. The vesicles were then stained with the dye Rho-DPPE and imaged in the fluorescent channel. Scale bar = 10 μm [107].



## Aim of the study

Bacterial L-forms have been known for a long time. However, detailed knowledge on the proliferation mode has been scarce. The aim of this study was to investigate a new mode of replication employed by stable *Listeria monocytogenes* L-forms. The first intention was to characterize the *Listeria* L-forms on the morphological level and to gain insights on the division mechanism. Various microscopy analyses revealed a multitude of shape deformations, including intracellular and extracellular vesiculation. The main goal of the thesis included the evaluation of the viability of the formed vesicles by newly developed methods. In a second step, the molecular mechanism of reproduction should be elucidated. Unlike binary fission, L-form proliferation does not represent a controlled process. Identification and analysis of the driving force for L-form proliferation constituted another task of this thesis.

# References Introduction

- [1] E.G.D. Murray. A disease of rabbits characterized by a large mononuclear leucocytosis, caused by a hitherto undescribed bacillus *Bacterium monocytogenes* (n. sp). *J. Pathol. Bacteriol* 29:407-39, 1926.
- [2] J. A. Vázquez-Boland, M. Kuhn, P. Berche, T. Chakraborty, G. Domínguez-Bernal, W. Goebel, B. González-Zorn, J. Wehland, and J. Kreft. *Listeria* pathogenesis and molecular virulence determinants. *Clin Microbiol Rev*, 14(3):584–640, 2001.
- [3] N. E. Freitag, G. C. Port, and M. D. Miner. *Listeria monocytogenes* - from saprophyte to intracellular pathogen. *Nat Rev Microbiol*, 7(9):623–628, 2009.
- [4] M. B. Cole, M. V. Jones, and C. Holyoak. The effect of pH, salt concentration and temperature on the survival and growth of *Listeria monocytogenes*. *J Appl Bacteriol*, 69(1):63–72, 1990.
- [5] J. Rocourt, J. M. Alonso, and H. P. Seeliger. [Comparative virulence of the 5 genomic groups of *Listeria monocytogenes* (sensu lato)]. *Ann Microbiol (Paris)*, 134A(3):359–364, 1983.
- [6] T. Ryser and E. H. Marth. *Listeria, listeriosis and food safety*. Marcel Dekker, Inc. New York, 1991.
- [7] M. Peel, W. Donachie, and A. Shaw. Temperature-dependent expression of flagella of *Listeria monocytogenes* studied by electron microscopy, SDS-PAGE and western blotting. *J Gen Microbiol*, 134(8):2171–2178, Aug 1988.
- [8] J.M. Farber and P.I. Peterkin. *Listeria monocytogenes*, a food-borne pathogen. *Microbiol Rev* 55(3): 476-511, 1991.
- [9] H. Hof and P. Hefner. Pathogenicity of *Listeria monocytogenes* in comparison to other *Listeria* species. *Infection*, 16 Suppl 2:S141–S144, 1988.
- [10] T. Mainou-Fowler, A. P. MacGowan, and R. Postlethwaite. Virulence of *Listeria* spp.: course of infection in resistant and susceptible mice. *J Med Microbiol*, 27(2):131–140, 1988.

- 
- [11] D. Jones. *Foodborne listeriosis*, volume 336. Lancet, 1990.
- [12] M. Schuppler. How the interaction of *Listeria monocytogenes* and *Acanthamoeba* spp. affects growth and distribution of the foodborne pathogen. *Appl Microbiol Biotechnol*, 98(7):2907–2916, Apr 2014.
- [13] M. Hamon, H. Bierne, and P. Cossart. *Listeria monocytogenes*: a multifaceted model. *Nat Rev Microbiol*, 4(6):423–434, 2006.
- [14] P. Schnupf and D. A. Portnoy. Listeriolysin O: a phagosome-specific lysin. *Microbes Infect*, 9(10):1176–1187, 2007.
- [15] L. G. Tilney and D. A. Portnoy. Actin filaments and the growth, movement, and spread of the intracellular bacterial parasite, *Listeria monocytogenes*. *J Cell Biol*, 109(4 Pt 1):1597–1608, 1989.
- [16] J. Pizarro-Cerdá and P. Cossart. Subversion of cellular functions by *Listeria monocytogenes*. *J Pathol*, 208(2):215–223, 2006.
- [17] M. Schuppler and M. J. Loessner. The Opportunistic Pathogen *Listeria monocytogenes*: Pathogenicity and Interaction with the Mucosal Immune System. 2010:704321–, 2010.
- [18] P. N. Rao and R. T. Johnson. Mammalian cell fusion: studies on the regulation of DNA synthesis and mitosis. *Nature*, 225(5228):159–164, 1970.
- [19] J. R. McIntosh, M. I. Molodtsov, and F. I. Ataullakhanov. Biophysics of mitosis. *Q Rev Biophys*, 45(2):147–207, May 2012.
- [20] David W. Adams and Jeff Errington. Bacterial cell division: assembly, maintenance and disassembly of the Z ring. *Nat Rev Microbiol*, 7(9):642–653, Sep 2009.
- [21] L. G. Monahan, A. F. Liew, A. L. Bottomley, and E. J. Harry. Division site positioning in bacteria: one size does not fit all. *Front Microbiol*, 5:19, 2014.
- [22] J. Lutkenhaus. Assembly dynamics of the bacterial MinCDE system and spatial regulation of the Z ring. *Annual review of biochemistry*, 76:539–562, 2007.
- [23] S. K. Ghosh, S. Hajra, A. Paek, and M. Jayaram. Mechanisms for chromosome and plasmid segregation. 75:211–41–, 2006.
- [24] H. C. Lim, I.V. Surovtsev, B.G Beltran, F. Huang, J. Bewersdorf, and C. Jacobs-Wagner. Evidence for a DNA-relay mechanism in ParABS-mediated chromosome segregation. *Elife*, 3:e02758, 2014.

- 
- [25] K. P. Lemon and A. D. Grossman. The extrusion-capture model for chromosome partitioning in bacteria. 15:2031–41–, 2001.
- [26] S. Jun and A. Wright. Entropy as the driver of chromosome segregation. 8:600–7–.
- [27] J. L. Ptacin, S. F. Lee, E. C. Garner, E. Toro, M. Eckart, L. R. Comolli, W. E. Moerner, and L. Shapiro. A spindle-like apparatus guides bacterial chromosome segregation. 12:791–8–, 2010.
- [28] J. Moller-Jensen, J. Borch, M. Dam, R. B. Jensen, P. Roepstorff, and K. Gerdes. Bacterial mitosis: ParM of plasmid R1 moves plasmid DNA by an actin-like insertional polymerization mechanism. *Mol Cell*, 12(6):1477–1487, Dec 2003.
- [29] N. Pavlendova, K. Muchova, and I. Barak. Chromosome segregation in *Bacillus subtilis*. 52:563–72–, 2007.
- [30] N. L. Sullivan, K. A. Marquis, and D. Z. Rudner. Recruitment of SMC by ParB-parS organizes the origin region and promotes efficient chromosome segregation. 137:697–707–, 2009.
- [31] W. Vollmer, D. Blanot, and M. A. de Pedro. Peptidoglycan structure and architecture. *FEMS Microbiol Rev*, 32(2):149–167, 2008.
- [32] Thomas J. Silhavy, Daniel Kahne, and Suzanne Walker. The bacterial cell envelope. *Cold Spring Harb Perspect Biol*, 2(5):a000414, 2010.
- [33] K. Kamisango, H. Fujii, H. Okumura, I. Saiki, Y. Araki, Y. Yamamura, and I. Azuma. Structural and immunochemical studies of teichoic acid of *Listeria monocytogenes*. *J Biochem*, 93(5):1401–1409, May 1983.
- [34] K. H. Schleifer and O. Kandler. Peptidoglycan types of bacterial cell walls and their taxonomic implications. *Bacteriol Rev*, 36(4):407–477, Dec 1972.
- [35] H. Bierne, S. Mazmanian, M. Trost, G. Pucciarelli, G. Liu, P. Dehoux, G. Jansch, F. Garcia-del Portillo, Olaf Schneewind, Pascale Cossart, and European *Listeria* Genome Consortium. Inactivation of the *srtA* gene in *Listeria monocytogenes* inhibits anchoring of surface proteins and affects virulence. *Molecular microbiology*, 43(4):869–881, February 2002.
- [36] A. L. Lovering, S. S. Safadi, and N. C. Strynadka. Structural perspective of peptidoglycan biosynthesis and assembly. 81:451–78–, 2012.

- [37] J. van Heijenoort. Formation of the glycan chains in the synthesis of bacterial peptidoglycan. *Glycobiology*, 11(3):25R–36R, 2001.
- [38] S. K. Mastronicolis, A. Berberi, I. Diakogiannis, E. Petrova, I. Kiaki, T. Baltzi, and P. Xenikakis. Alteration of the phospho- or neutral lipid content and fatty acid composition in *Listeria monocytogenes* due to acid adaptation mechanisms for hydrochloric, acetic and lactic acids at pH 5.5 or benzoic acid at neutral pH. 98:307–16–, 2010.
- [39] R. Mercier, Y. Kawai, and J. Errington. Excess membrane synthesis drives a primitive mode of cell proliferation. *Cell*, 152(5):997–1007, 2013.
- [40] Y. Zhang and L. C. Yu. Single-cell microinjection technology in cell biology. 30:606–10–, 2008.
- [41] K. Matsumoto, J. Kusaka, A. Nishibori, and H. Hara. Lipid domains in bacterial membranes. *Mol Microbiol*, 61(5):1110–1117, Sep 2006.
- [42] A. Nishibori, J. Kusaka, H. Hara, M. Umeda, and K. Matsumoto. Phosphatidylethanolamine domains and localization of phospholipid synthases in *Bacillus subtilis* membranes. *J Bacteriol*, 187(6):2163–2174, Mar 2005.
- [43] K. Simons and E. Ikonen. Functional rafts in cell membranes. 387:569–572–, 1997.
- [44] I. Barak and K. Muchova. The role of lipid domains in bacterial cell processes. 14:4050–65–, 2013.
- [45] E. Mileykovskaya and W. Dowhan. Cardiolipin membrane domains in prokaryotes and eukaryotes. *Biochim Biophys Acta*, 1788(10):2084–2091, Oct 2009.
- [46] N. C. Mykytczuk, J. T. Trevors, L. G. Leduc, and G. D. Ferroni. Fluorescence polarization in studies of bacterial cytoplasmic membrane fluidity under environmental stress. 95:60–82–, 2007.
- [47] S. Vanounou, D. Pines, E. Pines, A. H. Parola, and I. Fishov. Coexistence of domains with distinct order and polarity in fluid bacterial membranes. 76:1–11–, 2002.
- [48] J.B Finean and R.H. Michel. *Isolation, composition, and general structure of membranes*. Elsevier, New York, 1981.
- [49] N.J. Russell and N. Fukunaga. A comparison of thermal adaptation of membrane lipids in psychrophilic and thermophilic bacteria. *FEMS Microbiol Rev.*, 1990.



- 
- [50] A. Ann-Sofie, O. Leif, R. Greger, and L. GŽran. Total Lipids with Short and Long Acyl Chains from Acholeplasma Form Nonlamellar Phases. *Biophys J*, 1998.
- [51] L. Rilfors, G. Lindblom, Å. Wieslander, and A. Christiansson. Lipid bilayer stability in biological membranes. *Biomembranes*, 12:205–245, 1984.
- [52] M. C. Mansilla, L. E. Cybulski, D. Albanesi, and D. de Mendoza. Control of membrane lipid fluidity by molecular thermosensors. *J Bacteriol*, 186(20):6681–6688, Oct 2004.
- [53] M. Suutari and S. Laakso. Microbial fatty acids and thermal adaptation. 20:285–328–, 1994.
- [54] K. Gaus, T. Zech, and T. Harder. Visualizing membrane microdomains by Laurdan 2-photon microscopy. 23:41–8–, 2006.
- [55] S. A. Sanchez, M. A. Tricerri, and E. Gratton. Interaction of high density lipoprotein particles with membranes containing cholesterol. *J Lipid Res*, 48(8):1689–1700, Aug 2007.
- [56] L. A. Bagatolli, S. A. Sanchez, T. Hazlett, and E. Gratton. Giant vesicles, Laurdan, and two-photon fluorescence microscopy: evidence of lipid lateral separation in bilayers. *Methods Enzymol*, 360:481–500, 2003.
- [57] E. J. Allan, C. Hoischen, and J. Gumpert. Bacterial L-forms. *Advances in applied microbiology*, 68:1–39, 2009.
- [58] E. Klienberger. The natural occurrence of pleuropneumonia-like organisms in aparent symbiosis with streptobacillus moniliformis and its symbiont. *J. Path Bact*, 1935.
- [59] L. Dienes. Organisms of Klienberger and Streptobacillus moniliformis. *J Infect Dis*, 65:24–42, 1939.
- [60] J. Casadesús. Bacterial L-forms require peptidoglycan synthesis for cell division. *BioEssays : news and reviews in molecular, cellular and developmental biology*, 29(12):1189–1191, December 2007.
- [61] C. Pierce. Streptobacillus moniliformis, its associated L-form, and other pleuronpneumonia-like organisms. *J Bacteriol*, 43:780+, 1942.
- [62] L. Guze. *Microbial protoplasts, spheroplasts and L-forms*. The Williams & Wilkins Company, 1986.
- [63] S. Madoff. *The bacterial L-forms*. 1986.
- [64] G. Domingue, B. Turner, and J. U. Schlegel. Cell-wall deficient bacterial variants in kidney tissue. Detection by immunofluorescence. *Urology*, 3(3):288–292, March 1974.

- [65] M. T. Green, P. M. Heidger, and G. Domingue. Demonstration of the phenomena of microbial persistence and reversion with bacterial L-forms in human embryonic kidney cells. *Infection and immunity*, 10(4):889–914, October 1974.
- [66] J. Schmitt-Slomska, G. Drach, and R. Caravano. Incidence of cellular and humoral factors on group A streptococcal L forms. I. Microscopic study of the association of L forms with human polymorphonuclear leucocytes and mouse peritoneal macrophages. *Annales de microbiologie*, 124(3):329–350, October 1973.
- [67] S. Dell’Era, C. Buchrieser, E. Couvé, B. Schnell, Y. Briers, M. Schuppler, and M. J. Loessner. *Listeria monocytogenes* L-forms respond to cell wall deficiency by modifying gene expression and the mode of division. *Molecular microbiology*, 73(2):306–322, July 2009.
- [68] W. A. Glover, Y. Yang, and Y. Zhang. Insights into the molecular basis of L-form formation and survival in *Escherichia coli*. *PloS one*, 4(10), 2009.
- [69] M. Leaver, P. Dominguez-Cuevas, J. M. Coxhead, R. A. Daniel, and J. Errington. Life without a wall or division machine in *Bacillus subtilis*. *Nature*, 457:849–53–, 2009.
- [70] J. Errington. L-form bacteria, cell walls and the origins of life. *Open Biol*, 3(1):120143, Jan 2013.
- [71] P. Domínguez-Cuevas, R. Mercier, M. Leaver, Y. Kawai, and J. Errington. The rod to L-form transition of *Bacillus subtilis* is limited by a requirement for the protoplast to escape from the cell wall sacculus. *Mol Microbiol*, 83(1):52–66, Jan 2012.
- [72] R. Mercier, P. Domínguez-Cuevas, and J. Errington. Crucial role for membrane fluidity in proliferation of primitive cells. *Cell Rep*, 1(5):417–423, 2012.
- [73] Y. Briers, T. Staubli, M. C. Schmid, M. Wagner, M. Schuppler, and M. J. Loessner. Intracellular Vesicles as Reproduction Elements in Cell Wall-Deficient L-Form Bacteria. 7:–, 2012.
- [74] G. J. Domingue and H. B. Woody. Bacterial persistence and expression of disease. 10:320–&–, 1997.
- [75] M. Suchanova and F. Patocka. An attempt to isolate L forms of *Listeria monocytogenes*. *Cesk Epidemiol Mikrobiol Imunol*, 6(3):133–139, 1957.
- [76] A. M. Brem and W. C. Eveland. Inducing L Forms in *Listeria monocytogenes* Types 1 through 7. *Appl Microbiol*, 15(6):1510, Nov 1967.

- [77] A. M. Brem and W. C. Eveland. L forms of *Listeria monocytogenes*. I. In vitro induction and propagation of L forms in all serotypes. *J Infect Dis*, 118(2):181–187, Apr 1968.
- [78] D. C. Edman, M. B. Pollock, and E. R. Hall. *Listeria monocytogenes* L forms. I. Induction maintenance, and biological characteristics. *J Bacteriol*, 96(2):352–357, 1968.
- [79] R. A. Siddiqui, C. Hoischen, O. Holst, I. Heinze, B. Schlott, J. Gumpert, S. Diekmann, F. Grosse, and Matthias Platzer. The analysis of cell division and cell wall synthesis genes reveals mutationally inactivated *ftsQ* and *mraY* in a protoplast-type L-form of *Escherichia coli*. *FEMS microbiology letters*, 258(2):305–311, May 2006.
- [80] D. Joseleau-Petit, J. C. Liebart, J. A. Ayala, and R. D’Ari. Unstable *Escherichia coli* L forms revisited: Growth requires peptidoglycan synthesis. 189:6512–6520–, 2007.
- [81] N. Nanninga. Morphogenesis of *Escherichia coli*. *Microbiology and molecular biology reviews : MMBR*, 62(1):110–129, March 1998.
- [82] J. Tamames, M. González-Moreno, J. Mingorance, A. Valencia, and M. Vicente. Bringing gene order into bacterial shape. *Trends in genetics : TIG*, 17(3):124–126, 2001.
- [83] G. Billings, N. Ouzounov, T. Ursell, S. M. Desmarais, J. Shaevitz, Z. Gitai, and KC Huang. De novo morphogenesis in L-forms via geometric control of cell growth. *Mol Microbiol*, Jul 2014.
- [84] N. Markova, L. Michailova, A. Vesselinova, V. Kussovski, T. Radoucheva, S. Nikolova, and I. Paskaleva. Cell wall-deficient forms (L-forms) of *Listeria monocytogenes* in experimentally infected rats. 286:46–55–, 1997.
- [85] L. H. Mattman. *Cell Wall Deficient Forms, Stealth pathogens*. Boca Raton, USA: CRC Press LLC, 2001.
- [86] L. Michailova, V. Kussovsky, T. Radoucheva, M. Jordanova, and N. Markova. Persistence of *Staphylococcus aureus* L-form during experimental lung infection in rats. 268:88–97–, 2007.
- [87] G. J. Domingue. Demystifying pleomorphic forms in persistence and expression of disease: Are they bacteria, and is peptidoglycan the solution? 10:234–46–, 2010.
- [88] G. J Domingue. *Cell wall-deficient bacteria: basic principles and clinical significance*. 1982.
- [89] M. E. Onwuamaegbu, R. A. Belcher, and C. Soare. Cell wall-deficient bacteria as a cause of infections: a review of the clinical significance. *J Int Med Res*, 33(1):1–20, 2005.

- 
- [90] K. Wang and L. Chen. Helicobacter pylori L-form and patients with chronic gastritis. *World J Gastroenterol*, 10(9):1306–1309, 2004.
- [91] B. Schnell, T. Staubli, S. DellEra, N. Harris, M Kopf, M. Schuppler, and M. Loessner. Attenuated virulence of *L. monocytogenes* L-forms due to down-regulation of hly and induction of a TLR-dependent immune response. pages –, 2014.
- [92] M. O’Riordan, C. H. Yi, R. Gonzales, K. Lee, and D. A. Portnoy. Innate recognition of bacteria by a macrophage cytosolic surveillance pathway. *Proc Natl Acad Sci U S A*, 99(21):13861–13866, Oct 2002.
- [93] S. Stockinger, T. Materna, D. Stoiber, L. Bayr, R. Steinborn, T. Kolbe, H. Unger, T. Chakraborty, D. E. Levy, M. Müller, and T. Decker. Production of type I IFN sensitizes macrophages to cell death induced by *Listeria monocytogenes*. *J Immunol*, 169(11):6522–6529, Dec 2002.
- [94] H. J. Morowitz, B. Heinz, and D. W. Deamer. The chemical logic of a minimum protocell. 18:281–7–, 1988.
- [95] D. W. Deamer and J. P. Dworkin. Chemistry and physics of primitive membranes. 259:1–27–, 2005.
- [96] P. L. Luisi. *The emergence of life : from chemical origins to synthetic biology*. Cambridge University Press, Cambridge, 2006.
- [97] I. A. Chen and P. Walde. From Self-Assembled Vesicles to Protocells. 2:–, 2010.
- [98] D. W. Deamer. *First life : discovering the connections between stars, cells, and how life began*. University of California Press, Berkeley, 2011.
- [99] P. Carrara, P. Stano, and P. L. Luisi. Giant vesicles "colonies": a model for primitive cell communities. 13:1497–502–, 2012.
- [100] K. Adamala and J. W. Szostak. Nonenzymatic template-directed RNA synthesis inside model protocells. 342:1098–100–, 2013.
- [101] H. J. Morowitz. *Beginnings of cellular life : metabolism recapitulates biogenesis*. Yale University Press, New Haven, 1992.
- [102] J. W. Szostak, D. P. Bartel, and P. L. Luisi. Synthesizing life. 409:387–90–, 2001.

- 
- [103] M. M. Hanczyc and J. W. Szostak. Replicating vesicles as models of primitive cell growth and division. *Curr Opin Chem Biol*, 8(6):660–664, 2004.
- [104] K. Adamala and P. L. Luisi. Experimental systems to explore life origin: perspectives for understanding primitive mechanisms of cell division. *Results Probl Cell Differ*, 53:1–9, 2011.
- [105] Y. Briers, P. Walde, M. Schuppler, and M. J. Loessner. How did bacterial ancestors reproduce? Lessons from L-form cells and giant lipid vesicles. *Bioessays*, 34:1078–1084–, 2012.
- [106] E. V. Koonin and A. Y. Mulkidjanian. Evolution of Cell Division: From Shear Mechanics to Complex Molecular Machineries. 152:942–944–, 2013.
- [107] K. Oglecka, J. Sanborn, A. N. Parikh, and R. S. Kraut. Osmotic gradients induce bio-reminiscent morphological transformations in giant unilamellar vesicles. 3:120–, 2012.
- [108] T. Fuhrer, D. Heer, B. Begemann, and N. Zamboni. High-throughput, accurate mass metabolome profiling of cellular extracts by flow injection-time-of-flight mass spectrometry. *Anal Chem*, 83(18):7074–7080, Sep 2011.

## 3 Manuscript 1

### **Towards a top-down model for protocell evolution: cell wall-deficient L-form bacteria can fuse and take up extracellular DNA and proteins**

Titu Staubli<sup>1,#</sup> and Patrick Studer<sup>1,#</sup>, Thaddäus Perrot<sup>1</sup>, Yves Briers<sup>2</sup>, Markus Schuppler<sup>1</sup>, and Martin J. Loessner<sup>1,\*</sup>

<sup>1</sup> Institute of Food, Nutrition and Health, ETH Zurich, Schmelzbergstrasse 7, CH-8092 Zurich, Switzerland

<sup>2</sup> Department of Biosystems, Catholic University Leuven, Leuven, Belgium

# These authors contributed equally to this work

#### **Contributions of Titu Staubli to this manuscript:**

- designed the project and wrote the manuscript
- performed the following experiments: uptake of extracellular DNA and proteins, measurement of the membrane fluidity, part of the membrane fusion experiments, isolation and analysis of single L-form cells, isolation and differentiation of single L-form cells

\* Corresponding author.

Martin J. Loessner, Phone: +41 44 632 3335, E-mail: martin.loessner@ethz.ch

## Abstract

Putative pre-biological processes in hypothetical protocells on early earth have so far been investigated mainly by bottom-up approaches using singular giant lipid vesicles. We used a different and unique top-down approach, and employed cell wall-deficient *Listeria monocytogenes* L-form cells to probe possible properties and constraints of primordial life. Due to their morphological similarity to giant lipid vesicles and ability to aggregate to huge colony-like assemblies, we believe L-forms may well resemble primitive cell communities. We found that L-form cells feature a high membrane permeability and fluidity, which can support uptake of extracellular DNA and proteins from the growth environment, without specific enhancers or external stimuli. Furthermore, L-forms were observed to undergo membrane fusion, resulting in heteroploid cells with mixed genetic traits and phenotypes. Isolated single heteroploids undertook spontaneous and rapid differentiation to monoploids which may provide insights on DNA distribution in primitive cellular systems. Altogether, our findings contribute to a convergence of bottom-up and top-down approaches to better understand processes that may have taken place in protocell evolution.

## Introduction

It is assumed that precursor structures of the first cells (protocells) have formed about four billion years ago [1, 2, 3, 4]. Yet, evolution to "contemporary" cells remains elusive, and it is important to shed light on mechanisms that could have driven early evolutionary processes. Crucial properties such as uptake of extracellular biomolecules as well as cellular fusion may have allowed primitive cells to exchange molecules and information and allowed evolution towards sophisticated cellular processes. Although artificial cells such as giant lipid vesicles (GVs) may be used to address some cellular functions in a limited fashion [2, 3, 5, 6, 7, 8, 9], they are non-viable and lack the complexity brought about by interaction of biomolecules. In particular, elucidation of DNA inheritance in a primitive cellular system is limited due to the inability of GV's to replicate indefinitely. Bacterial L-forms represent a self-replicating and attractive alternative model system to improve our understanding of mechanism relevant for the evolution of early life.

L-form bacteria lack a cell wall, but are still capable of growth and reproduction. The mechanisms they use are remarkably similar to the different reproduction modes of lipid vesicle systems, specifically on the morphological level [10, 11]. They do not carry out an orchestrated binary fission, but employ simplified modes of reproduction, by vesicle formation which is mainly driven by membrane dynamics. Surprisingly, these processes do not require the various structural elements usually involved in bacterial cell division [12, 13]. It seems as if the molecular mechanisms acquired throughout evolution to enable and optimize bacterial cell division become dispensable in L-forms, leading to an uncoordinated and less efficient division mode. The presence of polyploidy reflects the disorganization in cell wall deficient bacteria [13, 14]. Hence, the simplified cellular division mode of L-forms renders their study an interesting top-down approach to probe simple, possibly primordial cellular reproduction mechanisms [10, 11, 14]. In many studies about the origin of primitive cells, the focus has been only on the individual cell compartment and its interaction with the environment. It is however conceivable, that primitive cells, as many unicellular microbes, may have been existing in communities. It is therefore of great interest



and relevance to study entire systems of supposedly primitive cellular life, where neighboring compartments possess the ability to interact with each other and the environment. This concept has recently been applied by comparing properties of GVs aggregated to colony-like structures to isolated, single vesicles [8]. Interestingly, it was shown that aggregates of lipid vesicles consisting of 1-palmitoyl-2-oleoyl-sn-glycero-3-phosphatidylcholine (POPC) and oleate in a 2:1 ratio exhibit an enhanced permeability, indicated by the uptake of phosphate from the environment. These vesicles also showed enhanced fusion between adjacent compartments. With respect to the evolution of bacterial life, solute capture of functional biomolecules such as catalytic RNAs (ribozymes) and peptides from the environment, in combination with mutual exchanges of encapsulated materials by vesicle fusion, could have fueled evolution driven by competition and selection of the best adapted vesicles [10, 15]. Therefore, both processes may have been essential to enable the further development of protocells, and help cellular organisms to adapt to changing environments.

Besides the uptake of extracellular biomolecules and the ability to re-assort genomes by fusion, faithful distribution of genetic material to the progeny cell was a prerequisite for an autonomously self-replicating system. Over the past billions of years, contemporary cells have developed an elaborated mechanism to ensure accurate distribution of genomes to their progeny cells [16]. The earliest cells on earth did certainly not possess machinery for the inheritance of DNA [17]. Instead, genetic distribution probably occurred by a random undirected assortment. The containment of a certain level of polyploidy likely accounted for the absence of a sophisticated system.

We here studied fusion and solute capture by living L-form systems that could resemble primitive cell colonies and allows comparison to abiotic GV colony-like assemblies. In addition, we employed the reduction in cell division elements and occurrence of polyploidy in L-forms to gain insights on the chromosome distribution process as it might have occurred in primordial cells. Specifically, we used *Listeria monocytogenes* L-forms as a model system. These spherical cells are heterogeneous in size and multiply by forming intracellular and extracellular membrane vesicles

---

within giant aggregated colonies, which behave intriguingly similar to GVs [18, 19].

## Results

### Uptake of extracellular DNA and protein by L-form cells

An essential requirement for the evolution of protocells into a complex "modern" cell is the ability to capture and take up macromolecules and nutrients from the environment, such as nucleobases and amino acids. It was therefore an important milestone to determine the permeability for macromolecules in artificial membrane vesicles [20]. We here assessed the ability of *Listeria* L-forms to directly take up extracellular plasmid DNA (eDNA) and proteins from the environment, i.e., the growth medium. Towards this goal, we exposed *Listeria* L-forms cells to plasmid DNA encoding CFP as a fluorescent reporter for successful uptake and gene expression. No other reagents known to support transformation, such as polyethylene glycol or lipid reagents were added. After 7 days, cells were removed and analyzed by fluorescence microscopy for presence of fluorescent markers. We found that a small fraction of L-forms did exhibit CFP fluorescent signals, indicating uptake and expression of the extracellular genetic information (Figure 1A.1-A.2). It is important to note here that *Listeria monocytogenes* lacks a functional competence system and is therefore not naturally competent or known to be able to take up extracellular DNA [21]. Our observation that L-forms cells are proficient for uptake and expression of eDNA raised the question as to whether proteins would also be able to permeate the vesicle membranes. To test this, we used a very simple assay, and exposed GFP tagged L-forms to purified red fluorescent protein (RFP) added to the growth medium. After incubation, cells were washed and analyzed by microscopy. Figure 1B shows that red fluorescent signals were in fact observed inside the *Listeria* L-forms. Verification that proteins did not simply diffuse or translocate through damaged membranes into non-viable cells was provided by the intracellular GFP signal, whose expression we used as an indicator for viability and membrane integrity. Another control experiment relating to the absence of cross-talk between the emission spectra of GFP and RFP is shown in supplementary Figure S1.

As a possible explanation for the enhanced permeability, we reasoned an alteration in the

membrane conformation, such as "gel-phase" or a more fluid "liquid-crystalline phase". The membrane fluidity depends on the degree of saturation and chain lengths of the fatty acid moiety of phospholipids [22]. It is well conceivable that L-form membranes are composed of different phospholipids. Therefore, the overall membrane fluidity in L-forms and parental cells was measured using Laurdan generalized polarization (GP) as described by Strahl *et al.*, 2013 [23]. The analysis revealed an significant increase in fluidity in L-form membranes compared to the parental cells indicated by a lower GP value (p-value < 0.0001)(Figure 1C). A more fluidic phospholipid membrane likely attributes to the observed enhanced permeability of DNA and proteins in *Listeria* L-forms.

### ***Listeria* L-forms cells can undergo membrane fusion**

Membrane fusion is a rather unfavorable and energy costly event. It has been reported to occur with both plant-derived [24] and bacterial protoplasts [25]. In those experiments, fusion was supported by addition of polyethylene glycol (PEG), which induces aggregation and initiates the fusion event. In order to monitor spontaneous fusion of cells within *Listeria* L-forms colonies, we constructed two fluorescently labeled *Listeria monocytogenes* strains featuring chromosomally encoded cyan fluorescent protein (CFP) or Citrine as fluorescent markers, which have no spectral overlap. Starting from the constructed parental *Listeria monocytogenes* strains, L-forms were generated by exposure to the penicillin G [18, 19]. Both CFP and Citrine-tagged L-form cells were then mixed and co-incubated. In rare cases, L-form cells were identified which expressed both the cyan and citrine fluorescent proteins, indicating fusion of two cell types (Figure 2A.1-A.2). Although the fusion frequency appeared low, we were able to monitor and therefore demonstrate the proposed fusion and generation of heterokaryons using time-lapse microscopy. As shown in Figure 2B, fusion events between adjacent cells could be observed in the bright field as well as in the fluorescent channel (Figure 2C). It is noteworthy that the process spanned over several minutes, unlike in the case of GVs, where fusion of lipid bilayers was reported to occur within less than a second [26]. In conclusion, our findings indicate that L-form vesicles can undergo

membrane and cell fusion, possibly resulting in heterokaryons with mixed properties.

### **Heteroploidic L-forms undergo spontaneous and rapid differentiation to monoploids**

Bacterial L-forms lack the complex set of structural elements which are usually essential in bacterial cell division [18, 10]. The proliferation mechanism is rather disorganized, less coordinated and most likely does not involve a directed apparatus for chromosome segregation. Due to this reduction and the presence of multiple chromosomes detailed knowledge of DNA distribution in L-forms may provide valuable information to understand how genetic material could have been inherited in primitive cells.

In order to assess chromosome inheritance in L-forms, a strain was constructed that contains two different chromosomes either encoding GFP or RFP. This was achieved by cloning the *rfp* gene, under the control of the constitutive xylose promoter (Schmitter et al., unpublished), into vector pPL2. The vector harbors a chloramphenicol resistance gene and a PSA integrase which integrates the plasmid at the 3' end of the tRNA<sup>Arg</sup> gene on the *Listeria* chromosome. A similar approach was performed for the plasmid encoding GFP. Instead of the vector pPL2, the vector pPL3 was used which differs in the antibiotic resistance (erythromycin) and site of integration (*comK*). *L. monocytogenes* L-forms were then transformed with either the pPL2- or pPL3 construct giving rise to two L-form strains either expressing RFP or GFP. Fusion of the two strains was then induced by applying PEG followed by selection with chloramphenicol and erythromycin (see material and methods) producing heteroploid L-forms ("mixed L-form"). Analysis of the cells grown on plates revealed expression of both fluorescent proteins confirming the successful fusion event (Figure 3A). Due to the almost identical back bone sequence of pPL2 and pPL3 plasmids, there is the possibility of homologues recombination which could lead to one *Listeria* chromosome exhibiting both fluorescent genes. In order to preclude this event and to confirm the occurrence of the fluorescent genes on two different chromosomes, PCR analysis on single cell was applied. Isolation of single heteroploids was conducted by micromanipulation as described

in Studer and Staubli *et al.* (see Manuscript 2) and then subjected to PCR. Primers were used which annealed specifically on the chromosome and on the respective antibiotic resistance gene. PCR analysis resulted in two distinct products indicating the containment of two different chromosomes and the ability of L-forms to express genes from multiple chromosomes simultaneously (Figure 3C, #2). As a control, single L-forms containing only one type of fluorescent proteins were used.

Monitoring the faith of chromosomes in the generated heteroploids enabled us to gain insights on the distribution of genetic material in *Listeria* L-forms. It was of interest to evaluate propagation of chromosomes in the absence of selection pressure (no antibiotics) over a period of several days. Heteroploids were grown in medium without antibiotics and then plated on agar plates supplemented with chloramphenicol and erythromycin. As a control, the cells were also plated on agar plates without antibiotics. The relative colony forming units (cfu) per ml were then determined. Already after two days, hardly any of the initially heteroploidic cells still contained both chromosomes, indicated by the inability to grow in the presence of chloramphenicol and erythromycin (Figure 4).

In order to ascertain rapid discrimination of the two different chromosomes, pure initial culture is a prerequisite. Sub-cultivation of an L-form culture, previously grown in the presence of chloramphenicol and erythromycin, into media without antibiotics does not guarantee a pure culture of heteroploids. There is the possibility of an L-form cell, having only obtained chromosomes of one type, to overgrow the neighboring "mixed L-forms" as soon as the antibiotic pressure is released. To exclude this scenario, chromosome differentiation was monitored originating from one single "mixed L-form". We applied a micromanipulator technique (described in Studer and Staubli *et al.*) to isolate a single L-form cell which was then re-inoculated into fresh media with and without antibiotics (Figure 5). After 3 to 4 days, cells were analyzed under the microscope showing almost exclusively either green or red fluorescent L-form cells in case of no selection. As expected, in cultures supplemented with chloramphenicol and erythromycin cells contained GFP and RFP. Selection with only one antibiotic resulted in a culture with L-forms expressing

either type of the fluorescent proteins (Figure 5).

The outcome clearly demonstrates a rapid differentiation from a heteroploid to monoploid state indicating the inheritance of just a fraction of chromosome copy numbers to the progeny cells.

## Discussion

We describe a top-down approach employing bacterial L-form vesicles to demonstrate two important properties that could have supported evolution of the earliest cell types: the ability of vesicles to fuse and exchange intracellular material, and to take up DNA and proteins from their surroundings. Both processes would have facilitated a high genetic flux where dissimilar genomes faced the chance to re-assort and recombine, thereby driving development towards a sophisticated cell. How complex macromolecules could have passed the lipid barrier of putative protocells is more difficult to conceive, as these first precursors of modern cells did likely not have membrane pores or active transport systems, neither featured these membranes an energy-generating electron transport system and an oriented charge. However, monoacyl lipids, as plausible prebiotic compound of primitive vesicles, show higher lipid fluidity and may also support limited solute passage [27].

Interestingly, *Listeria* L-forms membranes are characterized by higher membrane fluidity as observed for *B. subtilis* L-form membranes [14]. Correlation of membrane fluidity and permeation has been shown in GV [28]. Hence, the change in membrane fluidity and dynamics in L-forms not only is thought to support cell multiplication, it probably also result in significantly higher permeability of L-form membranes. Recent comparison of the lipid composition between L-forms and parental *Listeria* disclosed a significant higher abundance of positively charged phospholipids in cell wall-deficient cells (data not shown). We therefore envisage that this alteration in the membrane composition enables interaction with extracellular DNA resulting in the higher detected permeation.

Uptake of DNA and proteins from the environment and the possibility of cell fusion seem especially relevant in light of the observation that *Listeria* L-forms grow in dense, aggregated colonies. It was recently shown that giant lipid vesicles in similar "colony-like" assemblies are also capable to capture solutes and undergo fusion, which was not observed for individual, separated GVs [8]. The authors attributed the enhanced membrane permeability and increased fusion



frequency to the cationic poly-L-arginine (PLA) which acts as a molecular "glue" to maintain the arrangement of the negatively charged GVs. In the case of L-forms, it is conceivable that the vast amount of extracellular DNA originating from lysed L-form debris (Figure S2) may aid to hold the lipid vesicles together. Furthermore, the high concentration of extracellular DNA might also constitute an important driving force for fusion of L-form cells, since DNA may directly act as a fusogenic agent, drawing together positively charged liposomes [29].

Early forms of life were only equipped with primitive cellular functions, certainly lacking a stringent mechanism for chromosome segregation as it is present in contemporary cells [16]. It is therefore of interest to elucidate how primitive cells assured successful DNA partitioning. A valid hypothesis proposes the occurrence of multiple chromosomes which were distributed by a random fashion [17]. The feasibility of an undirected and non-protein-mediated DNA distribution was recently demonstrated in artificial vesicles. It was shown that spontaneous division of GVs was accompanied by partitioning of the encapsulated DNA. Furthermore, authors conclude that DNA-membrane interactions were solely responsible to operate and drive GV division [30]. Such artificial system delivers useful insights, however self-reproduction is limited which prevents monitoring of DNA partitioning over several generations. On the contrary, bacterial L-forms display similar features but represent a viable entity with the ability to reproduce indefinitely [10, 12]. Thus, they provide a great opportunity to probe DNA inheritance in the absence of a regulated segregation mechanism in a living and polyploidic system. Here, we found that heteroploid L-forms, containing several chromosomes of two types, undergo rapid and spontaneous differentiation. The outcome supports the idea of an undirected and random DNA assortment in *Listeria* L-forms by analogy to high copy number plasmids. It is conceivable that most viable reproduction units only obtain by chance some amount of chromosome accounting for the observed spontaneous and rapid differentiation. Imaging analysis of time-lapse movies monitoring proliferation revealed an approximate generation time of 5 h for *Listeria* L-forms (data not shown). Assuming there is an active process in use, DNA segregation would be more efficient leading to a longer time of period for the discrimination for the two types of chromo-

somes. It is tempting to speculate that the mode of DNA partitioning in *Listeria* L-forms mimics primitive processes used in primordial cells.

Our study represents a good example for the convergence of observations following bottom-up and top-down approaches to probe possible primitive cells, and provides support for the hypothesis that a community or "colony" organization may have had beneficial "cooperative" properties. In conclusion, our observations may contribute towards a better understanding of the origin of the first living entity, and the key processes occurring in early cells.

## Material and Methods

### Induction and growth of L-forms

We used vector pPL2/ $P_{Xyl}$  (Schmitter et al., unpublished data) which features a constitutively active xylose promoter ( $P_{Xyl}$ ) to drive expression of codon-optimized genes encoding CFP [31] and Citrine [32]. Vectors pPL2/ $P_{Xyl}$ -citrine and pPL2/ $P_{Xyl}$ -*cfp* were transformed into *Listeria monocytogenes* using electroporation [33]. Integration of the vectors into the bacterial chromosomes was verified by PCR, and reporter gene expression by fluorescence microscopy. Starting from parental *Listeria monocytogenes* L-forms were generated by exposure to the penicillin G, followed by sequential subculture in osmotically stabilizing media (37 g BHI, 150 g sucrose, 2.5 g  $MgSO_4 \cdot 7H_2O$ , 1% horse serum per 1 liter distilled water). After several passages, parental cells completed the transition into a stabilized (i.e. non-reverting) L-form state and began to actively multiply and grow in large galaxy-shaped colonies.

### Fusion of L-forms

The generated CFP and Citrine-tagged L-form cells were mixed in a 1:1 ratio, and co-incubated for up to 96 hours. Using confocal laser scanning microscopy, L-form cells were screened for the expression of both fluorescent proteins. Time-lapse microscopy was conducted by cultivating L-forms in 2-well glass-bottom microscope chambers (ibidi GmbH, Munich, Germany) embedded in soft agar medium, and monitored for 24 hours. Cell membranes were made visible by dropping FM1-43 on top of the prepared ibidi chambers prior to imaging (final concentration 10  $\mu g/ml$ ).

### Construction of the plasmid pMK4/ $P_{Rha}$ -*cfp*

The  $P_{Rha}$  promoter region was amplified from pLF1 [34] using the primers  $P_{Rha}$ -forw (5'-TTT GAA TTC TAT TCC GTG ATA ATT TGG-3') and  $P_{Rha}$ -rev (5'-TTT GTC GAC ACT CAT TTT TAG TTA AGC GC-3'). Following digestion with EcoRI and SalI the amplified fragment was inserted into pMK4 to yield pMK4/ $P_{Rha}$ . In order to enhance the expression, we used a *Listeria* codon-optimized cyan fluorescent protein which was kindly provided by P. Cossart (Institut Pasteur, France)[31]. The codon-optimized *cfp* was amplified using a forward primer

that added a SalI site (5'- $\eta$ TTT TTG TCG ACG GTT AAA AAA TGT AGA AG-3') and a reverse primer (5'-TTT TTC CCG GGT TAT TTG TAG AGT TCA TCC -3') containing a SmaI restriction site. The amplified gene was then digested with SalI and SmaI and cloned into pMK4/P<sub>Rha</sub> to yield pMK4/P<sub>Rha</sub>-*cfp*.

### **Uptake of extracellular DNA and proteins by *Listeria* L-forms**

Uptake of extracellular DNA by *Listeria* L-forms was achieved by incubating cells overnight in broth containing the plasmid pMK4/P<sub>Rha</sub> -*cfp* 10 $\mu$ g/ml which features a rhamnose-inducible promoter [34], followed by subculture in soft agar tubes supplemented with 10 mM rhamnose. Uptake of extracellular RFP was conducted by co-incubating L-forms constitutively expressing GFP with recombinant RFP for 120 hours. Prior to microscopy, the cells were washed with broth medium.

### **Construction of the chromosomally encoded fluorescent proteins**

In order to construct fluorescently labeled *Listeria monocytogenes* the vector pPL2/P<sub>Xyl</sub> was used (Schmitter et al., unpublished). The fluorescent proteins were cloned under the constitutive xylose promoter (P<sub>Xyl</sub>). The citrine fluorescent protein was kindly provided by R. Tsien (University of California, San Diego, USA)[32]. As the original citrine was not functional in *Listeria*, it had to be codon-optimized and newly synthesized. The optimized citrine was then used for cloning. The codon-optimized version of *rfp* for *L. monocytogenes* was kindly provided by D. Portnoy (University of California, Berkeley, USA). The vector pPL2 harbors a chloramphenicol resistance gene and a PSA integrase which integrates the plasmid at the 3' end of the tRNA<sup>Arg</sup> gene. Successful integration into the chromosomes was verified by PCR and microscopy. For the construction of the GFP labeling, the pPL3 was used. In contrast to pPL2, it harbors an erythromycin resistance gene and PSA integrase for the insertion of the vector at the *comK* gene. The constructed vectors were then transformed into *Listeria monocytogenes* strains EGDe using electroporation [33]. Integration of the vectors into the bacterial chromosomes was verified by PCR and reporter gene expression by fluorescence microscopy.

## Construction of heteroploid L-forms by PEG mediated fusion

50  $\mu$ l of GFP and 50  $\mu$ l of RFP expressing L-forms were pooled and mixed by pipetting. Subsequently, 900  $\mu$ l of PEG solution (5.5 g PEG6000 dissolved in 10 ml LLM) was added and mixed by pipetting for 1 min. This culture was then plated on LLM plates supplemented with 5  $\mu$ g/ml erythromycin and 10  $\mu$ g/ml chloramphenicol. The plates were sealed with parafilm to prevent the agar from drying out, and incubated at 32°C until colonies were visible.

## Monitoring differentiation of heteroploids to haploid L-forms over time

1 ml of an L-form culture grown in presence of 5  $\mu$ g/ml erythromycin and 10  $\mu$ g/ml chloramphenicol was centrifuged at 1000 g for 2 min, the supernatant was discarded and the pellet resuspended in 1 ml LLM not containing antibiotics. This L-form suspension was diluted 1:1000 in LLM, vortexed and 1 ml aliquots were prepared. These aliquots were incubated at 32°C and at different time points three of them were plated in parallel on LLM plates without antibiotics and on LLM plates supplemented with 5  $\mu$ g/ml erythromycin and 10  $\mu$ g/ml chloramphenicol. The plates were sealed with parafilm and the colonies enumerated after three weeks at 32°C. Since L-forms reach stationary phase after 2-3 d, the cultures were passaged after 2, 4, 7, 9, 11, 14, 16 d by diluting them 1:1000 in fresh LLM. After every passage the old cultures were discarded and only the new ones used for plating and subsequent passaging.

## Isolation of single heteroploid L-forms

Isolation was conducted as previously published in Studer and Staubli *et al.*. Briefly, 80  $\mu$ l of solution containing L-form cells were spotted on a slide and then placed under the microscope. Using a micromanipulator (Vaudau-Eppendorf TransferMan NK2) in combination with a CellTram Air (Vaudaux-Eppendorf) single cells were aspirated into a capillary (diameter of 6  $\mu$ m). Subsequently, the single cell was released into 100  $\mu$ l medium which was then used for re-inoculation into fresh media.

## Determination of the membrane fluidity

Membrane fluidity in L-forms and parental *Listeria* were grown to exponential phase in LLM-broth at 32°C. Subsequently, the cells were washed with pre-warmed buffer (sucrose 150g/l, MgSO<sub>4</sub> 2.5g/l, NaCl 7.5g/l) followed by incubation with 10  $\mu$ M Laurdan (). The cells were then washed two times with pre-warmed buffer and then analyzed by Tecan Infinite spectrometer. Laurdan fluorescence intensity were measured at  $435 \pm 5$  nm and  $490 \pm 5$  nm upon excitation at  $350 \pm 10$  nm. The GP value was calculated according to the formula  $GP = \frac{I_{435} - I_{495}}{I_{435} + I_{495}}$ . In order to assess significance differences of the determined GP values, statistical analysis was performed using PASW Statistics for Windows version 18.0 (SPSS Inc., Chicago). The two groups were subjected to student independent sample t-test which resulted in a p-value  $< 0.0001$ .

## Expression and purification of RFP

The gene encoding the red fluorescent protein (RFP) was amplified using a forward primer (5'-ATG GTG TCT AAG GGCGAA GAG CTG-3') that added *StuI* restriction site and reverse primer (5'-TTT GAG CTC CTT GTA CAG CTC GTC CAT GCC-3') containing a *SacI* restriction site. The vector pQE20 was then digested with the respective restriction enzymes. pQE30 contains an IPTG inducible T5 promoter and a hexa histidine-tag. *E. coli* JM109 was transformed with the resulting pQE30/*rfp*. A positive colony was selected and four overnight cultures with 10 ml LB Amp<sup>100</sup> were inoculated. These cultures were then used to inoculate four 250 ml cultures in LB Amp<sup>100</sup> and were grown to OD<sub>600</sub> nm = 0.6 before IPTG was added (final concentration = 0.2 mM). The bacteria were again grown for 4 h at 37°C in presence of IPTG to induce protein expression and subsequently centrifuged 10 minutes at 10000 g. Each pellet was resuspended in 4 ml of buffer A and then all samples were pooled. To lyse the bacteria, two french press treatments were performed sequentially, using a 20K cell. The cell debris were pelleted by centrifugation with 20000 g for 30 minutes. The supernatant, containing the RFP, was loaded onto columns, containing 5 ml of low density nickel. The column was washed with 15 ml of buffer A until no unbound protein was eluted anymore. Next, RFP was eluted with 7 ml of buffer B in 0.5 ml fractions. A dialysis was performed with PBS pH 7.0 overnight. The

concentration of the different fractions was determined with nanodrop measurements and the purity evaluated with a SDS protein gel.

## **Acknowledgements**

We gratefully acknowledge Peter Walde (Department of Materials, ETH Zurich) for many supportive discussions, comments and suggestions to improve this manuscript. We thank Pascale Cossart (Institute Pasteur, France) and Roger Tsien (University of California, San Diego, USA) for sending us plasmid DNA encoding the cyan and citrine fluorescent proteins. Last, we would like to thank David Deamer (University of California, Santa Cruz, USA) for inspiring discussions.

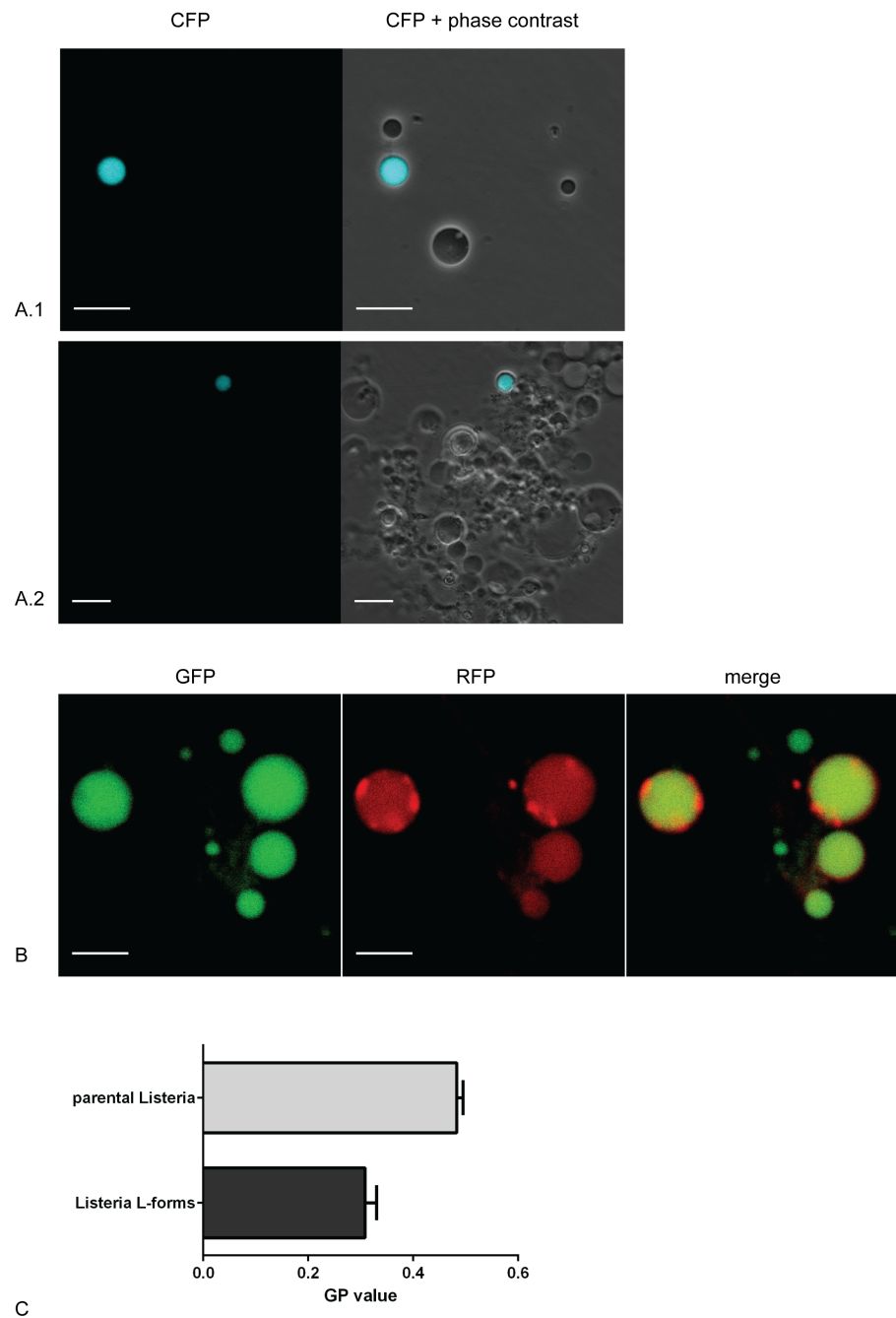


**Figure 1:** Uptake of extracellular plasmid DNA and red fluorescent protein (RFP) by *Listeria* L-forms cells. A.1-A.2). The L-form cells were incubated for six hours at 32°C in medium containing plasmid DNA encoding the cyan fluorescent protein (CFP) at concentration of 10  $\mu\text{g/ml}$ , followed by transfer and subcultivation in soft agar tubes. Successful uptake and expression of plasmid DNA was detected by the expression of CFP in L-form cells. B) Uptake of extracellular protein by L-form cells was demonstrated by incubation of GFP-tagged cells in medium supplemented with purified RFP (0.3 mg/ml), for six days at 32°C. Cells were carefully washed with broth medium prior to confocal fluorescence microscopy. C. Determination of the membrane fluidity using Laurdan. The cells were incubated with Laurdan followed by fluorescence intensity measurement. The resulting GP-value for L-forms is lower, indicating a higher membrane fluidity. The scale bar indicates 5  $\mu\text{m}$ .



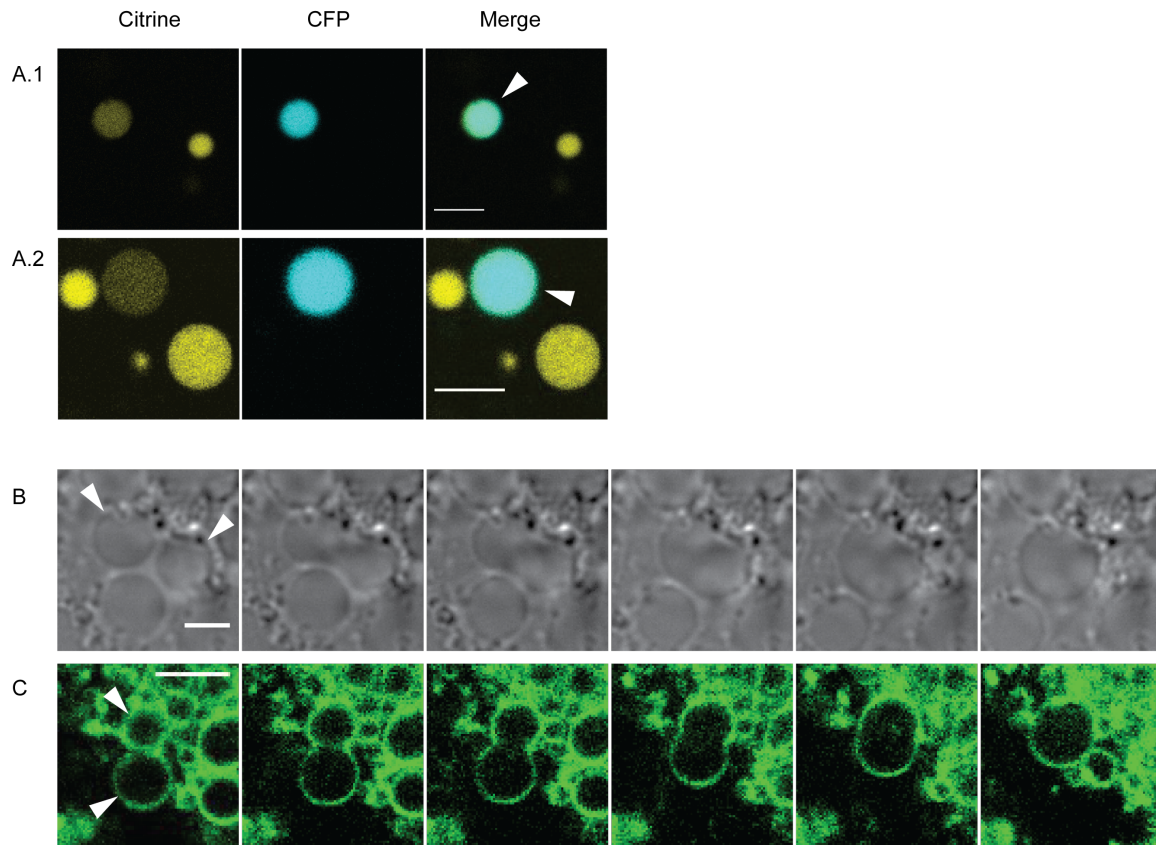


**Figure 2:** Generation of heteroploid *Listeria* L-forms through vesicle fusion. (A.1-A.2) Two *Listeria* L-forms strains expressing either citrine or cyan fluorescent protein, respectively, were co-incubated for five days at 32°C. Fusion of cells was indicated by colocalization of cyan and yellow fluorescence signals (arrows) in single cells. Images of two different samples are shown. B) Time-lapse series of bright field images of two *Listeria* L-forms cells (arrow heads) undergoing fusion. Images were taken every 4 minutes. C) Time-lapse series of two fusing *Listeria* L-forms cells stained with the green fluorescent membrane dye FM1-43. Images were taken at 0, 35, 75, 265, 345, and 895 min, respectively. The scale bar indicates 5  $\mu\text{m}$ .

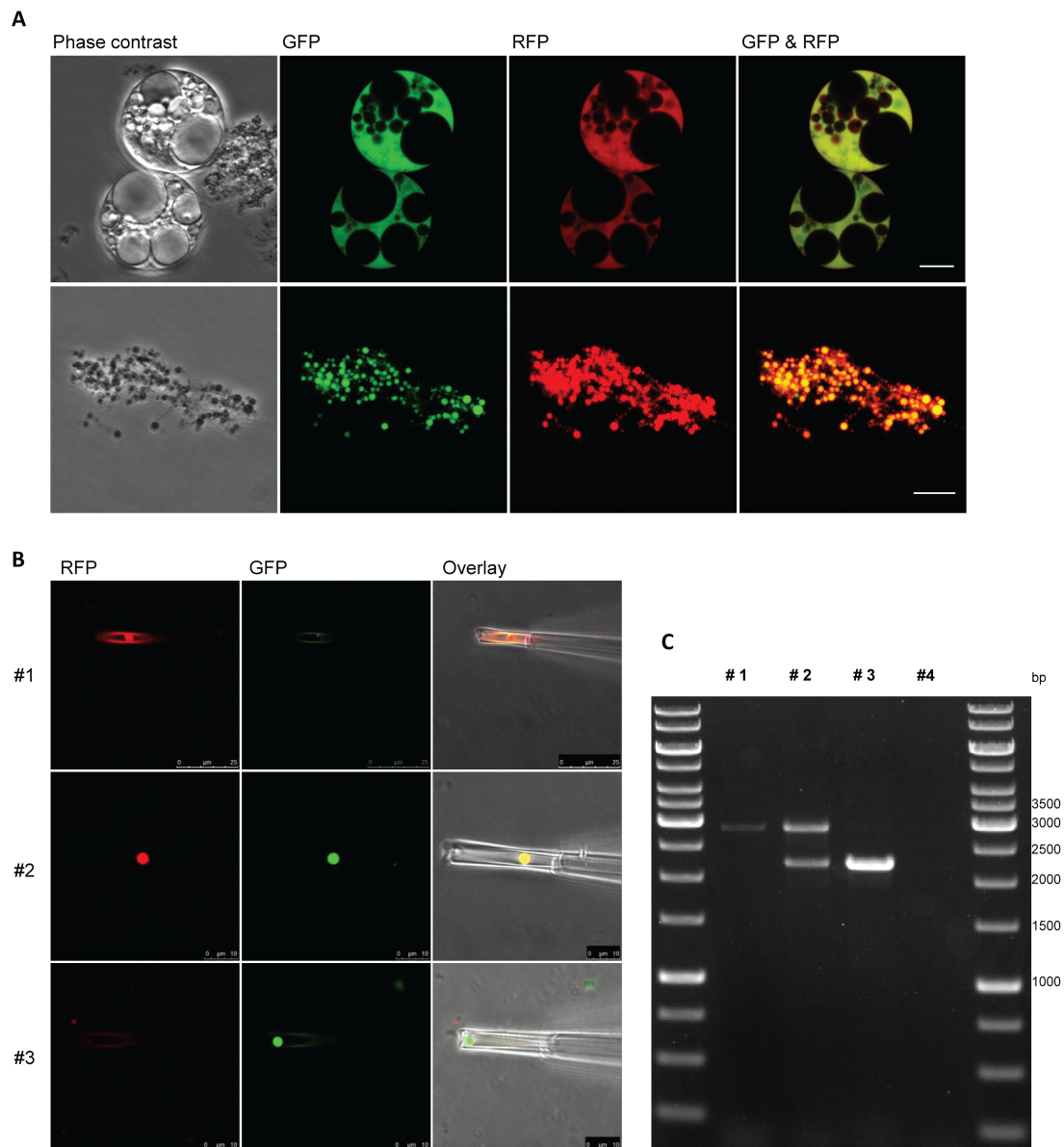


**Figure 3:** *Listeria* L-forms heteroploids are able to express genes from different types of chromosomes. Heteroploids were generated by induced vesicle fusion of GFP and RFP labeled L-forms. Selection occurred with chloramphenicol and erythromycin. A) *Listeria* L-forms expresses GFP and RFP indicating its heteroploidic state. The scale bar indicates 5  $\mu$ m. B) Single L-form cells were isolated using a micromanipulator and then subjected to PCR. #1: RFP expressing cell, #2: Heteroploid L-form containing two different chromosomes, each encoding one fluorescent protein. #3: GFP expressing cell. #4: As a negative control a small volume of extracellular liquid was aspirated into the capillary. The scale bar indicates 10 or 25  $\mu$ m. C) Primers were used which anneal to the antibiotic resistance genes and *Listeria* chromosome, allowing detection and differentiation of the two types of chromosomes. A successful integration of the pPL2/P<sub>Xyl-rfp</sub> yields a PCR product of about 3kb whereas the pPL3/P<sub>Xyl-gfp</sub> results in a PCR product at around 2kb. The result confirms the containment of two different chromosomes in L-forms indicated by the two PCR products in sample #2.

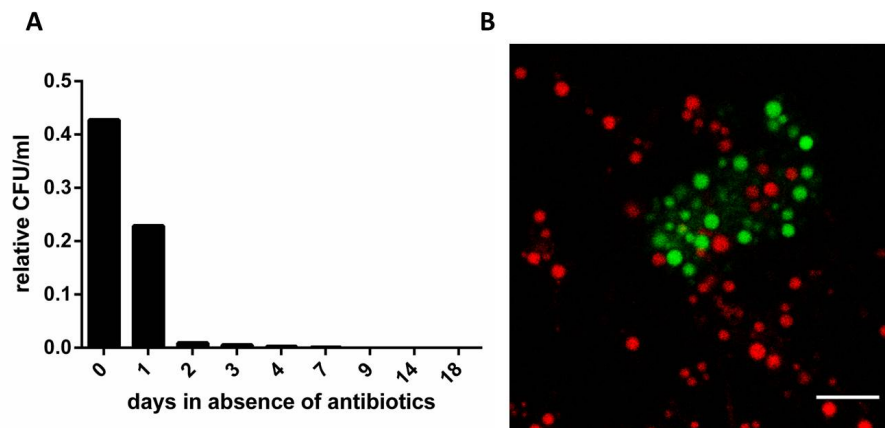


**Figure 4:** Loss of heteroploidy was monitored over time. Cells expressing both fluorescent proteins and previously grown in the presence of antibiotic pressure ( $\text{Cm}^{10}$  and  $\text{Ery}^5$ ) were sub-cultivated into media without antibiotics. After a certain period of time, the cells were plated on agar plates containing both antibiotics. The determined relative CFU/ml shows the differentiation to monoploids. B) Initial heteroploid L-forms were grown in the absence of antibiotics leading to cells containing one type of chromosome only. The scale bar indicates 5  $\mu\text{m}$ .

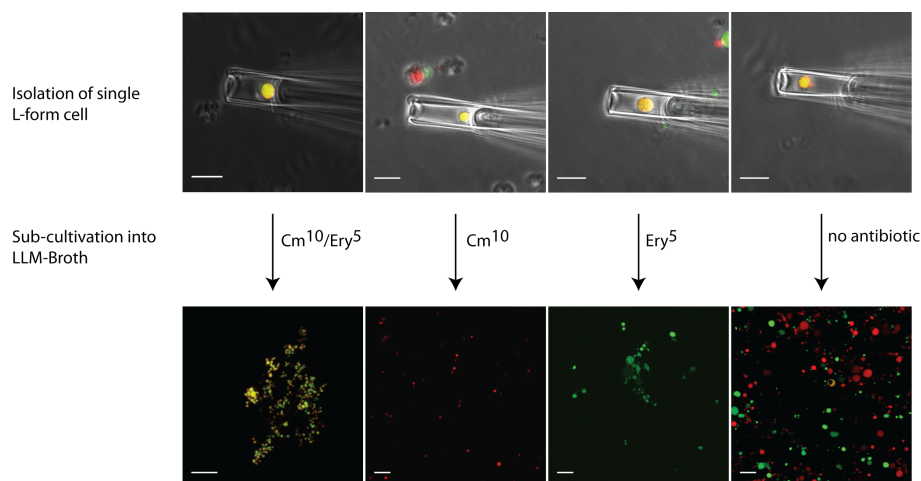


**Figure 5:** Isolation of single heteroploid L-forms using a micromanipulator followed by sub-cultivation into fresh LLM-Broth with and without antibiotics. In the absence of antibiotic pressure the single heteroploids differentiate spontaneously into monoploid red and green L-forms. In media supplemented with erythromycin or chloramphenicol, single heteroploids develop into pure cultures containing only one type of chromosomes. Selection with both antibiotics results in L-forms expressing GFP and RFP. Scale bars indicates 10  $\mu\text{m}$ .

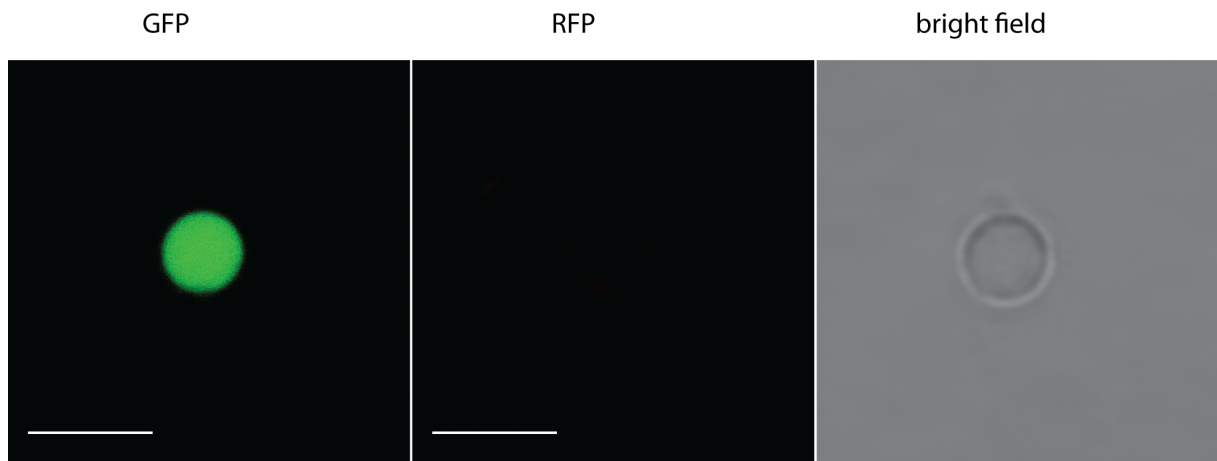


**Figure 6:** Supplementary Figure S1: Absence of cross-talk between the fluorescence emitted from GFP and RFP. A single GFP-tagged *Listeria* L-forms cell was recorded with the same settings as in Figure 1. Scale bars indicates 5  $\mu\text{m}$ .

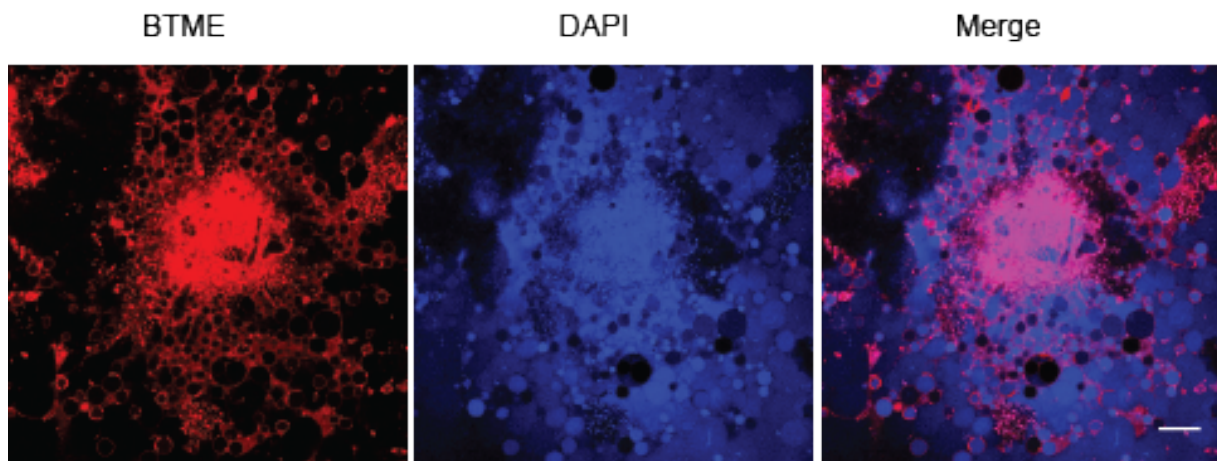


**Figure 7:** Supplementary Figure S2: *Listeria monocytogenes* L-form cells growing in colonies are surrounded by extracellular DNA released from dead and lysed cells. A) The DNA was stained with DAPI (blue), and membranes with CellTrace BODIPY TR methyl ester (red). Scale bar = 50  $\mu\text{m}$ .

# References Manuscript 1

- [1] H. J. Morowitz. *Beginnings of cellular life : metabolism recapitulates biogenesis*. Yale University Press, New Haven, 1992.
- [2] D. W. Deamer. *First life : discovering the connections between stars, cells, and how life began*. University of California Press, Berkeley, 2011.
- [3] P. L. Luisi. *The emergence of life : from chemical origins to synthetic biology*. Cambridge University Press, Cambridge, 2006.
- [4] J. W. Szostak, D. P. Bartel, and P. L. Luisi. Synthesizing life. *Nature*, 409:387–90–, 2001.
- [5] H. J. Morowitz, B. Heinz, and D. W. Deamer. The chemical logic of a minimum protocell. *Orig Life Evol Biosph*, 18:281–7–, 1988.
- [6] D. W. Deamer and J. P. Dworkin. Chemistry and physics of primitive membranes. *Springer Verlag Berlin*, 259:1–27–, 2005.
- [7] I. A. Chen and P. Walde. From Self-Assembled Vesicles to Protocells. *Cold Spring Harbor Perspect Biol*, 2:–, 2010.
- [8] P. Carrara, P. Stano, and P. L. Luisi. Giant vesicles "colonies": a model for primitive cell communities. *ChemBioChem*, 13:1497–502–, 2012.
- [9] K. Adamala and J. W. Szostak. Nonenzymatic template-directed RNA synthesis inside model protocells. *Science*, 342:1098–100–, 2013.
- [10] J. Errington. L-form bacteria, cell walls and the origins of life. *Open Biol*, 3(1):120143, Jan 2013.
- [11] Y. Briers, P. Walde, M. Schuppler, and M. J. Loessner. How did bacterial ancestors reproduce? Lessons from L-form cells and giant lipid vesicles: multiplication similarities between lipid vesicles and L-form bacteria. *Bioessays*, 34(12):1078–1084, Dec 2012.
- [12] R. Mercier, P. Domínguez-Cuevas, and J. Errington. Crucial role for membrane fluidity in proliferation of primitive cells. *Cell Rep*, 1(5):417–423, May 2012.

- 
- [13] M. Leaver, P. Dominguez-Cuevas, J. M. Coxhead, R. A. Daniel, and J. Errington. Life without a wall or division machine in *Bacillus subtilis*. *Nature*, 457:849–53–, 2009.
- [14] R. Mercier, Y. Kawai, and J. Errington. Excess membrane synthesis drives a primitive mode of cell proliferation. *Cell*, 152:997–1007–, 2013.
- [15] V. Norris and D. J. Raine. A fission-fusion origin for life. *Orig Life Evol Biosph*, 28:523–537–, 1998.
- [16] J.R. McIntosh, M. I. Molodtsov, and F. I. Ataullakhanov. Biophysics of mitosis. *Q Rev Biophys*, 45(2):147–207, May 2012.
- [17] A. L. Koch. Evolution vs the number of gene copies per primitive cell. *J Mol Evol*, 20(1):71–76, 1984.
- [18] Y. Briers, P. Walde, M. Schuppler, and M. J. Loessner. How did bacterial ancestors reproduce? Lessons from L-form cells and giant lipid vesicles. *PloS one*, 34:1078–1084–, 2012.
- [19] S. Dell’Era, C. Buchrieser, E. Couve, B. Schnell, Y. Briers, M. Schuppler, and M. J. Loessner. *Listeria monocytogenes* L-forms respond to cell wall deficiency by modifying gene expression and the mode of division. *Mol Microbiol*, 73:306–22–, 2009.
- [20] J. P. Schrum, T. F. Zhu, and J. W. Szostak. The Origins of Cellular Life. *Cold Spring Harbor Perspect Biol*, 2:–, 2010.
- [21] L. Rabinovich, N. Sigal, I. Borovok, R. Nir-Paz, and A. A. Herskovits. Prophage excision activates *Listeria* competence genes that promote phagosomal escape and virulence. *Cell*, 150:792–802–, 2012.
- [22] M. Suutari and S. Laakso. Microbial fatty acids and thermal adaptation. *Critical Reviews in Microbiology*, 20:285–328–, 1994.
- [23] H. Strahl, F. Bürmann, and L. W. Hamoen. The actin homologue MreB organizes the bacterial cell membrane. *Nat Commun*, 5:3442, 2014.
- [24] M. R. Davey, P. Anthony, J.B. Power, and K. C. Lowe. Plant protoplasts: status and biotechnological perspectives. *Biotechnol Adv*, 23(2):131–171, Mar 2005.
- [25] D. V. Gokhale, U. S. Puntambekar, and D. N. Deobagkar. Protoplast fusion: a tool for intergeneric gene transfer in bacteria. *Biotechnol Adv*, 11(2):199–217, 1993.
- [26] G. H. Lei and R. C. MacDonald. Lipid bilayer vesicle fusion: Intermediates captured by high-speed microfluorescence spectroscopy. *Biophysical Journal*, 85:1585–1599–, 2003.
- [27] S. S. Mansy. Membrane transport in primitive cells. *Cold Spring Harbor Perspect Biol*, 2:a002188–, 2010.

- 
- [28] T. Shimanouchi, H. Ishii, N. Yoshimoto, H. Umakoshi, and R. Kuboi. Calcein permeation across phosphatidylcholine bilayer membrane: effects of membrane fluidity, liposome size, and immobilization. *Colloids Surf B Biointerfaces*, 73(1):156–160, Oct 2009.
- [29] B. Sternberg, F. L. Sorgi, and L. Huang. New Structures in Complex-Formation between DNA and Cationic Liposomes Visualized by Freeze-Fracture Electron-Microscopy. *FEBS Letters*, 356:361–366–, 1994.
- [30] K. Kurihara, M. Tamura, K. Shohda, T. Toyota, K. Suzuki, and T. Sugawara. Self-reproduction of supramolecular giant vesicles combined with the amplification of encapsulated DNA. *Nat Chem*, 3(10):775–781, Oct 2011.
- [31] P. Cossart, D. Balestrino, M. A. Hamon, L. Dortet, M. A. Nahori, J. Pizarro-Cerda, D. Alignani, O. Dussurget, and A. Toledo-Arana. Single-Cell Techniques Using Chromosomally Tagged Fluorescent Bacteria To Study *Listeria monocytogenes* Infection Processes. *Applied and Environmental Microbiology*, 76:3625–3636–, 2010.
- [32] O. Griesbeck, G. S. Baird, R. E. Campbell, D. A. Zacharias, and R. Y. Tsien. Reducing the environmental sensitivity of yellow fluorescent protein. Mechanism and applications. *J Biol Chem*, 276:29188–94–, 2001.
- [33] S. F. Park and G. S. Stewart. High-efficiency transformation of *Listeria monocytogenes* by electroporation of penicillin-treated cells. *Gene*, 94:129–32–, 1990.
- [34] L. Fieseler, S. Schmitter, J. Teiserskas, and M. J. Loessner. Rhamnose-inducible gene expression in *Listeria monocytogenes*. *PlosOne*, 7:e43444–, 2012.



## 4 Manuscript 2

### **The diverse modes of reproduction in stable *Listeria monocytogenes* L-forms**

Patrick Studer<sup>1,#</sup>, Titu Staubli<sup>1,#</sup>, Noemi Wieser<sup>1</sup>, Patrick Wolf<sup>1</sup>, Markus Schuppler<sup>1</sup> and Martin J. Loessner<sup>1,\*</sup>

<sup>1</sup> Institute of Food, Nutrition and Health, ETH Zurich, Schmelzbergstrasse 7, CH-8092 Zurich, Switzerland

#### **Contributions of Titu Staubli to this manuscript:**

- wrote the manuscript (excl. material & methods) based on a draft by Patrick Studer
- developed and performed the micromanipulation technique to isolate single L-form cells

# These authors contributed equally to this work

\* Corresponding author.

Martin J. Loessner, Phone: +41 44 632 3335, E-mail: martin.loessner@ethz.ch



## Abstract

Bacteria are continuously faced with changing environments to which they have to adapt in order to ensure their survival. The rigid peptidoglycan layer surrounding the cellular membrane represents an important component in maintaining the structural integrity of bacteria under unfavorable conditions. However, the cell wall is not only beneficial as it provides a suitable target for antibiotics and also serves as a molecular recognition pattern for the innate immune system during infection of a host cell. Given the right osmotic environment bacteria are able to live without an intact peptidoglycan layer. These cell wall-deficient variants are commonly referred as L-forms which are implicated to be favorable under certain conditions compared to their parent walled forms. In this report, we investigated the mode of proliferation of a stable, non-reverting L-form strain derived from the foodborne pathogen *Listeria monocytogenes*. Time-lapse microscopy revealed multiple reproduction mechanisms including the production of extracellular and intracellular progeny cells as well as protrusion-like structures. Isolation of single internal vesicles using a micromanipulator followed by re-growth to colonies demonstrated their viability. Furthermore, we observed that actively growing L-forms tend to remain connected to each other by thin strands where exchange of cytoplasmic content occurs. In contrast to parental bacteria, the cell division key player FtsZ seems to be dispensable in L-forms as the cell wall-deficient variants were able to proliferate in the presence of a potent FtsZ inhibitor. The here presented data indicate that *Listeria* L-form reproduction is driven by uncoordinated and less efficient division modes. Polyploidy as well as the production of interconnecting strands may help to assure faithful distribution of essential cellular components to the progeny cells in the absence of a sophisticated cytoskeletal machinery.

## Introduction

Bacteria are surrounded by a rigid peptidoglycan layer which confers stability and defines the cellular structure. Despite its pivotal role, numerous bacteria are able to undergo the transition into a cell wall-deficient state, so called L-form. This conversion occurs upon exposure to cell wall synthesis interfering compounds such as  $\beta$ -lactam antibiotics or lytic enzymes. Provided there is an osmotic favorable environment, L-forms cannot only survive but are actually capable of reproducing. The loss of the peptidoglycan layer is a drastic response forcing the bacteria to experience cell physiological and morphological changes.

Bacterial cell division represents a tightly regulated process which is orchestrated by various protein systems in order to ensure the faithful distribution of all essential components required for autonomous life. Rod shaped bacteria mostly proliferate by binary fission giving rise to two identical daughter cells. The tubulin homologue FtsZ is one of the central players during this process by assembling the Z ring at midcell which then recruits further cell division proteins [1, 2]. On the contrary, bacterial L-forms do not divide by simple binary fission. Instead, they employ a wide range of compensatory reactions including intracellular and extracellular vesiculation as well as extrusion-resolution structures [3, 4, 5]. Remarkably, FtsZ along with many other cell division proteins usually involved in proliferation become dispensable in *B. subtilis* L-forms [39]. As an alternative, *B. subtilis* L-forms proliferation is driven by an increased membrane synthesis in combination with an imbalance in the cell surface area to volume ratio [6, 7].

Generation of L-forms in the lab is commonly achieved by interference of the peptidoglycan synthesis or integrity followed by cultivation in osmotically protected medium. Upon several passages in the presence of the inducing agent, L-forms eventually accumulate mutations which inhibit the generation of new cell wall material and enable indefinite proliferation. At this stage the L-form is referred to as stable and can be cultivated in absence of the inducing agent without reverting to the walled state.

We have previously analyzed stable *Listeria* L-forms by biochemical and molecular methods

and disclosed evidence consistent with intracellular vesicles being potential reproduction units [8, 4]. Recently, the role of pathogenicity of *Listeria* L-forms has been assessed which revealed an attenuated pathogenicity as well as the inability to evade the immune system [9]. All presented studies have been conducted with *Listeria* L-form strains that were only able to grow in soft-agar. Most likely the fragile L-form bodies required a solid support to grow on which is provided by the agar matrix. However, growth in soft-agar hampered the application of powerful molecular, biochemical, physiological and genetic applications in their study and prompted us to select for a strain capable of growing in liquid culture.

We have successfully obtained a new stable L-form line derived from the strain EGDe which not only can be cultured in liquid media but also grows in soft-agar and on agar plates. Here, we have characterized the newly generated L-form strain and present the new modes of proliferation. During exponential growth phase we observed that L-forms tend to remain interconnected among each other enabling to exchange cytoplasmic material. Microscopy analysis unraveled various uncontrolled shape deformations giving rise to internal and external vesicles. Isolation of single internal vesicles using a micromanipulator followed by re-growth to colonies demonstrated their viability. Furthermore, it has become apparent that FtsZ is dispensable for proliferation in *Listeria* L-forms confirming the earlier observation made in *B. subtilis* L-forms.

In conclusion, this study provides further insights on the unusual modes of replication exerted by bacterial L-forms.

## Results

### ***Listeria* L-forms proliferate by various uncontrolled shape deformations**

In order to investigate the new mode of replication of the newly generated L-form strain, a method for long-term live cell imaging in a heated microscope chamber was established. Cells grown in liquid culture were spun onto an IBIDI glass bottom dish and overlaid with LLM soft-agar in order to minimize Brownian motion of the cells. This setup allowed us to image L-form proliferation for more than two days. Generally, time-lapse movies revealed a high degree of membrane dynamics leading to very aberrant shape perturbations which finally gave rise to new L-form cells. Often, proliferation resembled a budding mechanism where a cell forms an outgrowth leading to two daughter cells (Figure 1A, Movie S1A). In some cases formation of multiple evaginations were observed which resolved almost simultaneously into several smaller cellular structures (Figure 1B, Movie S1B). Interestingly, newly formed cells tend to remain connected with each other by thin strands of presumably membrane-like material (Fig 1 C-D). These strands often contained small granules that might represent potential progenies (arrowhead in Figure 1C). Due to the fast Brownian motion the strands and its granules could not be tracked by time-lapse microscopy (Movie S1C). The interconnection among L-forms leads to a meshwork that can be even seen by eye in a static liquid culture where long thread-like assemblies range from the bottom to almost the top of the culture (Figure 1D and 1F). In addition to the formation of external membrane perturbations, intracellular vesiculations have been found to be favored in L-forms grown in soft-agar medium. Remarkably, internal vesicles, appearing in the phase contrast light gray, harbor themselves one or more smaller vesicles which we called vesicles-within-vesicles (VWV). Based on the phase contrast image, it is likely that they contain cytoplasm from the mother cell indicated by the same grayscale (VWVs; Figure 1 E, arrowhead). The emergence as well as the fate of the internal vesicles and the VWVs turned out to be difficult to monitor by time-lapse microscopy. However, it became clearly evident that they grow and increase in size along with the mother cell (Movie 1D). Irrespective of the mode of reproduction we observed that upon

extensive multiplication L-forms stop dividing, however still increase in size for several hours.

### ***Listeria* L-forms reach stationary phase after two days and contain multiple chromosomes**

Due to the new mode of replication employed by EGDe L-forms, it was of interest to determine their growth kinetics in liquid culture. As it is well-known that quantification of L-form growth using different methods may lead to dissimilar results [11], three different methods have been applied. Determination of the chromosome copy number by real time PCR over time was consistent with the counted colony forming units (CFU), indicating that L-forms reach stationary phase only after two days (Figure 2). The followed consistency of the number of chromosomes confirms that there is no further replication occurring. The decrease of the CFU numbers over the next twelve days can be likely attributed to deprivation of nutrients. In contrast, the optical density measurements showed a slightly different outcome peaking only seven days later. These findings coincide well with the observations made during time-lapse microscopy where we learned that older, non-replicating L-forms still continue to metabolize and increase in size, explaining the late peak of the optical density measurement. Based on the above-presented data, the average chromosome number per cell could be deduced. During exponential phase (= day 1) *Listeria* EGDe L-forms contain in average 34 chromosomes per cell. The containment of multiple chromosomes is in accordance with the previously detected polyploidy of  $18.0 \pm 3.6$  for a different *Listeria* L-form strain [3].

### **Vesicle-with-vesicles (VWVs) represent viable progeny cells**

Microscopy analysis showed the formation of vesicles-within-vesicles which appeared to contain cytoplasmic material from the mother cell (Figure 1E). In order to verify this hypothesis and to assess the containment of all the essential components to start up life, specific reporters were used. First of all, the DNA stain Hoechst indicated the presence of nucleic acid within VWV and mother cell cytoplasm (Figure 4C, arrowhead). Transformation of the newly generated

L-form strain allowed us to induce constitutive expression of cytoplasmic fluorescent proteins (RFP and GFP). The subsequent confocal microscopy analysis indicated clear fluorescent signals within VWV confirming that they must have obtained cellular components from the mother cell (Figure 4A-B, arrowheads). On the contrary, internal vesicles harboring the VWV clearly did not contain any cytoplasmic material originating from the surrounding cell (Figure 4B, arrow). Although these results strongly support the idea of VWV representing viable reproduction units, the ultimate proof would involve the ability to re-grow to colony starting from isolated vesicles. Hence, a micromanipulation technique was applied to isolate VWVs. We first demonstrated the capability of this procedure by capturing single L-form cells using a 6  $\mu\text{m}$  wide capillary followed by spotting on to fresh LLM-Agar plates. After 12-16 days of incubation, L-form colonies appeared on plates, indicating that one single L-form can re-grow to a colony. In order to verify the capture of a single cell only, GFP and RFP expressing L-form were mixed in a 1:1 ratio. Thereof, either an individual green or red fluorescently labeled L-form was aspirated into the capillary and transferred into 100  $\mu\text{l}$  broth media which was then spotted on LLM-Agar plates without antibiotics. Analysis by microscopy of the appeared colonies revealed a pure culture of either GFP or RFP expressing L-form cells (Figure 3). The result strongly implies the capability of isolating single *Listeria* L-form cells by a our used system. Of course, one has to consider the fact that there is still the possibility of capturing two cells, expressing the same fluorescent protein, which could also lead to the same result. However, we conducted this experiment several times always resulting in a pure culture. Based on that out outcome, we were confident to reliably isolate VWV by our system. Single L-form cell containing large VWV was aspirated into a 6  $\mu\text{m}$  wide capillary (Figure 4D1). Subsequently, the VWV residing in the mother cell were released into the capillary by mechanically disruption of the surrounding membrane using a second 0.4  $\mu\text{m}$  micro-pipette (not depicted) (Figure 4D2). The liberated cells could then be transferred and re-inoculated into fresh soft-agar. Inoculation for 12 to 16 days resulted occasionally in L-form colonies (Figure 4D3). Following verification for GFP fluorescence under the microscope always corroborated the origin from the initial culture (Figure 4D4). Quantification revealed a successful

rate of 27% of VWV to re-grow to colonies. Important to point out that the positive control (= single isolated L-form cell) showed only a slightly higher percentage. The content of a ruptured single L-form cell devoid of any internal vesicles served as negative control. In only one case out of 20 the negative control also resulted in growth. It is conceivable that an L-form might have adhered to the outside of the capillary or very small VWVs invisible under the microscope were still present (Figure 4E).

These findings highly support the idea of VWV representing viable reproduction units which might be able to proceed to proliferate upon burst of the mother cell membrane. Considering the uncoordinated mode of reproduction in L-forms, it was not surprising that only a fraction of the isolated vesicles resulted in growth. Isolated VWV most probably do not always obtain all the essential components to be viable.

### **Interconnecting membranous strands enable exchange of cytoplasmic content**

During early phase of growth *Listeria* L-forms remain connected with each other by thin membranous strands (Figure 1C-D, F). We were interested in investigating whether these strands form a continuum and therefore allow an exchange of cytoplasmic material. Analysis of L-forms expressing constitutively GFP indicated the presence of fluorescent proteins implying continuous structures (Figure 5A). In order to measure an active exchange of cytoplasmic content fluorescence loss in photobleaching (FLIP) was applied where fluorescence signal of specific cells were bleached. Assuming there is continuity of membranous threads between the bleached cell and any neighboring L-form, a recovery of fluorophores should be observed. In a first approach multiple cells in a colony were bleached and fluorescence intensity was then monitored within the cells before and after bleaching (Figure 5D-E). As represented in Figure 5D-E only one cell (= ROI 10) showed partial fluorescence recovery revealing a connecting thread to a surrounding L-form. As a next step, we focused on cells showing a clear interconnection by membranous structures visible in the DIC channel. Photobleaching of one cell and simultaneously monitoring the fluorescent signal of all cells of interest indicated exchange of molecules. The result is summarized in Figure

5B-C indicating that the fluorescence of the bleached cell (ROI 1) decreased by more than 80% upon the laser beam followed by a gradual recovery. Consistently, the fluorescence signal of the neighboring cell (ROI 3) decreased after bleaching due to the GFP molecule movement into the adjacent L-form. An additional cell without any threads (ROI 2) served as control confirming no alteration in the fluorescent intensity over time of recording.

In conclusion, the conducted measurements strongly suggest movements of cytoplasmic components among interconnected *Listeria* L-form cells.

### **A functional FtsZ becomes dispensable in *Listeria* L-forms**

The central element in binary fission is the formation of the Z-ring exerting the constriction during the final step of cytokinesis. The Z-ring is composed of FtsZ monomers and localizes at the septum [10]. To gain more information on *Listeria* L-form reproduction, FtsZ localization was studied by constructing a mutant expressing a fusion protein of FtsZ-GFP. In parental cells FtsZ-GFP localized at the division sites as it has been described in the literature for other bacterial species, confirming the functionality of the mutant (Figure 6C). In the majority of L-forms FtsZ-GFP formed various foci within the cells (Figure 6A). In a few cases though, 3D reconstruction revealed long filaments composed of FtsZ-GFP molecules spanning throughout the cells. Formation of FtsZ filaments is therefore still possible in roundly shaped L-forms (Figure 6B, Movie S2). However, no ring-like structures could be observed implicating a role in L-form division. In order to verify the dispensability of the Z-ring, the FtsZ-inhibitor PC190723 (8  $\mu\text{g}/\text{ml}$ ) was used. Parental *Listeria* grown in the presence of the inhibitor resulted in long filamentous cells underlining the inability to form a proper division septum in the absence of a functional FtsZ ring (data not shown). In contrast, *Listeria* L-forms could readily replicate and displayed no morphological abnormalities if exposed to PC190723 (Figure 6E). We therefore conclude that FtsZ becomes dispensable in *Listeria monocytogenes* L-forms.



## Discussion

During the last few years, it became evident that bacteria can also survive and proliferate in the absence of its surrounding peptidoglycan layer. Here, we investigated the new mode of reproduction of cell wall-deficient *Listeria*. In contrast to parental cells, they do not divide by binary fission but rather proliferate by various shape deformations including internal and external vesiculation as well as budding-like processes (Figure 7). We found that cell division does not rely on a functional FtsZ ring and is characterized by a significant slower growth rate in comparison to its walled form. Most likely proliferation occurs independent of any major cytoskeleton cell division protein as it has been reported for *B. subtilis* L-forms [5, 6]. The intriguing question arising considers what is the driving force of *Listeria* L-form reproduction. The multiple forms of progeny cells seem to be the result of the high degree of membrane dynamics which became apparent during time-lapse microscopy. Excess of phospholipids induced by an imbalance of cell surface area to volume ratio or overproduction of membrane synthesis has been implicated as the decisive factor for L-form proliferation [7]. We assume that the idea of a purely biophysical directed replication mode also applies for *Listeria* L-forms. It would well explain the likely uncoordinated processes as well as the various forms of reproduction units. Interestingly, similar shape deformations can be induced in artificial lipid vesicles indicating the dispensability of any proteins in the process. Such experiments were conducted with giant unilamellar vesicles (GUVs) which are most suitable due to their huge size (more than 10  $\mu$ l). As proposed for L-forms, *in vitro* proliferation requires an excess of lipids which can be achieved by several applications. Common methods include feeding with fatty acids, exposition of GUVs to substances with long hydrocarbon chains or simply alteration of the osmolarity [11, 12, 13].

The undirected proliferation mode does not guarantee a faithful distribution of all essential components to the produced progenies. This is reflected by the fact that only a fraction of isolated VWVs are able to re-grow to colonies. Despite the absence of sophisticated protein systems and the reliance on simple random processes, it is intriguing that L-forms still manage to give rise

to a reasonable high number of viable daughter cells. In particular, the distribution of an entire chromosome to the progenies is difficult to conceive without the guidance of a segregation system. We therefore assume that the acquirement of polyploidy in L-forms is crucial by increasing the successful rate for a random distribution to newly formed entity. Recently, it has been shown that GUVs filled with DNA can undergo spontaneous division upon extracellular addition of vesicle membrane precursors. This process is accompanied by the distribution of the DNA into the new daughter GUVs. Remarkably, GUVs containing higher concentrations of DNA showed an elevated spontaneous division rate compared to GUVs comprising lower or no amounts of DNA [14]. It is therefore conceivable that the chromosomes themselves define at which site within an L-form new membrane bulges and protrusions are formed.

As an alternative strategy to partition essential components membranous thread like structures are employed. Upon proliferation the resulting progenies tend to remain connected allowing diffusion of important substances at later stages during cell division. This way not all the crucial molecules have to be entrapped at the time a cell is created, thereby increasing the chance of producing a viable reproduction unit. Finally, the thin strands rupture by a yet unknown factor.

Bacterial L-forms can be derived from many species. Although they all lack a cell wall they may differ in their physiology and mode of proliferation. *Listeria* L-form reproduction shares some similarities with *B. subtilis* L-forms characterized by uncoordinated shape deformations and subsequent production of external cells. However, the formation of viable vesicles-within-vesicles is likely a unique feature of *Listeria* L-forms. Proliferation of cell wall-deficient bacteria is not always restricted to unorganized and random processes independent of any known cytoskeletal protein. *E. coli* L-forms are actually more elaborate and still employ a Z-Ring for asymmetrical constrictions. Furthermore, they still require a functional peptidoglycan synthesis for successful division [15]. Very recently, reversion of *E. coli* L-forms to rod-shaped bacteria has been recorded. Quantification of subcellular localization studies revealed that the reconstitution of the cell wall occurs according to a well-defined trajectory guided by MreB filaments, underlining the more directed and sophisticated cell biology in *E. coli* L-forms. Additionally, the short time-scale to

convert from a parental cell to an L-form followed by reversion to rods, supports the idea that no genetic mutations are required [16]. In contrast, the generation and proliferation of gram-positive L-forms derived from *B. subtilis* clearly relies on two mutations [7]. The here presented *Listeria* L-form strain harbors several mutations as sequencing analysis revealed. However, it currently remains elusive as to whether any of the detected genetic alterations are relevant for the conversion and new mode of reproduction.

In conclusion, these findings contribute to a better understanding of the diverse modes of proliferation employed by bacterial L-forms. We provide further support that reproduction is simply based on biophysical processes leading to an uncoordinated and random distribution of all the essential components.

# Material and Methods

## L-form induction, stabilization and growth

The new L-form strain was generated as described previously [3]. Briefly, an overnight culture of walled *L. monocytogenes* EGDe was inoculated into *Listeria* L-form medium (LLM) (37 g/l BHI (Biolife, Italy), 150 g/l sucrose, 2.5 g/l  $\text{MgSO}_4 \times 7 \text{ H}_2\text{O}$ , 3 g/l milk serum powder, 3 g/l agar) for 2 h. 100  $\mu\text{l}$  was then plated on LLM-Agar plates supplemented with 50  $\mu\text{g/ml}$  penicillin G. After several days to weeks, growing colonies were isolated and further sub-cultivated in LLM soft-agar containing penicillin G. Stabilization was accomplished by gradually reducing the penicillin G concentration (50, 25, and 12.5  $\mu\text{g/ml}$ ) while passaging. L-forms able to grow in the absence of the  $\beta$ -antibiotic were used to inoculate into LLM liquid culture. After 1-2 weeks growth could be observed. Several passages followed in order to adapt the L-forms to the liquid medium. Finally, they were plated onto LLM-Agar plates (LLM with 1% agar). A single colony from this plate was then inoculated into liquid medium, and a glycerol stock was prepared from this culture. For the growth of L-forms in liquid culture we slightly adapted the medium. Milk serum powder was replaced by 1% of heat-inactivated horse serum (37 g/l BHI, 150 g/l sucrose, 2.5 g/l  $\text{MgSO}_4 \times 7 \text{ H}_2\text{O}$ , 3% heat-inactivated horse serum). L-forms were always cultivated statically in LLM at 32°C.

## Time-lapse analysis of L-form proliferation

A 1-3 day old L-form liquid culture was vortexed and diluted 1:100 in LLM. 500  $\mu\text{l}$  thereof was transferred into a IBIDI  $\mu$ -Slide 2 well glass bottom dish. After a centrifugation step at 250 g for 5 min, the supernatant was discarded and the attached cells overlaid with 1 ml of approximately

37°C warm LLM soft-agar. After the soft-agar solidified, the IBIDI dish was closed air-tight with Parafilm in order to minimize evaporation of the medium. Time-lapses were then recorded in a pre-warmed microscope chamber at 32°C using a Leica TCS SPE microscope.

## Quantification of L-form growth

A 1 day old L-form culture was diluted 1:10000 in LLM-Broth. Thereof, 1 ml cultures were prepared in 2 ml Eppendorf tubes. After 0, 1, 2, 3, 7 and 14 day(s) L-form growth was monitored by plating on LLM-Agar, optical density measurement and determination of chromosome numbers. For every time point and method, three of the 1 ml cultures were used. For chromosome number determination 25  $\mu$ l of a homogenized L-form culture was mixed with 25  $\mu$ l of 2% Triton X-100 and incubated at 99°C for 30 min, vortexing every 10 min. This extract was then diluted 1:100 in deionized water (Milli-Q) to minimize inhibitory effects during quantitative real time PCR measurements. qRT-PCR was performed on a Rotor-Gene<sup>TM</sup> 6000 device (Corbett Life Science) using KAPA SYBR FAST Universal qPCR Kit (Kapa Biosystems) according to the manufacturer's instructions. The *rpoB* gene was chosen as representative for chromosome numbers. The used primers were *rpoB*\_F: 5'-CGCGAATCAGTGAAGTACTTG-3' and *rpoB*\_R: 5'-ATCCTCAATTGGCGAAATATC-3'. *L. monocytogenes* EGDe chromosomal DNA was used to prepare a standard curve with a defined copy number allowing to quantify the absolute number of chromosomes in the extracts. All samples were measured in duplicates.

## *Listeria* L-forms transformation

Initially, we transformed our L-forms with an adapted protocol of a PEG-based method described earlier [17]. Briefly, 100  $\mu$ l of a 2-3 d old L-form culture was mixed with 20  $\mu$ l of plasmid and 150  $\mu$ l of PEG8000 solution (3 g PEG was dissolved in 10 ml LLM and filter sterilized). After gentle mixing, the solution was incubated for 10 min on ice, followed by 10 min at 32 °C. 1 ml of LLM was then added and the L-forms were incubated for 4 h at 32 °C before being plated on LLM-Agar supplemented with the appropriate antibiotics. Later during our experiments we observed higher transformation efficiencies by using electroporation. Briefly, 4 ml of a 2-3 d old

L-form culture was cooled on ice and washed two times (5,000 g, 5 min, 4 °C) with ice-cold sucrose-glycerol washing buffer (SGWB; 10% glycerol, 500 mM sucrose; pH adjusted to 7 with 100 mM NaOH; filter sterilized) that was described in an earlier publication. The final L-form pellet was resuspended in 50  $\mu$ l SGWB and mixed with 10  $\mu$ l of plasmid. After electroporation at 2 kV (400  $\Omega$ , and 25  $\mu$ F), 1 ml of LLM was added and the cells were recovered for 4 h at 32°C before being plated on LLM agar supplemented with appropriate antibiotics.

## Generation of L-forms expressing GFP and RFP

The GFP expressing L-form strain was generated by transformation with the integrative plasmid pPL3e/*gfp* [18] where GFP expression was placed under the control of the constitutive promoter  $P_{Hyper}$ . L-form mutant expressing RFP was generated by using the vector pPL2/ $P_{Xyl}$  (Schmitter *et al.*, unpublished). The *Listeria* codon-optimized *rfp* version was cloned under the regulation of the constitutive  $P_{Xyl}$  promoter using the primers PstI-RBS-LmRFP-F (5'-TTT CTG CAG AGG AGG GAA TCG ATA TGG TTG-3') and SalI-Stop-LmRFP-R (5'-TTT GTC GAC TTA ATT AAG TTT ATG GCC TAA TTT G-3'). The vector was then transformed into L-forms. Successful integration into the chromosomes was verified by PCR and microscopy.

## Construction of the FtsZ-GFP labeling mutant

For the labelling of FtsZ with GFP under the control of an inducible rhamnose promoter, we used two different plasmids (pAUL-A and pPL2). First, *ftsZ* was amplified from chromosomal *L. monocytogenes* DNA using the primers ftsZ-FkpnI (5'-CTT AAC TAA AAT GAG TGG TAG GAG GCA ATA ATA TGT TAG-3') and ftsZ-Rlinker (5'-CCT TTA CTC ATT TCT AAA CGA CTT CCG CGA CGG TTA CGG-3'). Next, the gene encoding GFP was amplified using the primers gfp-Flinker (5'-GTC GCG GAA GTC GTT TAG AAA TGA GTA AAG GAG AAG AAC-3') and gfp-RkpnI (5'-TCT AGA GGA TCC CCG GGT TTA TTT GTA TAG TTC ATC CAT-3'). The PCR products as well as the plasmid pAUL-A were linearized and assembled by "Gibson assembly" resulting in pAUL-A/ $P_{Rha}$ -*ftsZ*-*gfp* [19]. As an alternative, we constructed pPL2/ $P_{Rha}$ -*ftsZ*-*gfp* that harbors a chloramphenicol resistance gene and a PSA integrase which

integrates the plasmid at the 3' end of the *tRNA<sup>Arg</sup>* gene. The fragment *P<sub>Rha</sub>-ftsZ-gfp* was amplified from the constructed pAUL-A/*P<sub>Rha</sub>-ftsZ-gfp* using the primers *P<sub>Rha</sub>-pPL2-F-inv* (5'-AAT TCC TGC AGC CCG GGG GAT ATT CCG TGA TAA TTT GGT-3') and *gfp-Rinverted* (5'-CGC TCT AGA ACT AGT GGA TTA TTT GTA TAG TTC ATC CAT-3'). The PCR product was then ligated into linearized pPL2 by Gibson assembly. Successful integration into the chromosomes was verified by PCR and microscopy.

## Inhibition of FtsZ ring formation by the drug PC190723

A stock of PC190723 (Calbiochem; Merck Chemicals Ltd.) was prepared in DMSO. Overnight cultures of parent *Listeria* and 1 day old L-forms were diluted 1:10,000 in LLM supplemented with PC190723 or the same amount of DMSO as control and incubated static at 32 °C. For enumeration, the cultures were plated on LLM agar. Every sample was plated in duplicate and the whole experiment was performed in triplicate.

## Micromanipulation

The micromanipulator system consists of two TransferMan (Vaudau-Eppendorf TransferMan NK2) in combination with a CellTram Air (Vaudaux-Eppendorf) and a CellTram Vario (Vaudaux-Eppendorf). In order to isolate single cells 80  $\mu$ l of diluted liquid culture was placed on a cover slip and subjected to an inverted Leica TCS SPE microscope (Leica Microsystems GmbH, Wetzlar, Germany). TransferMan equipped with a 6  $\mu$ m capillary and connected to a CellTram Air was used to aspirate individual cells. To assure the capture of only one L-form, the Air bubble was pushed first all to the front to exclude trapping of unwanted structures. Subsequently, the capillary was positioned right in front of the cell of interest. Gently aspirating a small volume resulted in capture of the cell. The content was then temporary transferred into a 100  $\mu$ l LL-Broth which was later used inoculated into fresh media.

Isolation of vesicles-within-vesicles: Capture of a single L-form containing VWV was achieved as described above. Next, the second TransferMan equipped with a thin 0.4  $\mu$ l pipette was used to poke and mechanically rupture the cell membrane of the captured L-form. The freed structures

were released into the 6  $\mu\text{m}$  wide capillary which was then transferred and re-inoculated according to the procedure explained above.

## Microscopy

Confocal microscopy, except for the FLIP experiments, was performed on a Leica TCS SPE system (Leica Microsystems GmbH, Wetzlar, Germany). The following dyes were used: 50  $\mu\text{g}/\text{ml}$  FM<sup>®</sup> 4-64 (Life Technologies), 50  $\mu\text{g}/\text{ml}$  Hoechst 33342 (Life Technologies), 50  $\mu\text{M}$  CellTrace<sup>™</sup> BODIPY<sup>®</sup> TR methyl ester (Life Technologies). The cells were mixed with the dyes and following an incubation time of 5 min, observed without washing. The microscope pictures were prepared for publication using ImageJ Software (Version 1.48e).

## Fluorescent loss in photobleaching

Imaging was performed on a Leica TCS SP5 system maintained by the Center for Microscopy and Image Analysis at the University of Zurich. 4-5  $\mu\text{l}$  of an approximately 1 day old GFP expressing L-forms were spotted on a microscope slide and a cover slip was put on top of the cells. In certain cases, the L-forms were spotted onto an agar pad containing 500 mM sucrose in order to minimize the motion of the cells. Recording and bleaching of the cells was performed using a laser with a wavelength of 488 nm. The resolution of the photomultiplier was set to 12 bits and the laser intensity during measurement was adjusted to a value where no oversaturated pixels were detected. 2-3 bleach cycles were performed with a laser intensity of 80-100%. The DIC channel was recorded in parallel with the fluorescence channel in order to control that the focal plane stayed constant during the experiment and that the cells did not move too much.

## Acknowledgements

The authors acknowledge the assistance and support of the Center for Microscopy and Image Analysis, University of Zurich for performing FLIP experiments.



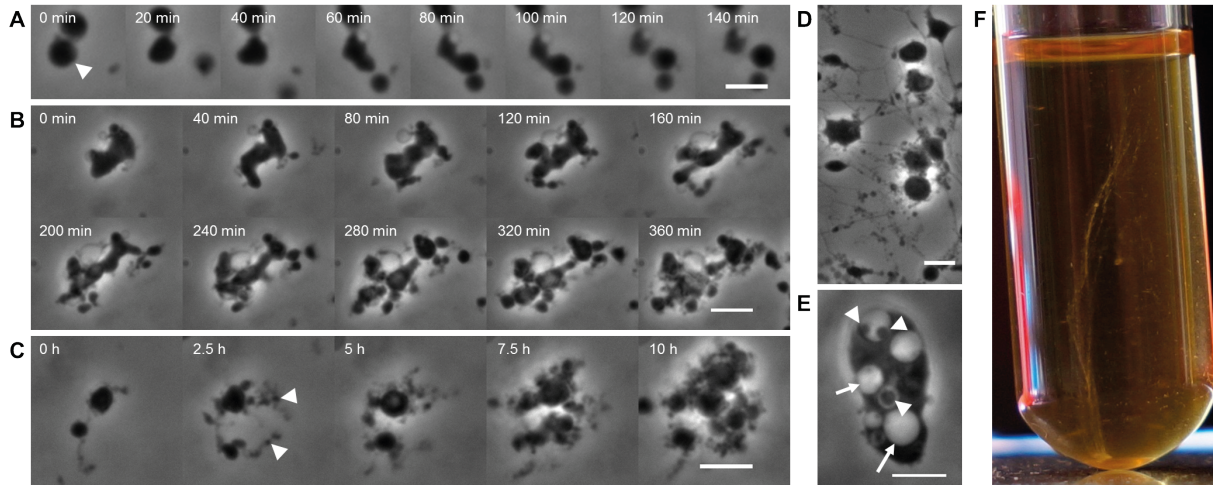


**Figure 1:** *Listeria* L-forms employ diverse modes of reproduction. A. Generation of a new L-form progeny by a budding-like process (cell highlighted by arrowhead). B. L-forms often produce multiple bulges and protrusions that eventually resolve into new progenies. C. During early growth phase L-forms tend to remain connected upon division by thin membraneous strands (arrowhead). D. Sometimes a massive network interconnecting multiple L-forms with each can be built. E. L-forms are able to form intracellular vesicles containing so called vesicles-within-vesicles (VWVs; arrowheads). The content of the VWV appears to exhibit the same grayscale as the mother cell cytoplasm whereas the appearance of the material within the vesicles (arrows) resembles the surrounding medium. F. The extensive interconnections among cells result in long thread-like assemblies ranging from the bottom to almost the top of static liquid culture. Scale bars: 4  $\mu\text{m}$  for A, 8  $\mu\text{m}$  for B-E.

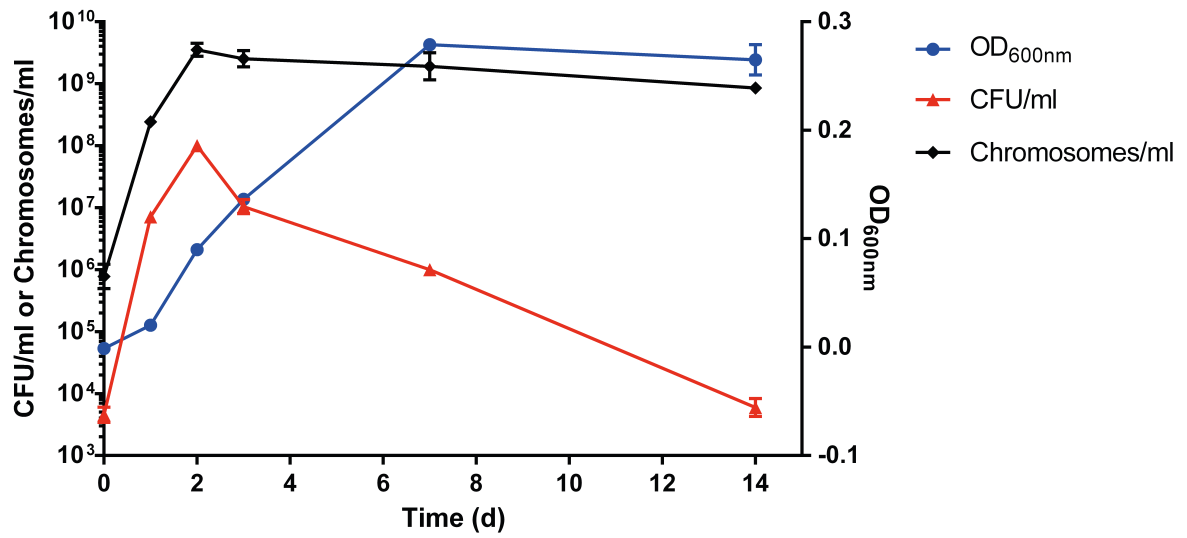


**Figure 2:** *Listeria* L-forms reach stationary phase after 2 days. Growth curve was determined by three different methods including optical density measurement, CFU determination and chromosome quantification by quantitative real time PCR. Note that the y-axis for CFU/ml and chromosomes/ml is in a logarithmic scale whereas the y-axis for OD<sub>600nm</sub> is represented in a linear scale.

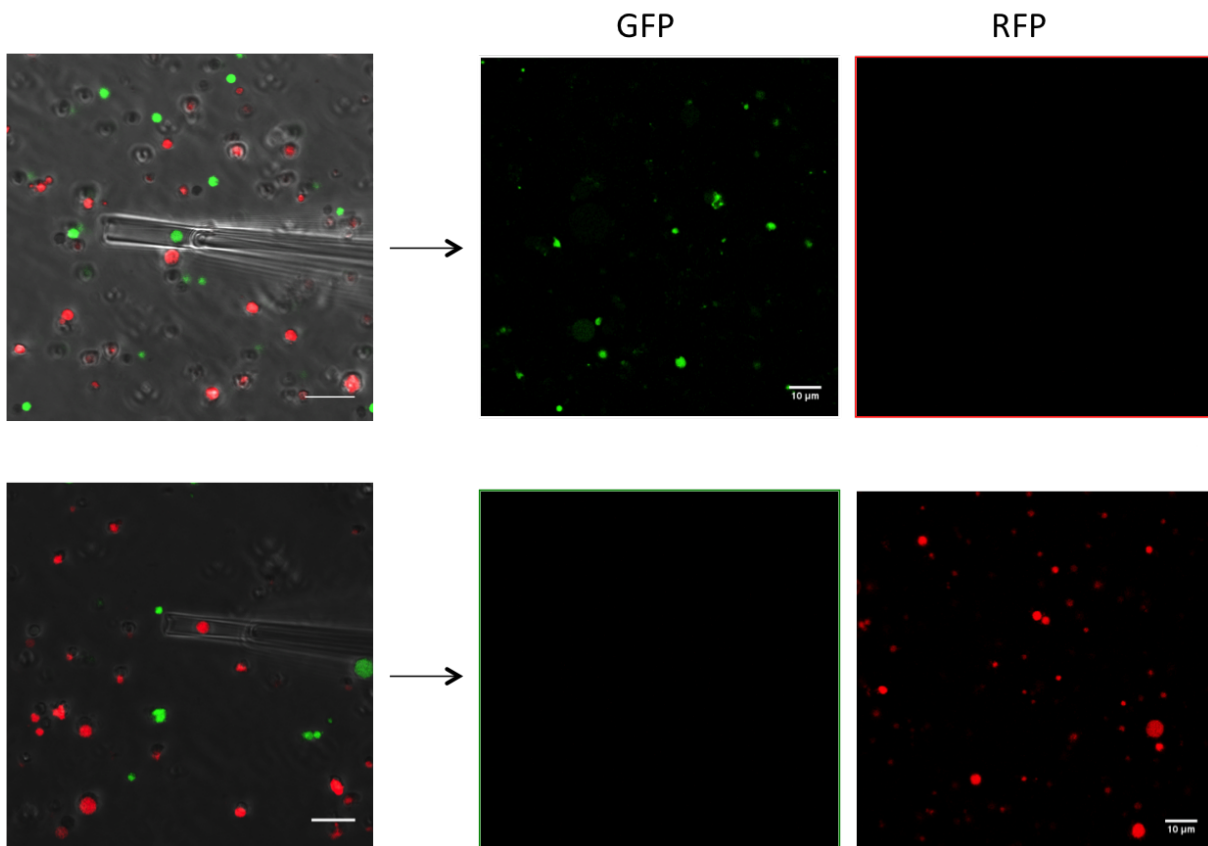


**Figure 3:** Proof of concept for the successful application of a micromanipulator to isolate single L-form cells which are then able to re-grow to colonies. Capture of individual cells out of a mixture of either GFP or RFP labeled L-forms resulted in colonies expressing the respective fluorescent protein only. Scale bars: 10  $\mu\text{m}$ .

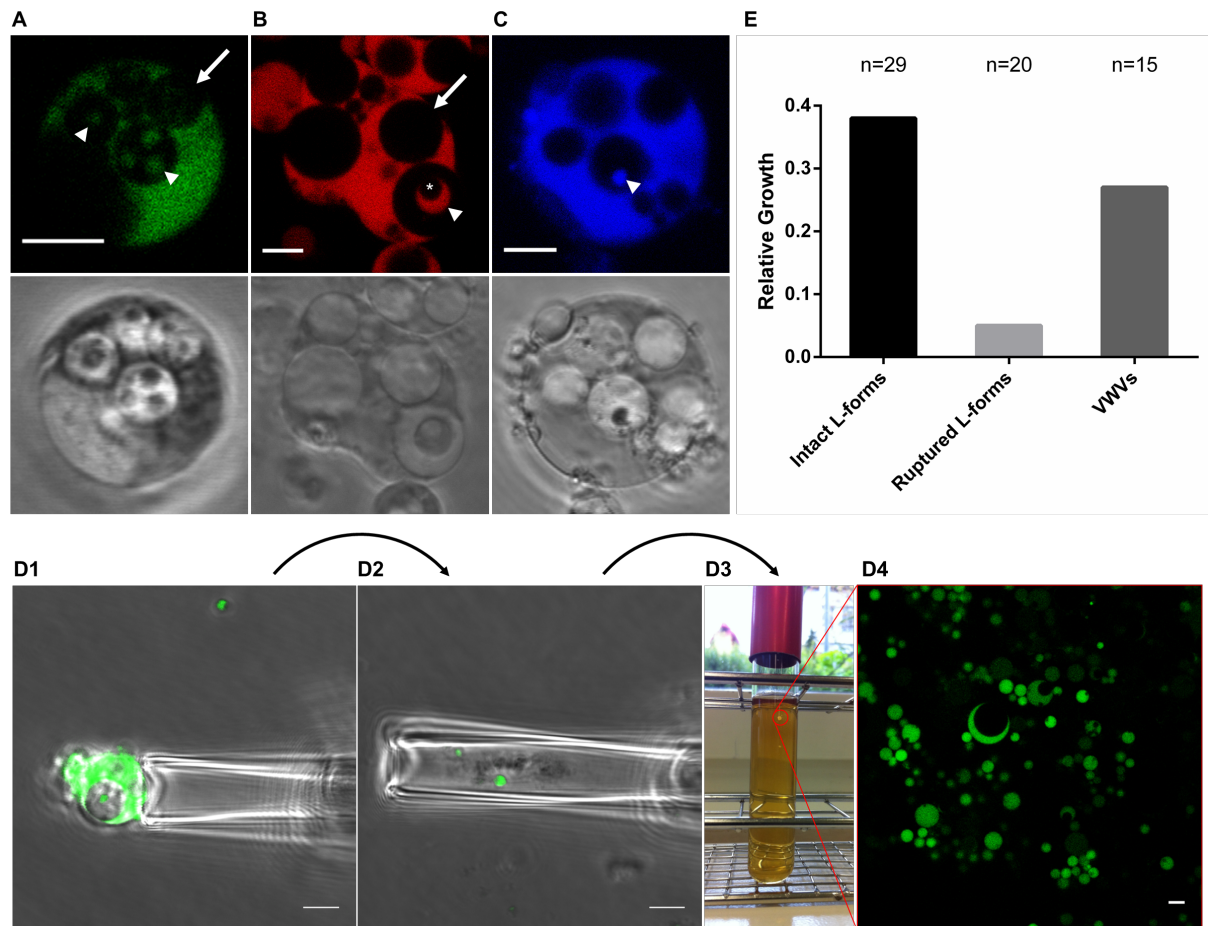


**Figure 4:** VWVs represent viable reproduction units indicated by specific markers and the ability to re-grow to colonies. A-C. VWVs (arrowheads) contain cytoplasmic content obtained from the surrounding mother cell. Confocal microscopy reveals the presence of GFP (A) and RFP (B) produced by the L-forms. VWVs contain DNA as indicated by the Hoechst33342 staining (C). D-E. Isolation of single VWV using a micromanipulation followed by re-growth to colonies indicates their viability. D1-D4 shows a representative image series of how single VWVs were isolated and observed for their capability to re-grow to a colony. E. Percentage of samples that show growth after being isolated by micromanipulation and re-inoculation into fresh soft-agar. Scale bars: 4  $\mu\text{m}$  for A-C, 5  $\mu\text{m}$  for D.

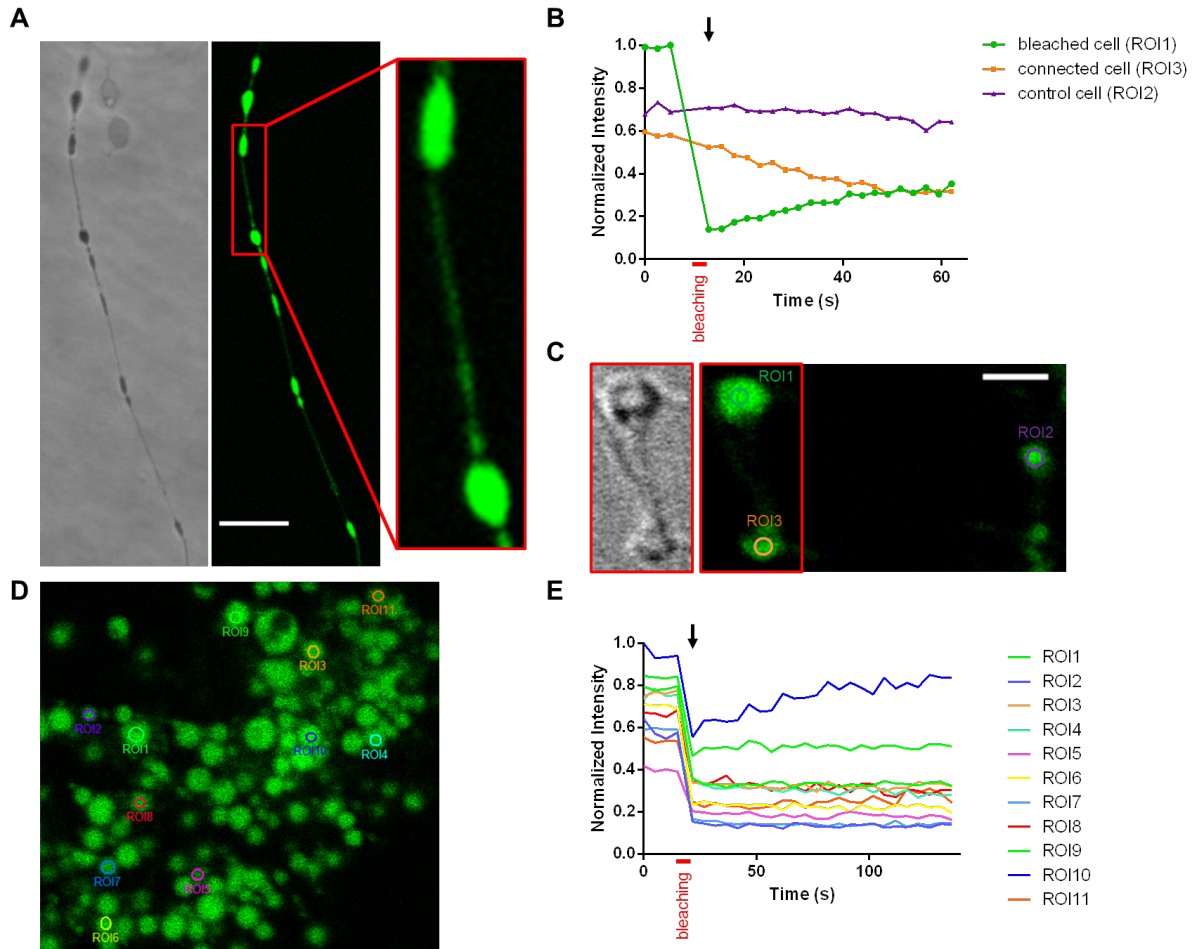


**Figure 5:** Thin strands interconnecting cells enables exchange of cytoplasmic material. **A.** Connecting structures are filled with cytoplasmic GFP produced by the L-forms. **B-C.** Fluorescence Loss in Photobleaching (FLIP) confirmed the formation of a continuum and the ability to exchange cytoplasmic material. After bleaching the signal within the bleached cell drops by more than 80%. An immediate recovery of the fluorescent signal can be measured whereas the intensity of the neighboring cell (ROI3) decreases. An unconnected cell in close proximity (ROI2) served as a control which remained unaffected throughout the experiment. Only a minority of L-forms are able to exchange cytoplasmic molecules. Eleven cells were bleached (**D**) and analyzed for fluorescence recovery. In only one cell (ROI10) an instant increase of GFP signal could be detected after bleaching (arrow in **E**).

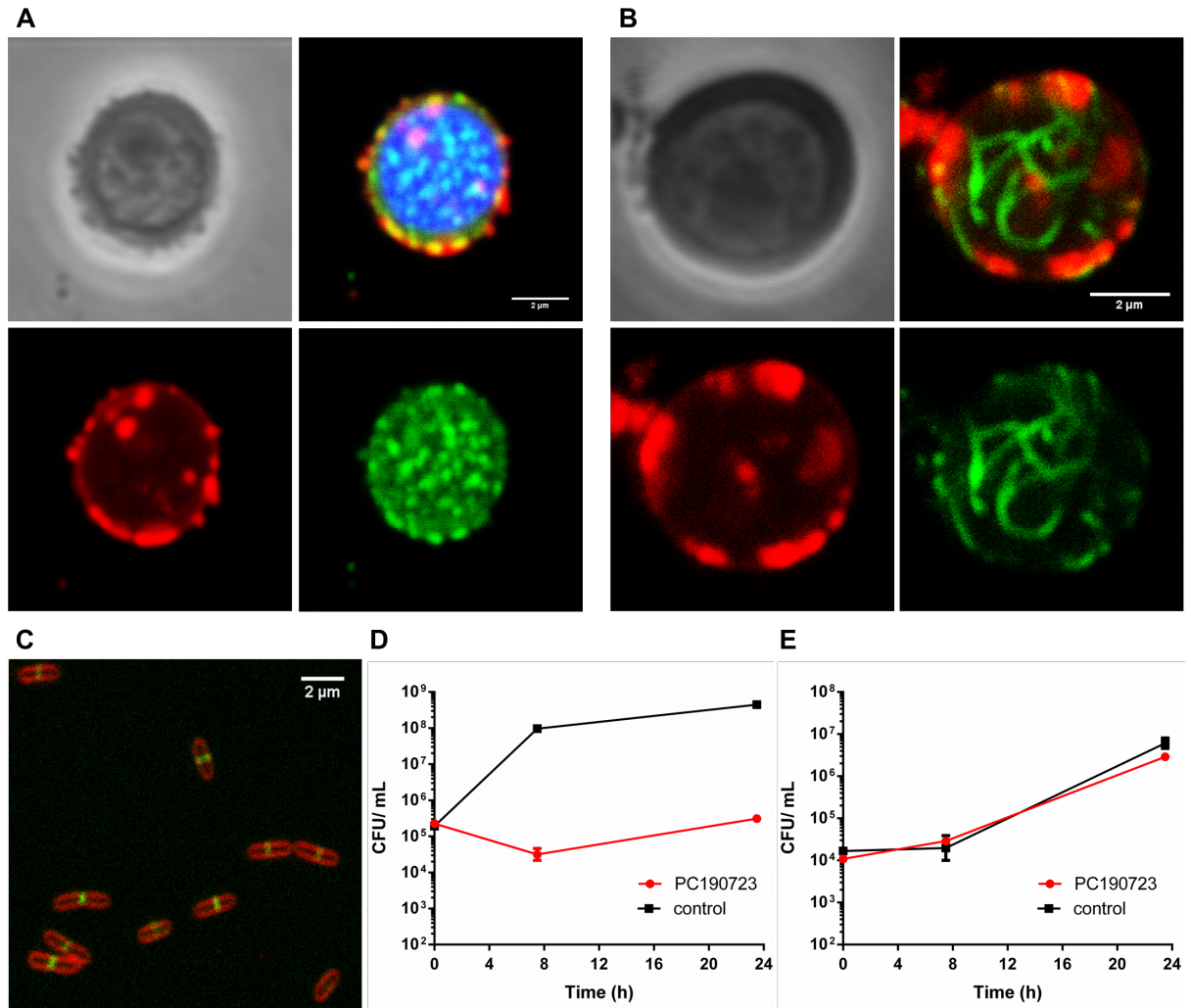


**Figure 6:** FtsZ is dispensable for L-form proliferation. A-B. Labelling of FtsZ with GFP shows two different localization patterns in L-forms. In most of the L-forms spotty GFP foci are detectable dispersed throughout the cell (A) whereas a few cells contain several FtsZ-GFP filaments (B). C. In parental cells FtsZ-GFP localizes to the septum. The cellular membrane was stained with FM4-64 (red). The DNA was stained with Hoechst 33342 (blue). D-E Growth analysis of parental cells and L-forms in the presence of the FtsZ inhibitor PC190823. D. Parental cells are not able to divide in the absence of functional FtsZ filaments. E. On the contrary, L-form proliferation is not dependent of a Z-ring.



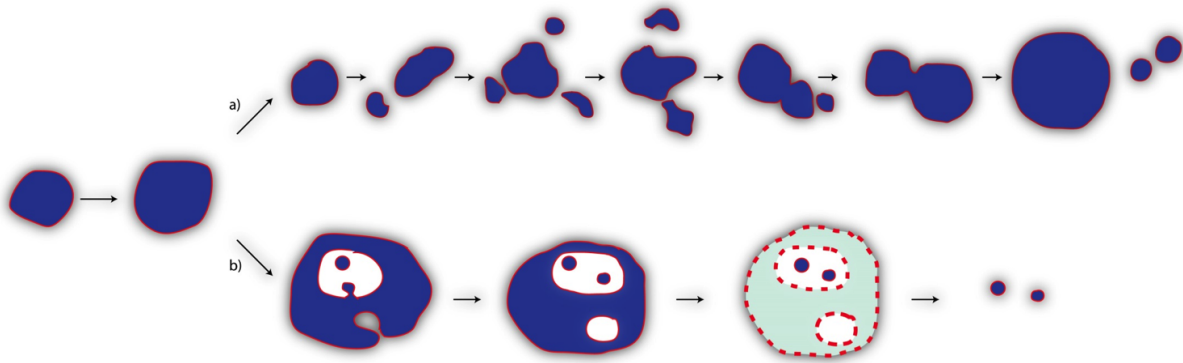


**Figure 7:** Schematic representation of the different modes of *Listeria* L-form reproduction. A. Various shape deformations including extrusions and budding-like structures lead to the formation of externally produced progeny cells. Newly formed cells may remain connected by thin membraneous strands allowing to exchange cytoplasmic compounds. B. The membrane can also bud inwards giving rise to internal vesicles which are released upon burst of the mother cell.

## References Manuscript 2

- [1] J. Lutkenhaus, S. Pichoff, and S. Du. Bacterial cytokinesis: From Z ring to divisome. *Cytoskeleton (Hoboken)*, 69(10):778–790, Oct 2012.
- [2] D. W. Adams and J. Errington. Bacterial cell division: assembly, maintenance and disassembly of the Z ring. *Nat Rev Microbiol*, 7(9):642–653, Sep 2009.
- [3] Y. Briers, T. Staubli, M. C. Schmid, M. Wagner, M. Schuppler, and M. J. Loessner. Intracellular Vesicles as Reproduction Elements in Cell Wall-Deficient L-Form Bacteria. *PlosOne*, 7:–, 2012.
- [4] S. Dell’Era, C. Buchrieser, E. Couve, B. Schnell, Y. Briers, M. Schuppler, and M. J. Loessner. *Listeria monocytogenes* L-forms respond to cell wall deficiency by modifying gene expression and the mode of division. *Mol Microbiol*, 73:306–22–, 2009.
- [5] M. Leaver, P. Dominguez-Cuevas, J. M. Coxhead, R. A. Daniel, and J. Errington. Life without a wall or division machine in *Bacillus subtilis*. *Nature*, 457:849–53–, 2009.
- [6] R. Mercier, P. Domínguez-Cuevas, and J. Errington. Crucial role for membrane fluidity in proliferation of primitive cells. *Cell Rep*, 1(5):417–423, May 2012.
- [7] R. Mercier, Y. Kawai, and J. Errington. Excess membrane synthesis drives a primitive mode of cell proliferation. *Cell*, 152:997–1007–, 2013.
- [8] Yves Briers, Peter Walde, Markus Schuppler, and Martin J. Loessner. How did bacterial ancestors reproduce? Lessons from L-form cells and giant lipid vesicles: multiplication similarities between lipid vesicles and L-form bacteria. *Bioessays*, 34(12):1078–1084, Dec 2012.
- [9] B. Schnell, T. Staubli, N. L. Harris, G. Rogler, M. Kopf, M. J. Loessner, and M. Schuppler. Cell-wall deficient *L. monocytogenes* L-forms feature abrogated pathogenicity. *Front Cell Infect Microbiol*, 4:60, 2014.
- [10] L. Rothfield, A. Taghbalout, and Y.L. Shih. Spatial control of bacterial division-site placement. *Nat Rev Microbiol*, 3(12):959–968, Dec 2005.



- 
- [11] P. Peterlin, V. Arrigler, K. Kogej, S. Svetina, and P. Walde. Growth and shape transformations of giant phospholipid vesicles upon interaction with an aqueous oleic acid suspension. *Chem Phys Lipids*, 159(2):67–76, Jun 2009.
- [12] T. F. Zhu and J. W. Szostak. Coupled growth and division of model protocell membranes. *J Am Chem Soc*, 131(15):5705–5713, Apr 2009.
- [13] T. Tanaka, R. Sano, Y. Yamashita, and M. Yamazaki. Shape changes and vesicle fission of giant unilamellar vesicles of liquid-ordered phase membrane induced by lysophosphatidylcholine. *Langmuir*, 20(22):9526–9534, Oct 2004.
- [14] K. Kurihara, M. Tamura, K. I. Shohda, T. Toyota, K. Suzuki, and T. Sugawara. Self-reproduction of supramolecular giant vesicles combined with the amplification of encapsulated DNA. *Nat Chem*, 3(10):775–781, Oct 2011.
- [15] D. Joseleau-Petit, J. Liébart, J. Ayala, and R. D’Ari. Unstable Escherichia coli L forms revisited: growth requires peptidoglycan synthesis. *Journal of bacteriology*, 189(18):6512–6520, September 2007.
- [16] G. Billings, N. Ouzounov, T. Ursell, S. M. Desmarais, J. Shaevitz, Z. Gitai, and K. C. Huang. De novo morphogenesis in L-forms via geometric control of cell growth. *Mol Microbiol*, Jul 2014.
- [17] C. Klessen, K. H. Schmidt, J. Gumpert, H. H. Grosse, and H. Malke. Complete secretion of activable bovine prochymosin by genetically engineered L forms of *Proteus mirabilis*. *Appl Environ Microbiol*, 55(4):1009–1015, Apr 1989.
- [18] A. Shen and D. E. Higgins. The 5’ untranslated region-mediated enhancement of intracellular listeriolysin O production is required for *Listeria monocytogenes* pathogenicity. *Mol Microbiol*, 57(5):1460–1473, Sep 2005.
- [19] D. G. Gibson, L. Young, R.Y. Chuang, J.C. Venter, C.A. Hutchison, and H. O. Smith. Enzymatic assembly of DNA molecules up to several hundred kilobases. *Nat Methods*, 6(5):343–345, May 2009.

## 5 Manuscript 3

### *Short Communication*

#### **DivIVA localization in *Listeria* L-forms supports the Molecular Bridging Model**

Titu Staubli<sup>1</sup>, Patrick Studer<sup>1</sup>, Markus Schuppler<sup>1</sup> and Martin J. Loessner<sup>1,\*</sup>

##### **Contributions of Titu Staubli to this manuscript:**

- designed the project and wrote the manuscript
- constructed and analyzed the mutant *L. monocytogenes* 1042::pPL2/P<sub>Rha</sub>-*divIVA-gfp*
- analysed the L-forms derived from the mutant *L. monocytogenes* EGDe::pPL2/P<sub>Rha</sub>-*divIVA-gfp*

<sup>1</sup> Institute of Food, Nutrition and Health, ETH Zurich, Schmelzbergstrasse 7, CH-8092 Zurich, Switzerland

\* Corresponding author.

Martin J. Loessner, Phone: +41 44 632 3335, E-mail: martin.loessner@ethz.ch

## Abstract

The bacterial cell division represents a tightly regulated process that is orchestrated by many proteins temporarily and spatially. Due to the absence of sub-cellular compartments, bacteria rely on biophysical means to recruit proteins to specific sites within the cytoplasm. The conserved protein DivIVA preferentially localizes at negative membrane curvature independently of any known factor. In Gram-positive bacteria DivIVA can be detected at the cell poles and division-sites where it indirectly positions at the division plane by interaction of the MinCD complex. The exact molecular mechanism underlying the primary cue dictating the recruitment has not been fully elucidated yet. We here exploited the extraordinary and diverse morphology of *Listeria* L-forms to provide further insights on the intrinsic property of DivIVA. We found a strong preference of DivIVA for localization between two bilayers where it experiences the greatest stabilization conferred by bridging the opposing membranes. Our results are well in agreement with the *Molecular Bridging Model* and therefore deliver additional support for the proposed hypothesis.

## Introduction

Cellular processes are regulated in detail by various biological molecules including lipids, nucleic acids and proteins. Precise localization of proteins within the cell is crucial to ensure an orderly cell division process. Unlike eukaryotes, bacteria do not contain compartments separated by specific membranes. It is therefore remarkable how proteins are able to find its place. Usually, proteins arrive at the intended destination through diffusion and interaction with another protein that previously localized at that site [1]. The intriguing question of how the very first protein is able to identify the appropriate place has been under debate for a long time. During the last few years, it has become apparent that bacteria employ biophysical processes in order to organize specific protein localization patterns [2].

Bacteria use two inhibitory systems to ensure the precise recruitment of the division machinery. The nucleoid occlusion system acts in close proximity of the nucleoid whereas the Min system prevents division at the poles [3, 4, 5]. The Min system consists of an inhibitory protein MinC which hinders the formation of FtsZ ring [4, 5]. MinC is recruited to the membrane by MinD and the formed MinCD complex depends on the localization of MinJ/DivIVA (applies for *B. subtilis*) [6, 7]. DivIVA represents a decisive factor in *B. subtilis* cell division by spatially regulating the Min system. Furthermore, the recruitment of the replication origin to the poles into spores of *B. subtilis* has been ascribed to the conserved protein as well [8]. DivIVA localizes independent of any other proteins or specific lipids and has therefore caused a lot of attraction recently [9]. However, the molecular mechanism underlying DivIVA localization has not been fully understood yet. Lernarcic and Ramamurthi have first proposed the idea of DivIVA accumulating at negatively curved membranes [10, 8]. They presented the Molecular Bridging Model, explaining DivIVA localization without the requirement of either intrinsic protein curvature or presence of specific lipids or proteins. DivIVA monomers are able to arrange themselves into hexa- to octamers by interaction of their C-terminal domains, forming doggy-bone like arrangements. These oligomers assemble into higher order structures that are able to span almost 25 nm. Due to the mutual

and irreversible interactions between the DivIVA molecules, the large structures are more stabilized by binding to strongly curved membranes. The percentage of stabilized oligomers thereby increases in correlation with the negative curvature of the membrane, to which the cluster is attached [10].

In order to further discern the molecular mechanism of DivIVA localization, we used *Listeria* L-forms. They exhibit a spherical shape and are able to form intracellular vesicles as well as membranous thin strands interconnecting cells. As described in Studer and Staubli et al. (see Manuscript 2) these structures form a continuum allowing exchange of cytoplasmic content. The different morphology enabled us to study DivIVA localization within various cell shapes. We found that DivIVA preferentially localizes at the interface between two double bilayers of mother cell and internal vesicles and at sites with highly negative membrane curvatures. In the cytoplasmic tubes, DivIVA bridges the two opposing membranes. In conclusion, the collected results support the Molecular Bridging Model suggesting proposed by Lenarcic *et al.*

## Results

### In parental *Listeria* DivIVA-GFP localizes to the poles and division sites in

Due to the various morphologies *Listeria* L-forms provide an interesting system to evaluate the suggested mechanism of DivIVA of sensing negative membrane curvatures. Therefore, a *Listeria* L-forms mutant was generated that expresses DivIVA-GFP under the control of an inducible rhamnose promoter. This was achieved by constructing pPL2/*P<sub>Rha</sub>-divIVA-gfp* and subsequent transformation of *L. monocytogenes*. An exponentially grown culture of the parental mutant supplemented with 10mM rhamnose was examined. Analysis revealed localization to the poles and/or to the division sites (Figure1). These findings are consistent with the literature where they describe a preferential localization as a ring to nascent cell division septa and to the cell poles [10, 8, 11]. The result confirms that the functionality of DivIVA is not hampered by the fusion to the GFP molecule and can be used for further analysis.

### DivIVA-GFP preferentially resides between two opposing membranes

The parental mutant was then exposed to the beta-lactam antibiotic penicillin G that induced the conversion into huge spherical L-forms containing internal vesicles. Due to the lack of a cell wall, L-forms had to be maintained in an osmoprotective media supplemented with 10mM rhamnose. Analysis under the confocal microscope revealed a primary DivIVA-GFP localization at the interface between mother and daughter cell. Z-Stacks and subsequent 3D representation nicely shows that DivIVA-GFP is dispersed over the entire interacting area of the two bilayers (Figure 2A-B). Moreover, at positions where the membrane is extremely negatively curved, DivIVA-GFP accumulation was observed as well (in the corner of the mother cell cytoplasm and internal vesicle) (Figure 2C-D).

As recently observed, *Listeria* L-forms derived from the strain EGDe shows a different growth behavior as well as a distinct morphology (see Manuscript 2). In the early growth phase, long lipid membranous tubes are formed which are filled with cytoplasmic material. These structures

interconnect L-form cells allowing the exchange of cytoplasmic material. It was of interest to assess preferential positioning of DivIVA in these threads. Generation of a DivIVA-GFP mutant in the background of the EGDe strain was conducted according to the same procedure as stated above. Subsequently, DivIVA-GFP recruitment was analyzed in these cytoplasmic threads. We indeed found a strong preference of DivIVA-GFP localizing in the membranous tubes where they formed distinct spots indicating the bridging of the two opposing membranes. Interestingly, the fusion protein could be hardly detected within the spherical L-form cells (Figure 3).

## Discussion

Bacterial cell division is a well-organized and tightly regulated process. In contrast to eukaryotic systems, bacteria are not partitioned into sub-cellular structures which would provide support in organization on the molecular level. They have to find other ways to establish cellular non-uniformity required for cellular processes. It has been shown that individual proteins are able to reside at specific sites by recognizing geometric cues [12]. DivIVA exemplifies such a protein and accumulates independently at division-sites and poles in Gram-positive bacteria [10, 8, 11]. The respective molecular mechanism underlying the observed recruitment has not been fully elucidated yet. Based on biophysical studies and Monte-Carlo-simulations the Molecular Bridging Model has been established providing an explanation for the ability to sense cellular architecture [10].

To assess the proposed model we made use of the diverse and unusual morphology of *Listeria* L-forms. In spherical L-forms containing intracellular vesicles, DivIVA-GFP preferentially resided at the interface of the two bilayers and at sites with a very high degree of negative membrane curvature. In principle, the outcome is consistent with the proposed model by Lenarcic and Ramaurthi of sensing negative membrane curvature. Although the prominent localization of DivIVA-GFP at the interface between the mother and daughter cell membrane seems to be surprising, it can be perfectly attributed to the Molecular Bridging Model. DivIVA oligomers employ the highest stabilization between the adjacent membranes due to the decreased exposed surface (Figure 4). It becomes obvious why the molecules do not demonstrate a uniformly distribution around the cell membrane as earlier reported in spherical protoplast lacking internal vesicles [13, 8].

*Listeria* L-forms derived from the strain EGDe exhibit the capability of forming membranous tubes in early growth phase which are filled with cytoplasmic material. Remarkably, DivIVA was almost exclusively found in these structures bridging the opposing membranes. The accumulation of DivIVA at distinct sites within the long membranous thread-like structures is also



well in accordance with the Molecular Bridging Model. DivIVA-GFP molecules bridge the two membranes directed by the law of having as many interaction partners as possible explaining why almost solely all DivIVA-GFP molecules can be found in the thin tubes (Figure 4).

Here, we employed the unusual morphology of *Listeria* L-forms to evaluate DivIVA localization in a living system. In two different cellular structures we could detect the preferential recruitment of the molecules between two adjacent membranes. Furthermore, DivIVA is also localized at sites with high degree of negative membrane curvature. We therefore provide further evidence for the Molecular Bridging Model that proposes how cell shape may serve as a regulatory role in biological processes.

## Material and Methods

### Induction and growth of L-forms

L-form were generated as described previously [14]. Briefly, an overnight culture of walled *L. monocytogenes* was inoculated into *Listeria* L-forms medium (LLM) for 2h and then inoculated into soft-agar (37 g/l BHI (Biolife, Italy), 150 g/l sucrose, 2.5 g/l  $\text{MgSO}_4 \times 7 \text{H}_2\text{O}$ , 3 g/l milk serum powder, 3 g/l agar) supplemented with 50  $\mu\text{g/ml}$  Penicillin G and incubated at 32°C. After a few days, spherical cell wall-deficient cells appeared which were then analyzed under the confocal laser scanning microscope. The formation of the thin membranous strands were observed in the *Listeria* L-forms strain EGDe which is able to grow in liquid culture. For the generation and further characteristics see Manuscript 2.

### Construction of *L. monocytogenes* mutant expressing DivIVA-GFP

To label the DivIVA with GFP under regulation of an inducible promoter, the plasmid pPL2 was used. The  $P_{Rha}$  promoter region was amplified from pLF1 [15] using the primers  $P_{Rha}$ -forw and  $P_{Rha}$ -rev and cloned into pPL2. The gene *divIVA* without the stop codon was amplified out of *Listeria* chromosomes using the primers *divIVA*-forw and *divIVA*-rev. The product was then ligated into pPL2/ $P_{Rha}$ . Next, the gene encoding GFP was inserted in frame into the vector pPL2/ $P_{Rha}$  yielding the final construct pPL2/ $P_{Rha}$ -*divIVA-gfp*. In order to facilitate DivIVA folding, a 24bp linker was inserted. The vector pPL2 harbors a chloramphenicol resistance gene and a PSA integrase which integrates the plasmid at the 3' end of the  $\text{tRNA}^{Arg}$  gene [16]. The constructed vector was then transformed into *L. monocytogenes* using electroporation [17]. Successful integration into the chromosomes was verified by PCR and microscopy.

### Microscopy

Microscopy analysis was conducted using a confocal laser scanning microscopy Leica TCS SPE system (Leica Microsystems GmbH, Wetzlar, Germany). The following dyes were used: 50  $\mu\text{g/ml}$  Hoechst 33342 (Life Technologies), 50  $\mu\text{M}$  CellTrace™ BODIPY® TR methyl ester

(Life Technologies). The cells were mixed with the dyes and following an incubation time of 5 min, observed without washing. 3D representation of the collected Z-Stacks were deconvoluted using Huygens-software provided by the Center for Microscopy and Image Analysis, University of Zurich and assembled in Imaris (Bitplane) and ImageJ Software (Version 1.48e).

**Table 1:** Primer used

<b>Primer Name</b>	<b>Primer Sequence</b>
$P_{Rha}$ -forw	5'-TTTGAATTCTATTCCGTGATAATTTGG-3'
$P_{Rha}$ -rev	5'-TTTGTCGACACTCATTTTTAGTTAAGCGC-3'
divIVA-forw	5'-TTTGGTACCCAATATAAATTCTAGGAAAAAGCTAG-3'
divIVA-rev	5'-TTTGTCGACTTGTAATAAATTCAATGTCT-AATTTACGTTCTTCTGATTC-3'
gfp-forw	5'-TTTGTCGACATGAGTAAAGGAGAAGAAGCTTTTC-3'
gfp-rev	5'-TTTGGTACCTTATTTGTATAGTTCATCCATGC-3'
<b>Linker</b>	<b>Linker Sequence</b>
divIVA (24bp)	5'-TTGTAAAAATTCAATGTCTAATTT-3'

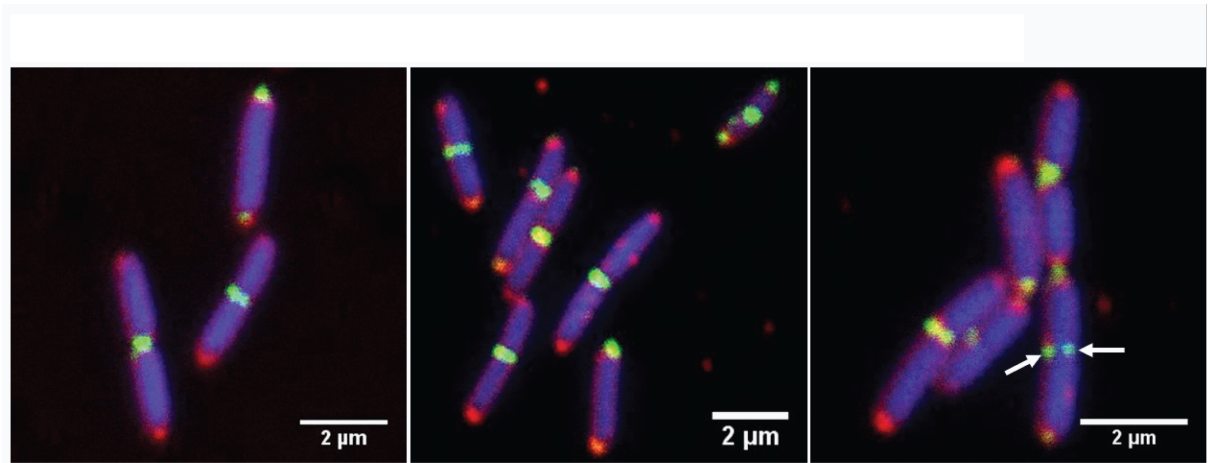


**Figure 1:** DivIVA localisation in parental *L. monocytogenes*. DivIVA was fused to GFP under the control of the rhamnose promoter. It localizes at the poles and at the newly formed septa (arrows). The cells were stained with the DNA stain Hoechst (blue) and the membrane was visualized with BTME (red).

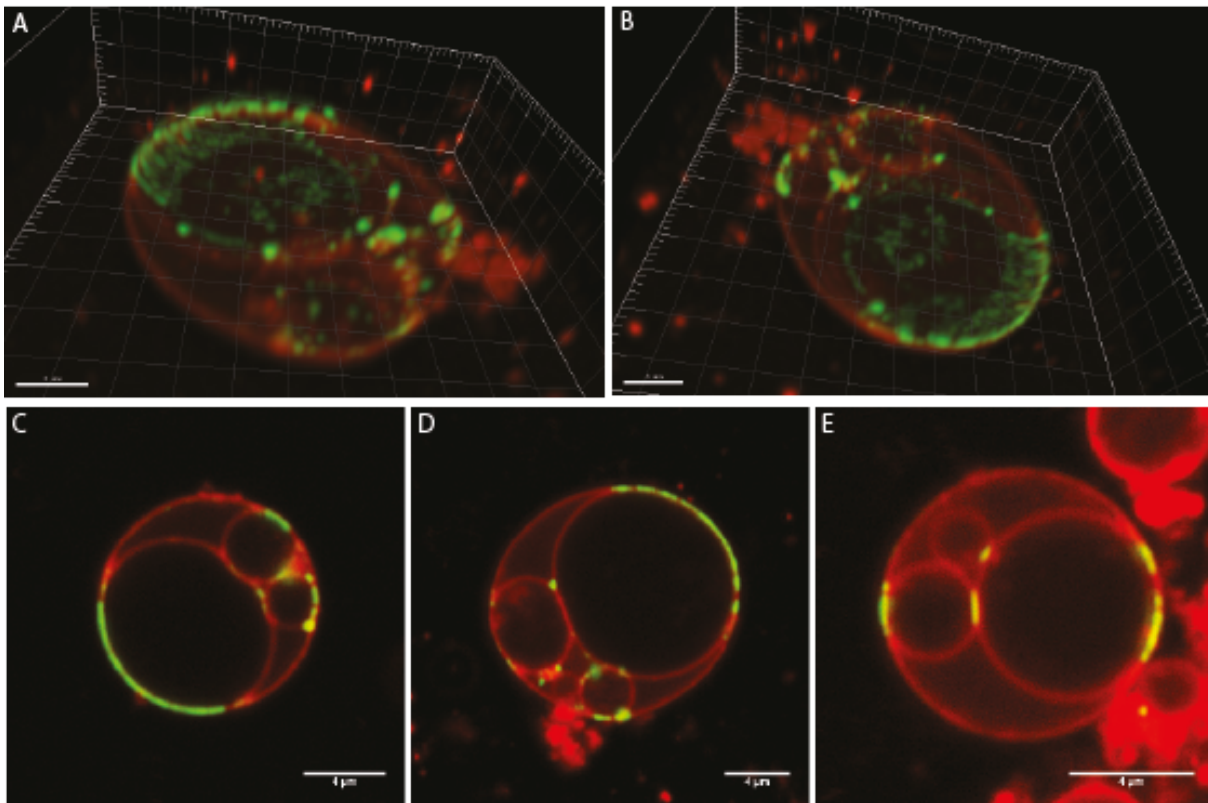


**Figure 2:** In L-forms containing internal vesicles, DivIVA preferentially resides at the interface of the mother and daughter cell membrane. In addition, it localizes at sites exhibiting the highest degree of negative membrane curvature (in the corner of mother cell cytoplasm and internal vesicle). The membrane was visualized with BTME (red).

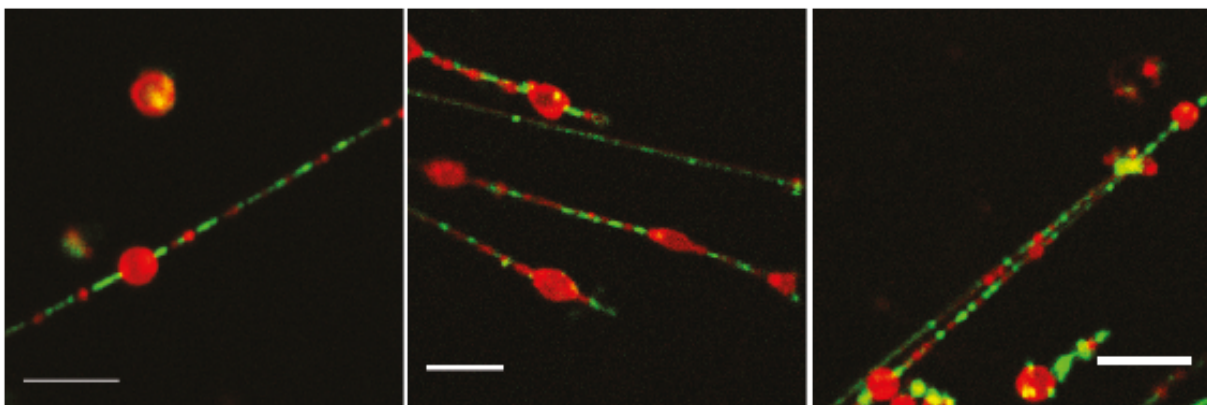


**Figure 3:** In L-forms forming membranous tubes, DivIVA-GFP accumulates at distinct sites within these structures. The high preference can be accounted by being able to bridge the two opposing membranes where clusters experience the highest stability. It can be hardly detected in spherical cells. The scale bar indicates  $5\mu\text{m}$ .

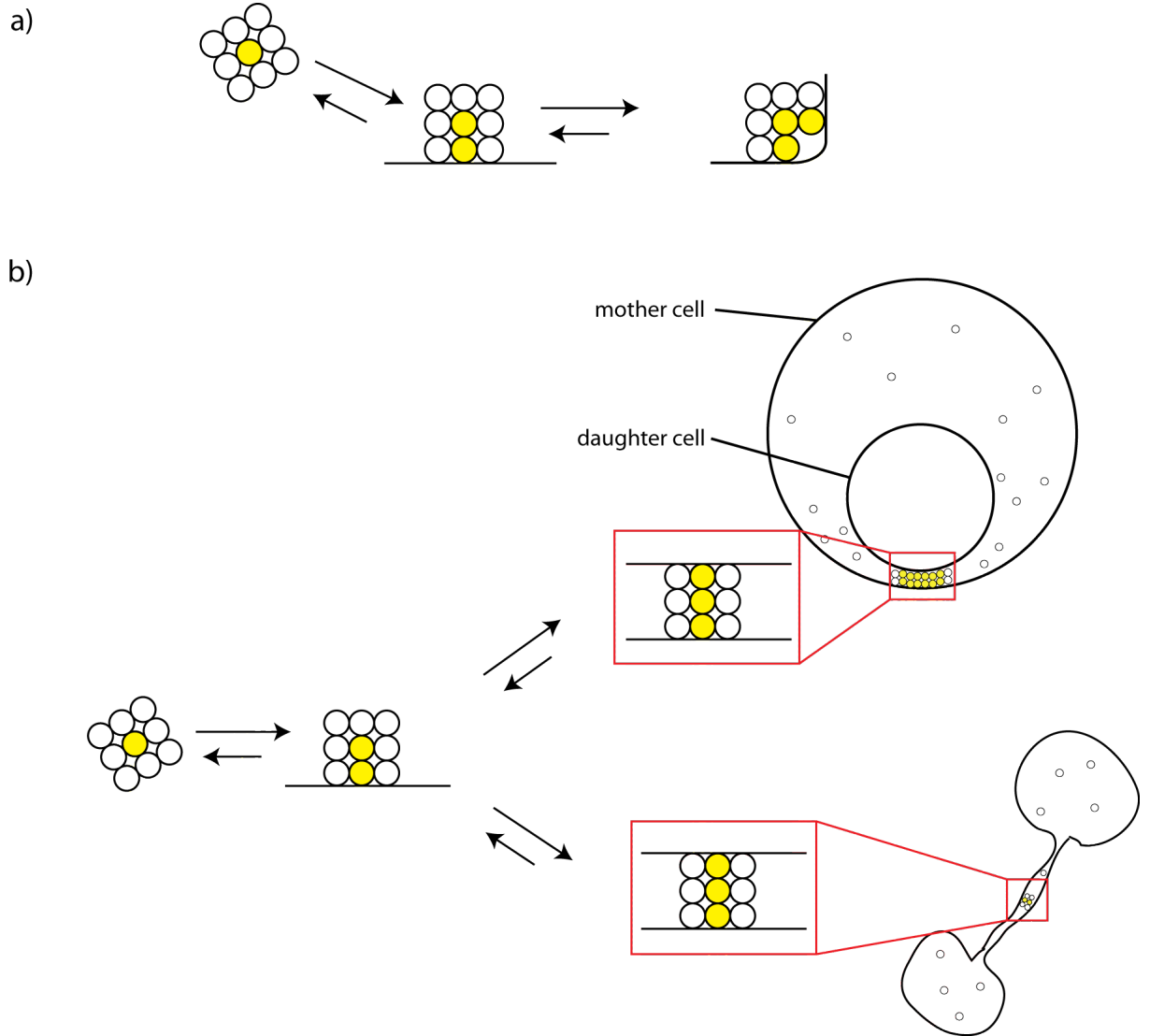


**Figure 4:** DivIVA localization in *Listeria* L-forms can be well attributed to the *Molecular Bridging Model* by Lenarcic et al. (2009). A. Schematic representation of the model illustrating how DivIVA recognizes negatively curved membranes. DivIVA oligomers are represented as spheres which form free floating clusters (left), a cluster attaching to the cell membrane (middle) or a cluster that bridges the corner of a curved membrane (right). White circles represent oligomers that can diffuse away whereas yellow circles indicate enclosed ones. Free floating clusters exhibit only a few entrapped oligomers. Due to fewer interaction partners they are not very stable and tend to detach from the cluster. When the cluster attaches to a straight membrane, the percentage of enclosed oligomers increases thereby stabilizing the entire structure. In a negatively curved membrane (in the corner) oligomers encounter their greatest stabilization due to the decreased surface exposure [10]. B. Schematic representation explaining DivIVA localization in *Listeria* L-forms. In spherical cells containing internal vesicles, oligomers prefer to reside at the interface between two membranes as they experience the biggest decrease in surface exposure. In L-forms lacking vesicles but forming membranous tubes, DivIVA oligomers obtain the most extensive support when bridging two opposing membranes as the membrane hinders the diffusion of the adjacent spheres.

## References Manuscript 3

- [1] L. Shapiro, H. H. McAdams, and R. Losick. Generating and exploiting polarity in bacteria. *Science*, 298(5600):1942–1946, 2002.
- [2] H. Strahl and L. W. Hamoen. Finding the corners in a cell. *Nature Communications*, 15:731–6–, 2012.
- [3] L. Rothfield, A. Taghbalout, and Y. L. Shih. Spatial control of bacterial division-site placement. *Nat Rev Microbiol*, 3(12):959–968, 2005.
- [4] E. Bi and J. Lutkenhaus. Interaction between the min locus and ftsZ. *J Bacteriol*, 172(10):5610–5616, 1990.
- [5] A. L. Marston and J. Errington. Selection of the midcell division site in *Bacillus subtilis* through MinD-dependent polar localization and activation of MinC. *Mol Microbiol*, 33(1):84–96, 1999.
- [6] D. H. Edwards and J. Errington. The *Bacillus subtilis* DivIVA protein targets to the division septum and controls the site specificity of cell division. *Mol Microbiol*, 24(5):905–915, 1997.
- [7] M. Bramkamp, R. Emmins, L. Weston, C. Donovan, R. A. Daniel, and J. Errington. A novel component of the division-site selection system of *Bacillus subtilis* and a new mode of action for the division inhibitor MinCD. *Mol Microbiol*, 70(6):1556–1569, 2008.
- [8] K. S. Ramamurthi, S. Lecuyer, H. A. Stone, and R. Losick. Geometric cue for protein localization in a bacterium. *Science*, 323:1354–7–, 2009.

- [9] D. H. Edwards, H. B. Thomaides, and J. Errington. Promiscuous targeting of *Bacillus subtilis* cell division protein DivIVA to division sites in *Escherichia Coli* and fission yeast. *EMBO Journal*, 19:2719–27–, 2000.
- [10] R. Lenarcic, S. Halbedel, L. Visser, M. Shaw, L. J. Wu, J. Errington, D. Marenduzzo, and L. W. Hamoen. Localisation of DivIVA by targeting to negatively curved membranes. *EMBO Journal*, 28:2272–82–, 2009.
- [11] H. Stahlberg, E. Kutejova, K. Muchova, M. Gregorini, A. Lustig, S. A. Muller, V. Olivieri, A. Engel, A. J. Wilkinson, and I. Barak. Oligomeric structure of the *Bacillus subtilis* cell division protein DivIVA determined by transmission electron microscopy. *Mol Microbiol*, 52:1281–90–, 2004.
- [12] K. C. Huang and K. S. Ramamurthi. Macromolecules that prefer their membranes curvy. *Mol Microbiol*, 76(4):822–832, 2010.
- [13] L. D. Renner, P. Eswaramoorthy, K. S. Ramamurthi, and D. B. Weibel. Studying biomolecule localization by engineering bacterial cell wall curvature. *PLoS One*, 8(12):e84143, 2013.
- [14] Y. Briers, T. Staubli, M. C. Schmid, M. Wagner, M. Schuppler, and M. J. Loessner. Intracellular Vesicles as Reproduction Elements in Cell Wall-Deficient L-Form Bacteria. *PlosOne*, 7:–, 2012.
- [15] L. Fieseler, S. Schmitter, J. Teiserskas, and M. J. Loessner. Rhamnose-inducible gene expression in *Listeria monocytogenes*. *PlosOne*, 7:e43444–, 2012.
- [16] P. Lauer, M. N. Chow, M. J. Loessner, D. A. Portnoy, and R. Calendar. Construction, characterization, and use of two *Listeria monocytogenes* site-specific phage integration vectors. *J Bacteriol*, 184(15):4177–4186, 2002.
- [17] S. F. Park and G. S. Stewart. High-efficiency transformation of *Listeria monocytogenes* by electroporation of penicillin-treated cells. *Gene*, 94:129–32–, 1990.





## 6 Conclusion and Outlook

Practically all bacteria are surrounded by a rigid cell wall responsible for mechanical integrity and for determining cell shape. Exposure to compounds interfering with peptidoglycan synthesis (e.g. Penicillin G) causes the bacteria to escape from its surrounding cell wall. Interestingly, given the right osmotic environment, the resulting protoplast may be able to develop into an L-form capable of reproduction.

The current study characterizes the unusual mode of reproduction employed by cell wall-deficient *Listeria* L-forms. Parental *Listeria* divide by binary fission, which is orchestrated by many proteins and tightly regulated. It was found that *Listeria* L-forms acquire a new mode of reproduction characterized by a multitude of proliferation mechanisms. Time-lapse imaging revealed a high degree of membrane dynamics leading to various shape deformations which finally result in the production of extracellular progeny cells. Remarkably, *Listeria* L-forms are also able to produce intracellular vesicles. Isolation of even smaller vesicles-within-vesicles followed by culture demonstrated the viability of these intracellular budding-like structures. The new proliferation modes appear to be occurring in an uncoordinated and random fashion, characterized by the dispensability of the cell division protein FtsZ. The polyploidy of L-forms further confirms the disorganization by the loss of synchronization of cell division, DNA replication and chromosome segregation. It is assumed that there is no involvement of any known cytoskeletal systems to induce membrane deformations in *Listeria* L-forms. Instead, it seems plausible that membrane dynamics driven by an excess of lipids governs the formation of new progeny cells. Distribution of the essential components to daughter cells apparently occurs in a random manner, explaining the slower growth rate and the inability of producing only viable progeny.

The cytoplasmic membrane plays a crucial role in the lifestyle of bacterial L-forms. Analysis of its biophysical properties revealed an increased membrane fluidity likely due to the alteration in the membrane lipid composition. It is thought that a more fluidic membrane is not only a pre-requisite for shape modulations required for proliferation, but also responsible for enhanced membrane permeability. The ability to take up plasmids may be based on the significant higher abundance of polar phospholipids, which can increase interactions between DNA and membrane.

In general, all bacterial L-forms feature cell wall-deficiency and are characterized by a heterogeneous morphology and structure. Their modes of reproduction vary significantly, depending on the organism and genetic background. It is conceivable that the diversity results from the absence of one or more regulatory mechanisms developed throughout evolution. *E. coli* L-forms seem to have retained most of the features of a sophisticated bacterial cell as they still require FtsZ. Whereas L-forms derived from Gram-positive bacteria (such as *B. subtilis* and *L. monocytogenes*) likely have reduced to a more primitive cellular entity, reflected by the dispensability of various cellular systems and the unusual replication mechanisms.

Due to the primitive modes of reproduction and the dispensability of a sophisticated cell division machinery, L-forms provide a suitable model to probe putative primordial cellular reproduction. In addition, the diverse morphologies of L-forms present an interesting system to study biophysical properties of bacterial proteins.

The development and application of a micromanipulator system allowed us for the first time to manipulate L-forms of a single cell level. Isolation of an individual L-form and its capability to re-grow to a new colony constituted a valuable tool for the presented project. Among others, it enabled us to investigate the fate of a single heteroploid L-form, and to unravel a spontaneous differentiation to monoploid cells. Due to the huge size, there is the possibility to develop an injection procedure. Although, it is certainly challenging to inject compounds into L-forms without harming the cell, I'm confident that this can be done. This would provide new approaches, such as injection of DNA or proteins which would help to elucidate the molecular mechanism *Listeria* L-forms reproduction.

In the future, it is vital to gain a better understanding of the generation of *Listeria* L-forms.

Directed induction of a parental *Listeria* L-forms cell to switch to the L-form state seems pivotal in order to elucidate the molecular mechanism of *Listeria* L-forms reproduction. Generation and analysis of knock-out mutants deficient in cell division genes will deliver further insights on the minimal set of proteins required for proliferation.

Moreover, a bottom up approach could be pursued by generating GUVs based on *Listeria* L-form extracts. Subsequent examination in a micro-fluid system would enable to probe what proportion of the shape deformations is the result of simple physical-chemical properties, and what might be actively governed by proteins. In order to show a putative purely passive distribution of genetic material, fluorescently labeled DNA could be encapsulated in GUVs. Induction of *in vitro* proliferation would lead to new progenies which then could be assessed for the containment of an entire chromosome.

Prospective *Listeria* L-forms research further includes the comprehension of the reversion process. It is intriguing to investigate the factors that would allow a cell wall-deficient cell to re-establish a peptidoglycan layer.

Overall, this thesis contributes to a better understanding of the diverse modes of proliferation employed by bacterial L-forms.



## 7 Addendum

### 7.1 *Listeria* L-forms membranes comprise significantly more polar phospholipids

*B. subtilis* L-forms seem to proliferate independently of known cytoskeletal proteins. Instead, biophysical properties of membranes have been ascribed to play a decisive role in driving L-form replication [6]. Characterization of the cellular membrane in *Listeria* L-forms revealed a significant increased membrane fluidity (see Manuscript 2) likely allowing the membrane deformations required for proliferation. Bacterial membranes maintain their fluidity by altering the phospholipid composition. It was therefore of interest to compare the phospholipid structure of L-forms with parental *L. monocytogenes* using mass spectrometry analysis. Extraction of the phospholipids was performed by a two-step protocol which included a Chloroform 17:1 Methanol and Chloroform 2:1 Methanol extraction procedure. Biomass of L-form and parental pellets were verified to be the same by determining the weight. Extracted organic phases were then vacuum dried and then resuspended in Acetonitrile 1:1 Methanol. Subsequently, lipid extracts were profiled using negative mode flow injection time of flight mass spectrometry. The detected ions were annotated according to previously reported methods [4]. Statistical analysis and principal component analysis allowed identification of several different components. Strikingly, polar phospholipids, such as phosphatidylethanolamine (PE), phosphatidylcholine (PG) and phosphatidylglycerol (PG), were more than 30x more abundant in L-forms than in parental cells. On the other hand, di- and triglycerides revealed to be less frequent in L-forms (1). Unfortunately, these data do not deliver conclusive insights on the chain length and the degree of saturation of the phospholipids.

However, they clearly indicate an alteration in the membrane composition between L-forms and parental cells which might ascribe to the different features we observed.

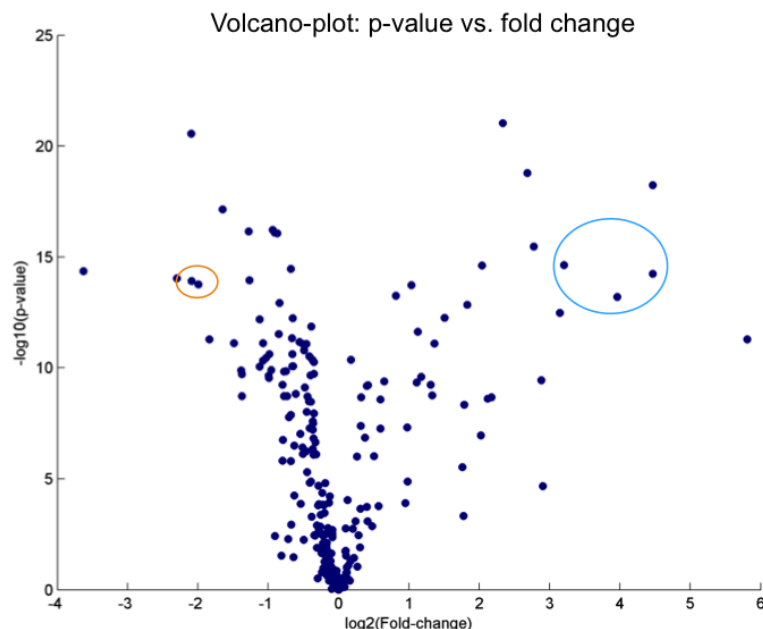


**Figure 1:** Mass Spectrometry analysis of membrane composition in L-forms and parental cells. Pairwise comparison of all detected components derived from lipid extraction are represented in a volcano plot. Spots circled in blue indicates the significant higher abundance of PG, PE and PC in L-forms whereas the orange circle highlights the down-regulation of di- and triglycerides.

## 7.2 Imaging analysis suggests a generation time of 265 minutes

Time-lapse microscopy demonstrated that stable *Listeria* EGDe L-forms grown in LLM-Broth mainly reproduce by forming extracellular vesiculation (see Manuscript 2). The diverse cell morphologies and the polyploidy exacerbate the determination of the generation time by conventional methods. Therefore, imaging analysis was used to estimate the doubling time. It automatically recognizes cell boundaries and calculates surface area of each cell over time. The software *morphometrics* was applied which is based on Matlab and was developed by Tristan Ursell, Stanford University, USA (unpublished). Despite the high fluctuation and not always clear cell boundaries, the software could identify surprisingly a high number of cells. Though, it

is important to bear in mind that the software sometimes mislabels cells for a few frames or cells move in and out of field of view. The measured surface area was then subjected to a function best describing bacterial growth (unpublished). The final calculation resulted in a generation time of 265 min for *Listeria* EGDe L-forms (Figure 2).

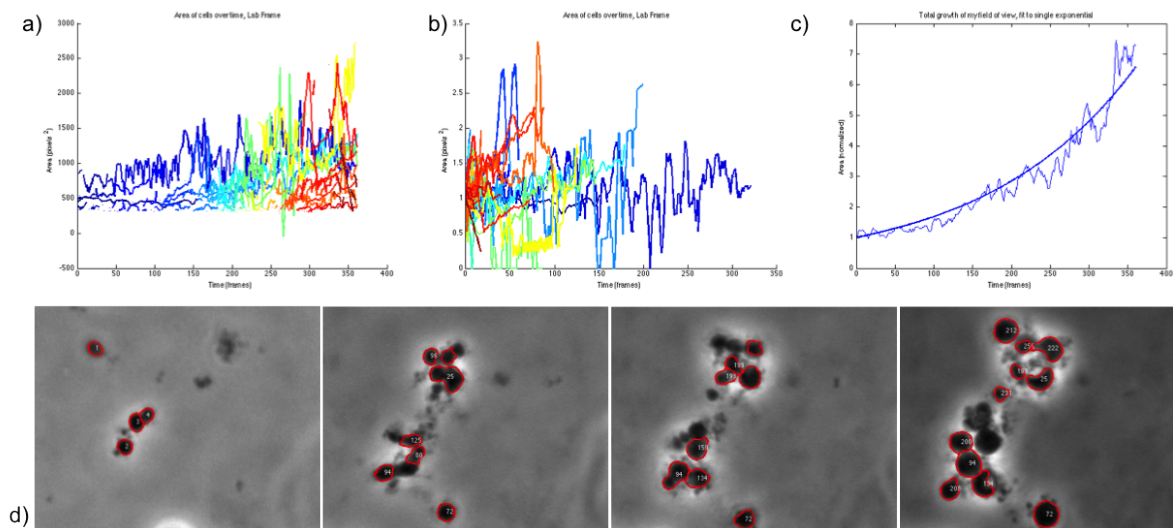


**Figure 2:** Imaging analysis of replicating L-forms. Time-lapse movie of multiplying L-form cells was subjected to the imaging software morphometrics. The software recognizes automatically cell boundaries in all the frames. (a) The surface area of individual cells was plotted over time frames. Each color represents a cell. (b) Surface area of each individual cell represented in cell frame and normalized. Rapid in- and decrease of surface area can be ascribed to cells going out and coming in of field view. (c) Sum of surface area of all cells was subjected to a function that fits the data to a growth curve. The calculated doubling time for the cells of this particular spot is 265 min. (d) Collection of time-lapse at different time points (1, 150, 569 and 724 min). Pictures were taken every minute.

### 7.3 DNA content and surface area correlate linearly over time

In order to elucidate the molecular mechanism of the DNA transfer in *Listeria* L-forms, detection and monitoring of DNA over time is required. As imaging of single chromosomes turned out to be difficult, other methods were examined. Here, we aimed at investigating the efficiency of chromosomes distribution using a digital imaging processing approach. To reliably and quantitatively assess the DNA content of L-form cells over time, a new MatLab script was written.



The algorithm processed each image, segmented cells based on the phase contrast channel and calculated the surface area of each segmented object. The recognized cell boundaries were then used as a mask to quantify the fluorescence in each segmented object in each frame. Analyses of several time-lapse series of DNA stained (SYTO45) EGDe L-forms images revealed a linear correlation of DNA content with surface area (Figure 3). This outcome implies that the newly formed vesicles obtain DNA which is then replicated and distributed to the next progeny cells.

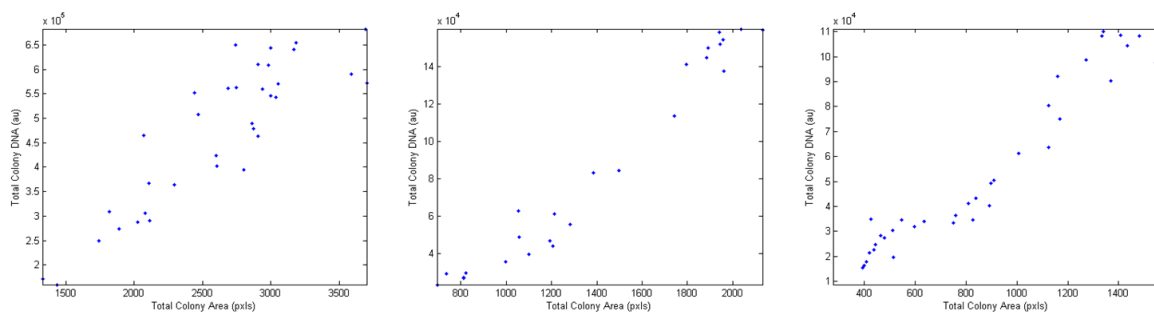


**Figure 3:** Analysis of time-lapse movies of EGDe L-forms stained with the DNA stain SYTO45 using MatLab. The written script automatically segments the cell, calculates the surface area and measures the fluorescence intensity of each identified object in each frame. Plotting the total amount of DNA versus the total surface area revealed a strikingly linear correlation.

## 7.4 Three Dimensional Structured Illumination Microscopy of stable L-forms

Super-resolution microscopy was performed with the intention to gain more information on the structure and localization of DNA within L-forms. In particular, we used Three Dimensional Structured Illumination Microscopy (3D-SIM) that projects a structured light pattern onto the sample, interacting with the present fluorescent probes. This leads to an interference pattern. By altering the illumination pattern, followed by collection and reconstitution of images using computational methods, a super-resolution images were obtained. L-form samples stained with DAPI and FM4-64 were imaged with 3-D Structured Illumination Microscopy (3D-SIM). Subse-

quently, 3D volume reconstruction was performed leading to the representation in Figure 4. In the upper pannel, a cell is depicted that appears to distribute some DNA to its progeny cell. In the lower row, it is nicely visible that the chromosomes sometimes exhibit a condensed structural organization indicated by not completely filling the entire cytoplasm.

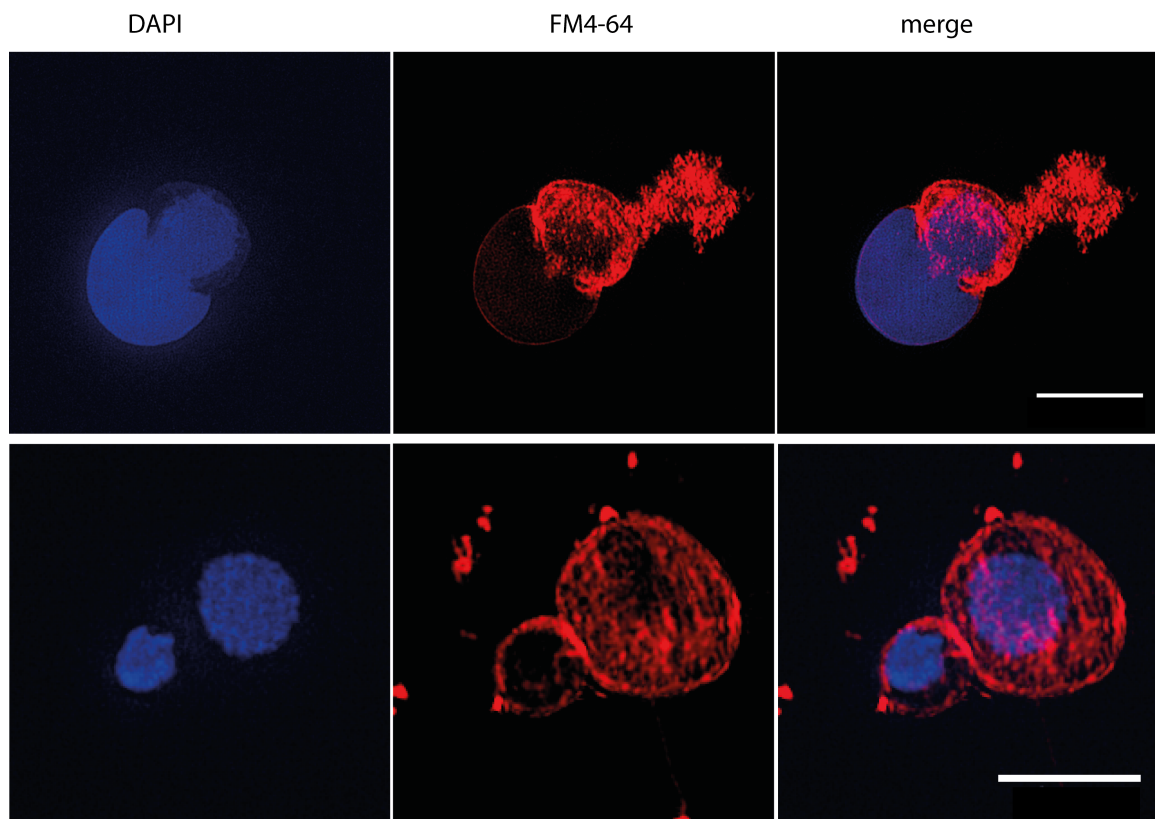


**Figure 4:** Structure illumination Microscopy and subsequent 3D reconstruction of *Listeria* L-forms. The cells were stained with DAPI and FM4-64. In the first row, it looks like as if a progeny cell filled with DNA buds off. In the second row two L-forms adjacent to each other contain clearly a condensed chromosome structure. The scale bar indicates 3  $\mu\text{m}$ .

## 7.5 Production of GUV with *Listeria* lipid extracts

*Listeria* L-forms reproduce by various shape deformations (see Manuscript 1 and 2) giving rise to internal or external progeny cells. L-form proliferation is speculated to occur in an uncoordinated manner devoid of any cytoskeletal protein supporting the faithful distribution of the essential components. In order to verify this hypothesis we aimed at generating GUV out of *Listeria*

L-form lipid. The idea was to probe what of the shape deformations and observed L-form characteristics is simply the result of physical and chemical properties and what is actively governed by proteins. The production of GUV from *Listeria* L-form extracts turned out to be extremely challenging. First approaches were conducted using an electro-formation protocol [1]. Briefly, *Listeria* L-forms were first subjected to an extruder to produce small unilamellar vesicles (SUV) with a diameter of about 400  $\mu\text{m}$ . Subsequently, SUV fusions were induced by electro-formation to produce GUVs. Even after several attempts, this approach was unsuccessful. Therefore, an alternative strategy was pursued, starting with crude lipids from *Listeria* L-forms extracts. GUVs were engineered according to inverted emulsion protocol [7]. The procedure is simple, fast and in addition allows encapsulation of components. Briefly, the extracted lipids were re-suspended in mineral oil and mixed with sucrose resulting in an inverted emulsion. This phase was then placed over an intermediate phase containing extracted lipids for the outer leaflet. The intermediate phase was then laid over an aqueous solution where monolayer of lipids could be formed at the interface. Finally, the emulsion was placed on top of the two phases. The sucrose droplets are heavier than oil and therefore sediment through the different layers leading to the formation of vesicles in the aqueous solution (Figure 5). Up to now, we have successfully produced GUV out of parental *Listeria* L-forms lipid extracts (Figure 5). However, the vesicles seem to be contaminated with an aqueous solution, may be originating from the lipid extraction procedure. The engineering of GUV of *Listeria* L-forms lipid extract has not been achieved yet. It is possible that the initial amount of lipids was too low.

## 7.6 *Listeria* protoplasts escape at the middle of the lateral wall

Exposure to antibiotics or lytic enzymes targeting the cell wall forces the bacteria to respond. Remarkably, bacteria do not die off immediately. Instead, provided the appropriate osmotic environment, they simply shed of their cell wall, become roundly shaped protoplasts, and eventually may convert into replicating L-forms [5, 2]. The first step of this transition has been monitored by time-lapse microscopy. Parental *Listeria* cells were coated with GFP-CBD500-CBD500, vi-

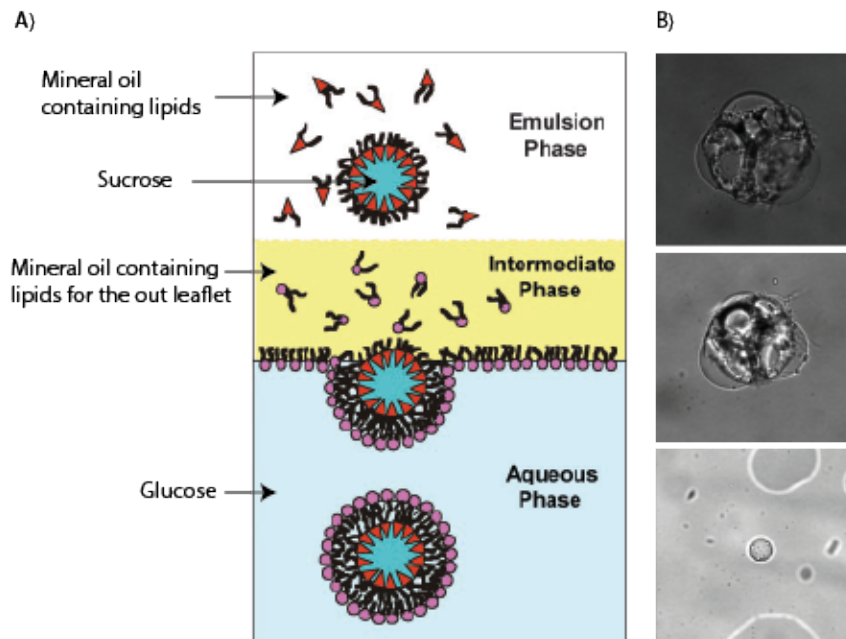


**Figure 5:** A. Schematic illustration of the applied inverted emulsion method (Pautot et al., 2003). B. GUV produced with *Listeria* L-forms lipid extracts using the inverted emulsion protocol.

sualizing the surrounding cell wall. Upon exposure to penicillin G, protoplasts bulged at the middle of the lateral wall. The emergence almost invariably occurred at mid-cell constrictions (Figure 6). This can be ascribed to the fact that at this position the peptidoglycan synthesis takes place. Thus, the cell wall integrity is reduced enabling the protoplast to squeeze out. Very similar observations have been made for *Bacillus subtilis* [3]. Induction of L-forms can be facilitated by two distinct genetic lesions what finally leads to the escape of the cell protoplast within 1-2h. On the contrary, *L. monocytogenes* takes about 20-30 h upon exposure to penicillin (200  $\mu\text{g/ml}$ ). Interestingly, Dominguez-Cuevas *et al.* were unable to induce *B. subtilis* protoplast by treatment with penicillin. They concluded that inhibition of PBP activity by PenG impairs the escape step in L-form generation [3]. Our results indicate that this seems not to be the case for *Listeria*.

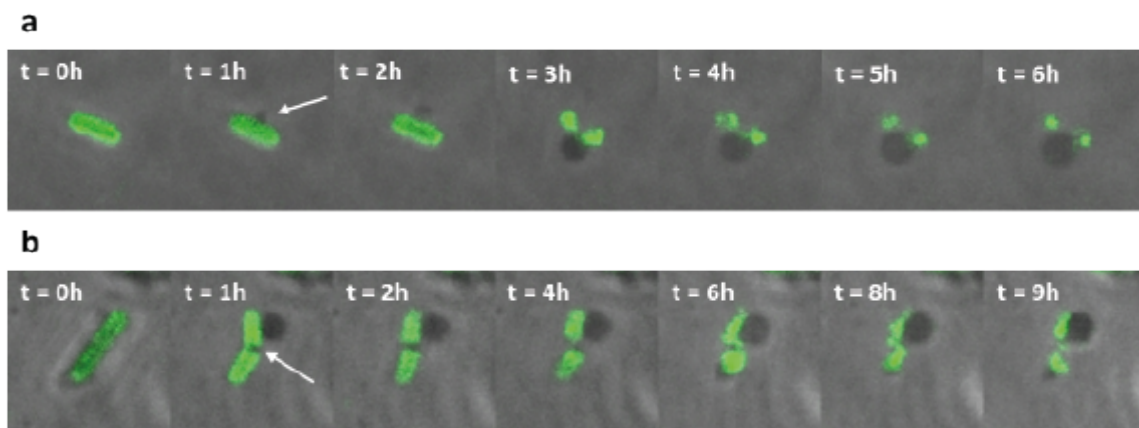


**Figure 6:** Exposure of parental *Listeria* to penicillin G induced protoplast escape at the middle of the lateral from its enveloping cell wall. The peptidoglycan layer was visualized by GFP-CBD500-CBD-500.

## References Addendum

- [1] M. Angelova, S. Meleard, P. Faucon, and F. Bothorel. Preparation of giant vesicles by external AC electric fields. Kinetics and applications. *Trends in Colloid and Interface Science*.
- [2] Y. Briers, T. Staubli, M. C. Schmid, M. Wagner, M. Schuppler, and M. J. Loessner. Intracellular Vesicles as Reproduction Elements in Cell Wall-Deficient L-Form Bacteria. *PlosOne*, 7:–, 2012.
- [3] P. Dominguez-Cuevas, R. Mercier, M. Leaver, Y. Kawai, and J. Errington. The rod to L-form transition of *Bacillus subtilis* is limited by a requirement for the protoplast to escape from the cell wall sacculus. *Mol Microbiol*, pages –, 2011.
- [4] T. Fuhrer, D. Heer, B. Begemann, and N. Zamboni. High-throughput, accurate mass metabolome profiling of cellular extracts by flow injection-time-of-flight mass spectrometry. *Anal Chem*, 83(18):7074–7080, Sep 2011.
- [5] M. Leaver, P. Dominguez-Cuevas, J. M. Coxhead, R. A. Daniel, and J. Errington. Life without a wall or division machine in *Bacillus subtilis*. *Nature*, 457:849–53–, 2009.
- [6] R. Mercier, P. Domínguez-Cuevas, and J. Errington. Crucial role for membrane fluidity in proliferation of primitive cells. *Cell Rep*, 1(5):417–423, May 2012.
- [7] S. Pautot, B. J. Frisken, and D. A. Weitz. Engineering asymmetric vesicles. *Proc Natl Acad Sci U S A*, 100(19):10718–10721, Sep 2003.



## 8 Material and Methods

### 8.1 Methods

#### 8.1.1 Lipid composition analysis by mass spectrometry

10 ml overnight *L. monocytogenes* and 150 ml L-form 2 days old cultures were used for the analysis. Lipid extraction occurred by a two-step protocol. The cells were washed with protoplast buffer. The pellet was weighed to verify the same biomass and then resuspended in 500  $\mu$ l 155mM  $\text{Na}_4\text{HCO}_3$ . 500  $\mu$ l Chloroform 17:1 Methanol was added and then placed on over-head rotator for 2h at 4°C. Subsequently, the tubes were spun down and the organic phase was collected. The second step included the addition of 500  $\mu$ l Chloroform 2:1 Methanol followed by 2h at 4°C on the over-head projector. Upon centrifugation, the organic phase was collected and pooled with the previous one. The samples were then vacuum dried and resuspended in 100  $\mu$ l Acetonitrile 1:1 Methanol which was then subjected to profiling using negative mode flow injection-time-of-flight mass spectrometry. Detected ions were annotated according to the previously reported procedure by Fuhrer *et al.*, 2011 [108]. Statistical analysis and principal component analysis was performed using Matlab R2010b (Mathworks, Natick, MA, United States). Pairwise comparisons of all detected ions was performed and its significance confirmed by t-tests ( $p < 0.05$ ).

#### 8.1.2 Infection of THP1-macrophages with EGDe L-forms

Human THP-1 macrophages (DSMZ ACC 16) were cultured in cell culture flasks in 90% RPMI 1640 + 10% FBS, and incubated at 37°C in a 5%  $\text{CO}_2$  gas atmosphere. One day prior to infection the cell density was adjusted to  $5 \times 10^5$  cell/ml and supplemented with PMA to final concentration of 5  $\mu$ g/ml. Stable EGDe L-forms grown for 2 days in LLM-Broth were used for the infection assay. The cells were washed three times with protoplast buffer and finally washed once more with pre-warmed RPMI medium. Centrifugation occurred at 1000g for 5 min. THP-



1 macrophages were then washed twice with PBS and subsequently challenged with L-forms for 2h at 37°C. Following the washing step of macrophages with PBS, the RPMI was replaced with fresh medium supplemented with 25  $\mu\text{g}/\text{ml}$  gentamicin and incubated at 37°C until usage. Staining of the infected macrophages with lysotracker red occurred by washing the cells three times with PBS followed by adding RPMI medium containing a final concentration of 2  $\mu\text{M}$  staining solution. Subsequently, the cells were incubated for 1.5h. Prior to analysis the cells were washed with PBS.

### 8.1.3 Imaging analysis

Time-lapse images were processed by a custom MATLAB (MathWorks) image processing code. This allowed segmentation of L-forms based on contours from phase contrast images and association of those outlines with cells in time. Fluorescent profiles were achieved by integration of the image fluorescence along the segmented cellular contours. For the determination of generation time of EGDe L-forms, automated segmentation was conducted by a custom MATLAB software package.

### 8.1.4 Time-lapse of protoplast escape from its enveloping wall

For live-cell imaging glass bottom dishes from MatTek Corporation were used. 200  $\mu\text{l}$  of a 1042 overnight culture grown in LLM broth was placed on the glass bottom dish and coated with LLM soft-agar, supplemented with 200  $\mu\text{g}/\text{ml}$  Penicillin G. The LLM soft-agar had a 1.5% agar concentration in order to reduce the dehydration rate during live-cell imaging. To label the cell wall of *Listeria*, 200  $\mu\text{l}$  of an overnight culture was centrifuged at 7000 g for 1 min. Subsequently, the supernatant was discarded and the pellet was resuspended in 100  $\mu\text{l}$  PBS, pH8 and 10  $\mu\text{l}$  GFP-GFP-CBD500-CBD500 (2.64 mg/ml), provided by Fritz Eichenseher. After an incubation time of 5 min, the bacteria were washed once in 500  $\mu\text{l}$  PBS, pH8 and resuspended in 200  $\mu\text{l}$  LLM broth. Finally, the bacteria were put on a glass bottom dish and coated with LLM soft-agar supplemented with 200  $\mu\text{g}/\text{ml}$  Penicillin G.

### 8.1.5 *Listeria* L-forms lipids were extracted using a two-step protocol

For parental cells, an overnight culture of 2 litres was centrifuged at 1500 g for 10 min. The cells were washed with PWB and resuspended in 155mM  $\text{NH}_4\text{HCO}_3$ . The following lipid extraction was conducted under the hood due to the toxic chemicals used. First, Chloroform 17:1 Methanol

was added to the tube which was then placed on a overhead-rotator for 2h at 4°C. Subsequently, the tube was spun down at max. speed for 1 min and the organic phase was collected. To the remaining aqueous solution, Chloroform 2:1 Methanol was added. The tube was put again for two hours on an overhead-rotator at 4°C and then spun down at max. speed for 1 min. The organic phase was collected and pooled with the previous one. Evaporation of the organic liquid was performed in a rotary evaporator under vacuum at room temperature.

#### 8.1.6 Generation of GUVs out of *Listeria* L-forms lipid extracts

Generation of GUV were produced using an inverted emulsion approach. The extracted phospholipids were dissolved in mineral oil (200  $\mu$ M) appr. 10 ml (= phospholipid solution, PS). Next, the solution was sonicated for 30 min and then stored overnight at RT. For the interface solution 500  $\mu$ l of the *hosting solution* (= 1M Glucose) and 200  $\mu$ l of the phospholipid solution were mixed and incubated for 10 min at RT. The water/oil (w/o)emulsion was prepared by adding 500  $\mu$ l of the PS solution and 50  $\mu$ l of the *droplet solution* (DS) to an EP which was then mechanically agitated. For the formation of GUV 500  $\mu$ l of the w/o emulsion was placed on top of the interface solution and centrifuged for 3 min at 1500 g. Subsequently, the oil was removed by an aspirator followed by centrifugation (3min, 1500 g, RT). Finally, about 150  $\mu$ l was removed by an aspirator to get rid of most of the remaining oil. GUV could be collected at the bottom of the tube.

## 8.2 Culture Media

### LB Media

Tryptone	10 g/l
Yeast Extract	5 g/l
NaCl	5 g/l
ddH <sub>2</sub> O	
pH 7.3 - 7.4	
<i>Autoclave</i>	

### LB Agar

Tryptone	10 g/l
Yeast Extract	5 g/l
NaCl	5 g/l
Agar	15 g/l
ddH <sub>2</sub> O	
pH 7.3-7.4	
<i>Autoclave</i>	

### BHI Agar

BHI	37 g/l
Agar	15 g/l
ddH <sub>2</sub> O	
<i>Autoclave</i>	

### BHI Medium

BHI	37 g/l
ddH <sub>2</sub> O	
<i>Autoclave</i>	

### LLM Agar

BHI	37 g
Sucrose	150 g
MgSO <sub>4</sub> x7H <sub>2</sub> O	2.5 g
Horse Serum	10ml/l
Agar	10 g
ddH <sub>2</sub> O	
<i>Autoclave</i>	

### LLM Softagar

BHI	37 g
Sucrose	150 g/l
MgSO <sub>4</sub> x7H <sub>2</sub> O	2.5 g/l
Horse Serum	10ml/l
Agar	2.88 g/l
ddH <sub>2</sub> O	
<i>Autoclave</i>	

### LLM Broth

BHI	37 g/l
Sucrose	150 g/l
MgSO <sub>4</sub> x7H <sub>2</sub> O	2.5 g/l
Horse Serum	10ml/l
ddH <sub>2</sub> O	
<i>Autoclave</i>	

### 8.3 Buffers and Solutions

#### Protoplast buffer

Sucrose	150 g/l
MgSO <sub>4</sub> ·7H <sub>2</sub> O	2.5 g/l
NaCl	7.59 g/l

#### SGWB (Sucrose glycerol washing buffer)

0.5M Sucrose  
 10% glycerol (sterile)  
*pH 7 adjusted with 100 mM NaOH*  
*filter sterilized*

#### Loading dye (6x)

Glycerol	20 ml
Bromophenol blue	10 mg
Xylene cyanole	10 mg
MilliQ (sterile)	80 g

#### 10x PBS

KCl	2 g/l
Na <sub>2</sub> HPO <sub>4</sub>	14.4 g/l
KH <sub>2</sub> PO <sub>4</sub>	2 g/l
NaCl	80 g/l
ddH <sub>2</sub> O	up to 1 l
<i>pH 7.4 adjusted with HCl</i>	

#### SOC

Tryptone	20 g/l
Glucose solution (1M)	20ml/l
Sodium chloride	0.5 g/l
KCl	0.2 g/l
MgSO <sub>4</sub> (1M)	20ml/l
ddH <sub>2</sub> O	up to 1 l
<i>pH 7.5 adjusted with NaOH</i>	

#### TAE 50x

Trise-base	242 g/l
Glacial acetic acid	57.1 ml/l
EDTA (0.5M pH 8)	100ml/l
ddH <sub>2</sub> O	up to 1 l
<i>pH 7.4 adjusted with HCl</i>	

#### TSS Transformation Buffer

LB	21.6ml
DMSO	1.25
MgCl <sub>2</sub>	167μl
KCl	0.2 g/l
MgSO <sub>4</sub> (1M)	20ml/l
PEG solution (67% per weight)	3.2ml
store at 4°C	



# Acknowledgements

The present thesis would have never been possible without the excellent assistance from various people.

First of all, I would like to extend my sincere gratitude to *Prof. Martin J. Loessner* for providing me the opportunity to conduct my PhD in his Laboratory. His expertise and support have proved invaluable in my growth and development as a scientist.

I would like to thank my thesis committee *Dr. Markus Schuppler* and *Dr. Yves Briers* for accepting the task as reviewers and introducing me into the fascinating world of bacterial L-forms.

I am very grateful to my students *Patrick Studer*, *Nicolas Annaheim*, *Thaddäus Perrot* and *James Tauber* for their valuable contributions to this thesis.

In particular I would like to thank Patrick Studer for his continuous friendship and support. I appreciated the close cooperation as well as the lively scientific exchange we have cultivated during the last couples of years.

I am indebted to *Prof. Peter Walde* for his effort and support as an expert on protocell chemistry. The fruitful discussions were extremely valuable for my thesis.

I would like to thank *Dr. Marcel Eugster*, *Sibylle Schmitter* and *Dr. Oliver Weingart* for their great support in the laboratory and readiness to help me out any time. Furthermore, I would like to show my appreciation to *Prof. KC Huang* and *Dr. Tristan Ursell* who enabled my research visit at Stanford University, USA.

I wish to thank *Dr. Rainer Lehmann* for his willingness to give useful advice whenever I sought help.

Special thanks goes to my collaborators. *Daniel Sévin* who conducted the mass spectrometry analysis and *Dr. Maik Hadorn* who was willing to accept the challenge and work on the production of GUV with *Listeria* lipid extracts.

Many thanks to all present and former members of the Laboratory of Food Microbiology for the pleasant working atmosphere and all the exciting activities.

My deepest gratitude goes to my family and Sibylle who have always supported me. I thank for their patience, faith and being always there when I needed them.

# Curriculum vitae

TITU STAUBLI

Born January 20, 1984

Citizen of Zurich (ZH)

---

## Education

2010 - 2014	PhD Student in the Laboratory of Food Microbiology, ETH Zurich, Switzerland
2008 - 2010	MSc in Biology (Major Biochemistry), ETH Zurich, Switzerland
2005 - 2008	BSc in Biochemistry, University of Zurich, Switzerland
2000 - 2004	High School, Matura, Gymnasium Unterstrass, Switzerland
1997 - 2000	Secondary School, Hirzel, Switzerland
1990 - 1997	Primary School, Stadt Zürich, Switzerland